ADDIS ABABA INSTITUTE OF TECHNOLOGY
SCHOOL OF GRADUATE STUDIES

Numerical Investigation on the Behaviour of Laterally Loaded Pile Embedded in Layered Soils of Addis Ababa

by

Fenta Nebiyou Mekonnen

A Thesis Submitted to School of Graduate Studies in
Partial Fulfillment of the Requirement for Degree of
Master of Science
in
Geotechnical Engineering

Advisor
Dr.–Ing. Henok Fikre
Assistant Professor of Civil Engineering
Addis Ababa University

October, 2019
Addis Ababa, Ethiopia

ADDIS ABABA INSTITUTE OF TECHNOLOGY
SCHOOL OF GRADUATE STUDIES

Numerical Investigation on the Behaviour of Laterally Loaded Piles Embedded in Layered Soils of Addis Ababa

By

Fenta Nebiyou Mekonnen

A Thesis Submitted to School of Graduate Studies in
Partial Fulfillment of the Requirement for Degree of
Master of Science
in
Geotechnical Engineering

Approved by Board of Examiners:

Dr.-Ing. Henok Fikre	_____	_____
Advisor	Signature	Date
Dr. Im So Been	_____	_____
Internal Examiner	Signature	Date
Dr.-Ing. Tensay Gebremedhin	_____	_____
External Examiner	Signature	Date
Dr.-Ing. Mebruk Mohammed	_____	_____
Chairperson	Signature	Date

DECLARATION

I, the undersigned, declare that this thesis is my original work performed under the supervision of my research advisor Dr.-Ing. Henok Fikre and has not been presented as a thesis for a degree in any other university. All sources of materials used for this thesis have also been duly acknowledged.

Name: Fenta Nebiyou Mekonnen

Signature _____

Place Faculty of Technology,

Addis Ababa Institute of Technology,

Addis Ababa.

October, 2019

ABSTRACT

A three-dimensional finite element technique was used to analyze behaviour of laterally loaded single pile subjected to pure static lateral load. The main objective of this study is to assess the influence of the pile diameter, pile length and site condition on the behaviour of laterally loaded single pile embedded in layered soils. Most of the studies were focused on the behaviour of laterally loaded pile embedded in homogenous soils, but in this study behaviour of laterally loaded pile embedded in layered soils was considered.

A lateral load behavior of single piles in three different sites located in Addis Ababa city were studied with different diameter and length of pile. The analysis was carried out by considering free headed flexible piles. Full scale field test result obtained from the literature was used for the validation of Plaxis 3D Foundation FEM. Lateral deflection, bending moment and shear force were calculated for piles with different diameter and length for each three sites and their results were presented.

In this study the result shows that the head deflection of a pile, lateral pile displacement, distribution of bending moment, distribution of shear force along the pile length and lateral soil resistance were influenced by pile diameter and site conditions. The analysis indicated that the head deflection of the pile decreased with increase in pile diameter since its stiffness was increased but remain constant with increase in length of pile since the embedded length of the pile is greater than its critical length. Increase in pile diameter increased in ultimate lateral load capacity, bending moment and shear force along the pile length and remain constant with increase in pile length. In addition, the location and the thickness of the hard stratum near to the ground surface has a great role in the response of laterally loaded piles.

Keywords: Laterally Loaded Piles; Layered Soil; Finite Element

ACKNOWLEDGEMENT

I would like to express my sincere gratitude to my advisor, Dr.–Ing. Henok Fikre, for his valuable advice, support, encouragement and friendship throughout the course of this work. His excellent guidance, thoughtful criticism, innovative ideas made this research an enjoyable and fruitful experience.

I am deeply grateful to all who have given me assistance on soil and rock laboratory results and obtaining the information and data, especially Best Consulting Engineer Private Limited Company, ARCON Design Building PLC, Geotechnical Service and Construction Design Share Company staffs in Addis Ababa related to this work.

It is not possible to acknowledge all of my friends who have contributed to the development of this thesis, but special deepest gratitude is extended to my family for their support and encouragement.

LIST OF SYMBOLS AND NOTATIONS

3D	Three Dimensional
2D	Two Dimensional
FEM	Finite Element Method
p-y	Horizontal Load verses Deflection
CBE	Commercial Bank of Ethiopia
AAICEC	Addis Africa International Convention and Exhibition Center
EBCS	Ethiopian Building Code of Standard
L_c	Critical embedded pile length
K_p	$\tan^2(45° + \phi'/2)$, the coefficient of passive earth pressure
$L(l)$	Embedded pile length
I_p	Moment of inertia of an equivalent solid cylinder pile
E_p	Young's modulus of an equivalent solid cylinder pile
D(Dia)	Diameter of a concrete pile
E_pI_p	*EI,* initial flexural rigidity of the pile
c	Cohesion
RMR	Rock Mass Rating
RQD	Rock Quality Designation
$u(x)$	Lateral pile displacement in the direction of *x*
$u(y)$	Lateral pile displacement in the direction of *y*
$u(z)$	Lateral pile displacement in the direction of *z*
SPT-N	Standard Penetration Number
PI	Plasticity Index
q_u	Unconfined Compressive Strength
γ_{sat}	Unit weight of the overburdened soil (saturated)
γ_{unsat}	Unit weight of the overburdened soil (unsaturated)
γ_w	Unit weight of water

λ	Relative stiffness ratio
ν_s	Poisson's ratio of a pile (soil)
σ_h	Horizontal stress
σ'_v	Effective overburden pressure
$\phi(\phi')$	Angle of friction of soil (effective ϕ)
USCS	Unified Soil Classification System
UCS	Unconfined compressive strength
R_{int}	Strength reduction factor for interface
H	Horizontal load
M	Bending moment
S	Shear force
δ	Lateral deflection
FE	Finite Element
y	Depth of pile
ε_e	Elastic strain
ε_p	Plastic strain

TABLE OF CONTENTS

LIST OF FIGURES

LIST OF TABLES

CHAPTER 1 : INTRODUCTION

1.1 Background

Many structures need deep foundations in order to utilize the bearing capacity of deeper and stronger soil layers. Piles are one particular type of deep foundations most widely-used for high structures. In addition to the vertical loads that must be carried by the piles, lateral loads may be present and must be considered in design. These lateral loads may be generated by earthquakes, waves, wind, ice flow, debris flow, river flow, earth movement, structural expansion and impacts. These transient loading conditions which may involve cyclic loading contribute to the complicated interaction between the structural foundation components and the surrounding soil.

Wind gusts are the most common cause of lateral force (and/or moment) that a pile has to support. The other major cause of lateral force is seismic activity. The horizontal shaking of the ground during earthquakes generates lateral forces that the piles have to withstand. Certain buildings are also acted upon by lateral earth pressures, which transmit lateral forces to the foundations. That apart, depending on the type of structure a pile supports, there can be different causes of lateral forces. For tall buildings and transmission towers, wind action is the primary cause. For offshore oil production platforms, quays, harbors, wharfs and jetties, wave action gives rise to lateral forces.

Piles are commonly used to transfer vertical (axial) forces, arising primarily from gravity (e.g., the weight of a superstructure). Examples of structures where piles are commonly used as foundations are tall buildings, bridges, offshore platforms, defense structures, dams and lock structures, transmission towers, earth retaining structures, wharfs and jetties. However, in all these structures, it is not only the axial force that the piles carry; often the piles are subjected to lateral (horizontal) forces and moments. In fact, there are some structures (e.g., oil production platforms, earth retaining structures, wharfs and jetties) where the primary function of piles is to transfer lateral loads to the ground.

The lateral load capacity of pile foundations is critically important in the design of civil structures. Although fairly reliable methods have been developed for predicting the lateral capacity of single piles under static loads, there is very little information to guide engineers in the design of piles embedded in layered soil particularly under static loads.

In past, many analytical/numerical methods for analysis of pile have employed simplified assumptions such as replacing the soil medium by Winkler springs, treating the soil medium as an elastic continuum, and neglecting the interaction between various components (namely, the piles and the soil medium).

In this study an investigation is made to assess the behaviour of laterally loaded pile foundation for three sites found in Addis Ababa city. In addition, a parametric study has been conducted to see the effect of pile diameter, pile length and location and thickness of hard stratum near the ground surface on response of laterally loaded pile foundation. In this study three different sites from Addis Ababa city has been taken as a case study. The complex geometry and interaction of pile foundation can be accounted for using Finite Element Method modelling. So, this method can be used for modelling and analyzing the laterally loaded pile foundation system. The present study was directed to understand the response of pile foundation subjected to lateral loads in layered soil.

1.2 Problem Statement

The lateral load capacity of pile foundations is critically important in the design of civil structures which may be subjected to wind load. Information about the lateral behavior of piles in layered soil profiles is very limited especially in the case of Ethiopian Building Code of Standard as a guide. It is noted that there is limited literature reporting on pile behavior under lateral loading in layered soil. Although fairly reliable methods have been developed for predicting the lateral capacity and behaviour of single piles embedded in layered soil under static loads.

Therefore, it is important to investigate the response of laterally loaded piles when it embedded in layered soils since in practice, most of soil deposits in nature are layered systems. Obviously, an educated guess might not result in optimal design. It is very important to find out how these layers in the layered system affect the analysis of laterally loaded pile foundation and therefore provide a more effective way for the design of laterally loaded pile foundations in layered soil systems. To address the lack of design guidance and quantitative information on the behaviour of laterally loaded single pile embedded in layered soils Addis Ababa was considered.

1.3 Research Objectives

1.3.1 General objective of the study

The overall objective of this study is focused on the investigation of behavior of laterally loaded piles embedded in layered soil using numerical modelling for three sites found in Addis Ababa.

1.3.2 Specific Objectives of the Study

This study has the following specific objectives:

- To develop load-displacement relationship of laterally loaded pile embedded in layered soils by varying pile diameter and pile length under static horizontal loads.
- To estimate the ultimate lateral resistance of laterally loaded pile by varying pile diameter and pile length under static horizontal loads.
- To study the variation of lateral deflection, bending moment and shear force along pile length that embedded in layered soil by considering the variation of pile diameter and pile length under static horizontal load.

1.4 Methodology

To meet the above objectives the following procedure was followed.

- Data collection

  All the necessary secondary data that helps for the modelling and analysis of the laterally loaded pile foundation were collected from investigation reports conducted in the lab and field tests. Different correlation techniques were also used to determine soil parameters that are not included in the soil investigation reports.
- Software modelling

  The finite element software Plaxis 3D Foundation was selected for simulating the laterally loaded pile foundation. The behaviour of laterally loaded pile foundation was analyzed based on different constitutive material behaviour. The material behaviour of soil was modelled with non-linear material constitutive model, whereas, piles were modelled with a linear elastic constitutive model.
- Finally, the results are interpreted, conclusions are drawn and recommendations made based on the obtained results.

The whole process is documented in the final report together with the important conclusions and recommendations. Figure 1.1 shows the general research process

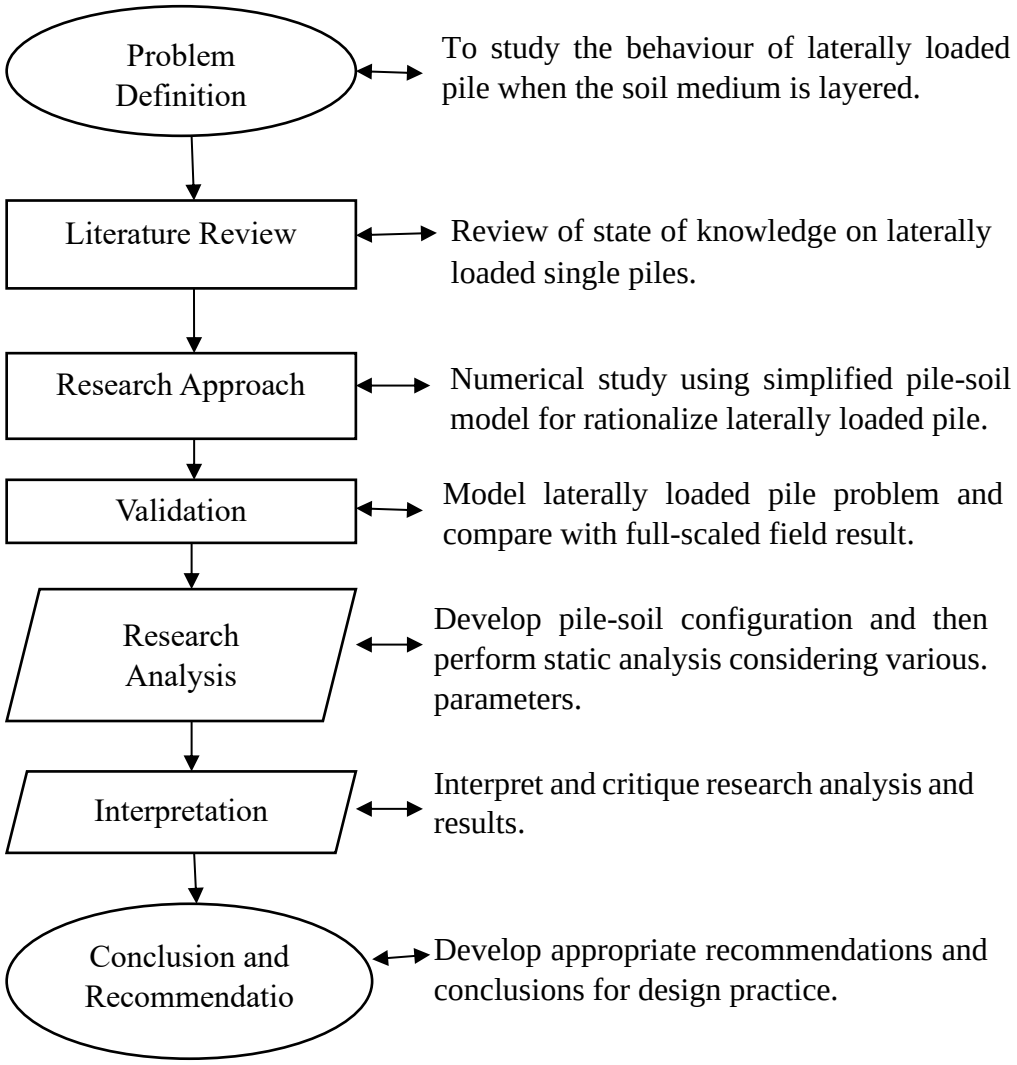

Figure 1.1 General research process

1.5 Scope and Limitations of the Present Study

The investigation was carried out using soil profiles in Addis Ababa where high-rise buildings are going to be constructed and have been already constructed. A three-dimensional finite element model for pile and soil was used for the study. This study is limited to investigate the effect of pile diameter and pile length, on deflection, ultimate lateral load capacity, bending moment and shear force when the pile was subjected by static lateral loads. This study is limited to investigate the effect of pile diameter and pile length, on deflection, ultimate lateral load capacity, bending moment and shear force when the pile is subjected by static lateral loads.

Elastic-perfectly plastic Mohr-Coulomb failure criterion was used in all analyses as soil and rock material model. Drained analysis was conducted for all layer type of ground materials.

1.6 Content of the Thesis

This thesis consists of six chapters. Chapter one introduces some ideas on the title and the main task of this work. Chapter two presents the general background of the use of laterally loaded pile foundations to support different types of structures. It also highlights the current available means for analyzing and designing laterally loaded pile foundations. A review of previous studies on laterally loaded pile foundations is also presented in this chapter. The third chapter deals with validation of numerical model and numerical modelling of selected laterally loaded pile and the details of the pile-soil modelling in Plaxis 3D Foundation, material modelling, and analytical programming procedure steps involved in modelling of the laterally loaded piles. In the fourth chapter, parametric study and analysis of laterally loaded for particular site conditions is discussed in details. In chapter five, conclusions and recommendations of the present study are given followed by the references.

CHAPTER 2 : LITERATURE REVIEW

2.1 Introduction

When a pile is subjected to lateral loading, the interaction that ensues between the pile and the surrounding soil is a topic replete with issues. The nature of soil is an obvious source of complexity, but so too are the pile and the dependence of its behavior on the nature of the soil present. Introduction of other piles nearby, or in other words consideration of pile group, provides further complexity through pile-soil-pile interaction and the physical repercussions of the group configuration. Further modification is possible due to construction-related issues such as the installation process, and this is to say nothing of other factors that can affect lateral response, such as the pile head fixity.

In answer to these various issues a basic framework of mathematical models supplemented with empirical rules has emerged. Playing a key role has been the understanding of single pile behavior, serving to identify both general pile-soil interaction issues as well as providing a benchmark from which group behavior can be assessed. Single pile behavior will therefore be reviewed in the current section.

Piles have been used to increase the vertical load carrying capacity of foundations for many decades. For the most part, design of pile foundations has been based on empirical formulations and procedures. To date, there has been much research effort focused on the design and behavior of pile foundations to meet increasing needs for efficient and cost-effective construction in more and more unfavorable grounds. Many analytical models which are based on sound engineering principles have been developed in the last two decades. These models generally represent the soil as an elastic medium (Poulos and Davis, 1970) or replace the soil with uncoupled, Winkler springs, termed p-y curves. The p-y curve methods have proved to be very versatile and useful as they can be non-linear and have different shapes and form which better represent the soil behavior. Unfortunately, due to the high cost of full-scale experiments on piles, soil parameters required for the various models have not been fully calibrated, nor have the models been fully verified yet. Fundamental aspects of soil-pile interaction are still poorly understood. This chapter serves as a review of the previous studies of laterally loaded pile design, analysis, and construction.

2.2 Linear Subgrade Reaction Theory

The response of an isolated, single pile to lateral loading is a typical soil-structure interaction problem whereby appreciation of both components and their dependence on each other is required in order to properly assess behavior. This basic need to consider the properties of both the soil and pile combined is epitomized by the classical beam-on-elastic-foundation problem as illustrated in Figure 2.1.

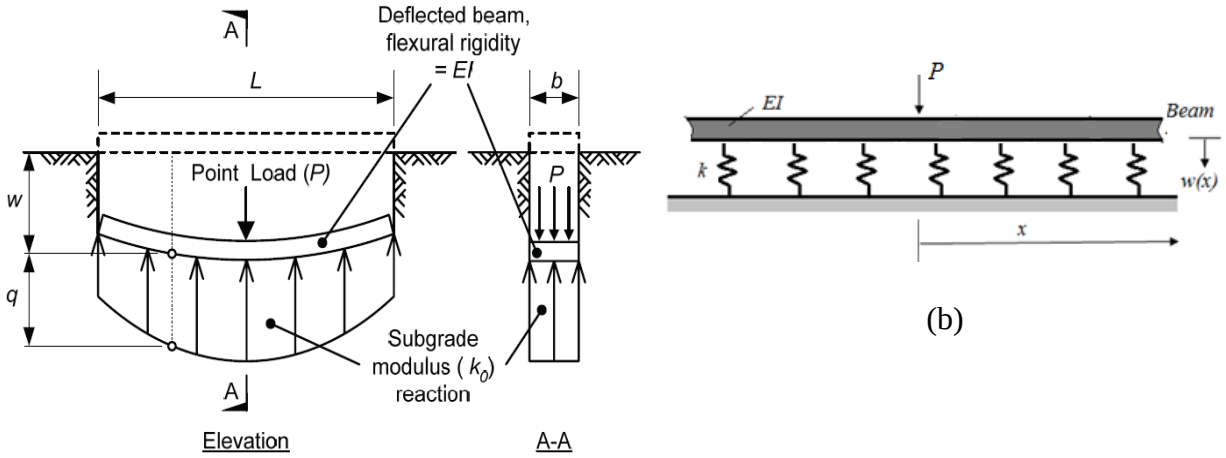

Figure 2.1 Beam-on-elastic-foundation problem (after Terzaghi, 1955)

Idealizing the soil foundation as a Winkler foundation Figure 2.1(a), consisting of a bed of infinitely closely spaced, independent springs Figure 2.1(b) each possessing a linear vertical pressure q per unit area versus vertical deflection w relationship as follows,

$$\frac{q}{w} = k_0 \text{ or } \frac{qb}{w} = k \qquad (2.1)$$

Where: k_o = subgrade modulus soil (FL^{-3} dimensions)

b = width of beam

$k = k_o b$ = subgrade modulus for soil (FL^{-2} dimensions)

The general differential equation governing the deflected shape of a beam resting on a Winkler medium is:

$$E_b I_b \frac{d^4 w}{dx^4} + kw(x) = p(x) \qquad (2.2)$$

The general solution of Equation (2.2) is given by:

$$w = (C_1 \cos \lambda x + C_2 \sin \lambda x)e^{\lambda x} + (C_3 \cos \lambda x + C_4 \sin \lambda x)e^{-\lambda x} \qquad (2.3)$$

Where C_1 through C_4 are constants, and

$$\lambda = \sqrt[4]{\frac{k}{4EI}} \quad (L^{-1} \text{ dimensions}) \qquad (2.4)$$

Consider now a beam of infinite length subjected to a concentrated force, P, as shown Figure 2.1 (b), from the boundary conditions; Equation 2.3 becomes,

$$w = (C_3 \cos \lambda x + C_4 \sin \lambda x)e^{-\lambda x} \qquad (2.5)$$

In equation 2.5, for the left side of the beam w(-x) = w(x) (M. Hetenyi, 1946).

The parameter λ is dependent on the properties of both the soil and beam, and its reciprocal represents a characteristic length of the soil-beam system. If the beam is very stiff compared with the soil then the characteristic length is large and a load applied to the beam will cause vertical deflections of the soil for a considerable distance from the point of load application; conversely, a beam that is very soft compared with the soil (i.e., a very stiff soil) will result in a small characteristic length and only cause vertical deflections in the immediate vicinity of the point load (Scott, 1981). Although use of subgrade reaction theory to depict soil is far removed from real soil behavior, identification of λ as an interactive measure dependent on the relative stiffness of the soil and structure, and in turn the dependency of behavior on such a measure, is a fundamental aspect of soil structure interaction.

In the context of laterally loaded piles, the dependence of behavior on relative stiffness has resulted in the need to distinguish between “short” (rigid) and “long” (flexible) piles. These definitions acknowledge a somewhat intuitive sense of pile behavior whereby a very short and relatively stiff pile (e.g., a fence strainer-post) would be expected to deflect in a rigid manner when laterally loaded, whereas a very long pile in the same situation would be expected to exhibit a different type of behavior due to the increased embedment and accompanying fixity that this implies. Reese (1986) discussed this dependence of lateral behavior on pile length, noting that short piles can

deflect a large amount at the ground line given movement of the pile tip, but with increasing depth of penetration the soil resistance at the pile tip increases until a point is reached at which ground line deflection reaches a limiting value. This type of behavior is depicted in Figure 2.2, for the case of both lateral load (P_t) and moment (M_t) applied at the ground line, assuming an elastic (E_pI_p) pile model and constant horizontal subgrade modulus (k_h) soil model. As shown, a so called "critical length" L_c exists, beyond which any additional pile length has no further influence on the pile head response.

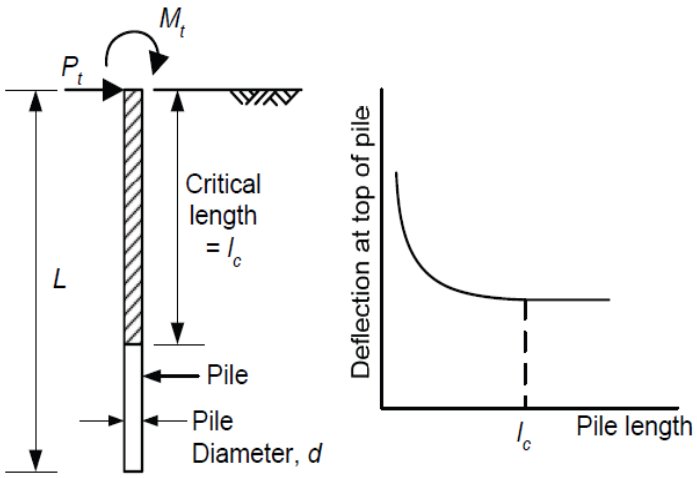

Figure 2.2 Critical length for a laterally loaded pile (after Reese and Van Impe, 2001)

Thus, a flexible pile is defined as a pile whose length equals or exceeds its critical length. In subgrade reaction terms such critical lengths have been established for the case of a horizontal subgrade modulus (k_h) that is constant with depth (as in Figure 2.2), in which case:

$$L_c = \frac{4}{\lambda} \tag{2.6}$$

Where: $\lambda = \sqrt[4]{\frac{k_h}{4E_pI_p}}$ (2.7)

k_h = Subgrade modulus for soil (FL^{-2} dimensions)

E_p = Young's modulus for pile,

I_p = Second moment of area for pile,

and for the case of a horizontal subgrade modulus increasing linearly with depth, in which case:

$$l_c = 4T \tag{2.8}$$

Where, $T = \sqrt[5]{\frac{E_p I_P}{n_h}}$ (2.9)

n_h = constant of horizontal subgrade reaction (FL^{-3} dimensions), given

$k_h = n_h z$ (FL^{-2}dimensions), where z is depth

While these critical length values are subject to the limitations inherent in idealizing the pile-soil system in such a simplistic way, the concept of a critical length is nevertheless of general validity and acknowledges the dependence of lateral behavior on a certain mobilized depth of soil that may or may not extend the entire length of the pile. As a comment aside, this physical attribute of lateral behavior is also suggestive of some form of normalization, an early example of which was the non-dimensional linear solutions derived by Matlock and Reese (1960) using principles of dimensional analysis.

Poulos and Hull (1989) method, a linear elastic soil response due to lateral pile movements was assumed. A critical length, L_c equation (2.10), exists for a laterally-loaded pile, over which any increase in pile length has no influence on the pile head deflection. The critical pile length, L_c is a function of the relative stiffness of pile and soil. For uniform soil, L_c can be calculated from the following equations:

$$L_c = 4.44\left(\frac{E_P I_p}{E_s}\right)^{0.25} \tag{2.10}$$

Where: $E_P I_p$ -Pile rigidity

E_s -Soil Young's Modulus of Elasticity

The initial preference towards subgrade reaction theory to assess lateral pile-soil interaction was understandable given that readily obtainable solutions were possible, but the selection of an appropriate subgrade modulus presented a real problem. Terzaghi (1955) expressed such concern in the now classic paper that serves as a reminder of both the basic limitations involved with subgrade reaction theory, and the difficulty of obtaining an appropriate value for the subgrade modulus. Besides his all-important remark that the theory was only approximately valid for pile-

soil contact pressures less than about one half the ultimate bearing capacity of the soil under lateral load, Terzaghi also emphasized the importance of soil type and the dimensions of the pile. These issues were considered as shown in Figure 2.3, where stiff (overconsolidated) clay and sand subgrade characteristics were idealized by constant and linearly increasing subgrade reaction models respectively, and pile dimensions were addressed utilizing the notion of differing horizontal pressure bulbs mobilized by different pile widths.

These simple ideas underlined the need to appreciate both the different deformation characteristics of soils, and possible effects of size due to differing volumes of the surrounding soil mass being affected by different loaded areas. The issue of flexural rigidity of a structure, such as a pile, and its effect on the subgrade modulus was only briefly mentioned by Terzaghi (1955), and only then in the context of theoretical work.

Rowe (1956), on the other hand, specifically pursued the response of a laterally loaded single pile in real sand and noted significant differences in the back-calculated values of subgrade modulus depending on whether the pile was considered to be rigid or flexible. Though weakened somewhat by use of some data from scaled-down 1-*g* laboratory pile-soil models and thus subject to scaling errors, this work by Rowe was of particular value given that it utilized subgrade reaction theory in conjunction with experimentally observed data. In doing so it served to demonstrate the highly variable nature of the subgrade modulus during lateral loading as a result of the actual nonlinear interplay between pile and soil. This resulted in a rather convoluted analysis procedure, relying on various assumptions and approximations in order to adapt the underlying subgrade reaction theory to agree with observed behavior.

That subgrade reaction theory is limited from both a physical and theoretical point of view is a fact that has long been recognized: Terzaghi himself expressed reservations in publishing his 1955 paper and only did so after numerous requests (Reese, 1986). Jamiolkowski and Garassino (1977) acknowledged this limitation in their review of soil moduli for laterally loaded piles, noting the important observation made earlier by McClelland and Focht (1958a) that the subgrade modulus is not a property exclusively of the soil, but simply a convenient mathematical parameter that expresses the ratio of soil reaction to pile deflection. In doing so, such a parameter depends on the characteristics of the pile (i.e., pile geometry, flexural rigidity, boundary conditions at the top and

bottom of the pile, etc.), the soil, and the manner in which the pile and soil characteristics change with the level of lateral loading applied.

In response to this complex state of affairs, two general categories of design approaches for single piles have emerged: a) Those that retain the basic qualities of subgrade reaction theory in the form of discrete, nonlinear load-transfer mechanisms along the pile length depicting the soil reaction to pile deflection relationship; and b) those that represent the soil as a continuum.

These approaches will be referred to here as the Discrete Load-Transfer and Continuum approaches, respectively. Prior to discussing these approaches, however, mention must also be made of limit equilibrium approaches, exemplified by the work of Broms (1964a, 1964b, 1965). This type of approach, representing a limit analysis, is confined to ultimate (failure) conditions where reasonable assumptions of lateral soil pressures can be made and solutions readily found by use of the equations of statics. While largely redundant now given the versatility and capabilities of the continuum and discrete load-transfer approaches, a brief account of the work of Broms will be given as it provides an instructive account of lateral soil-pile interaction and is an appropriate precursor to the more advanced continuum and discrete load-transfer approaches.

a. Soil type

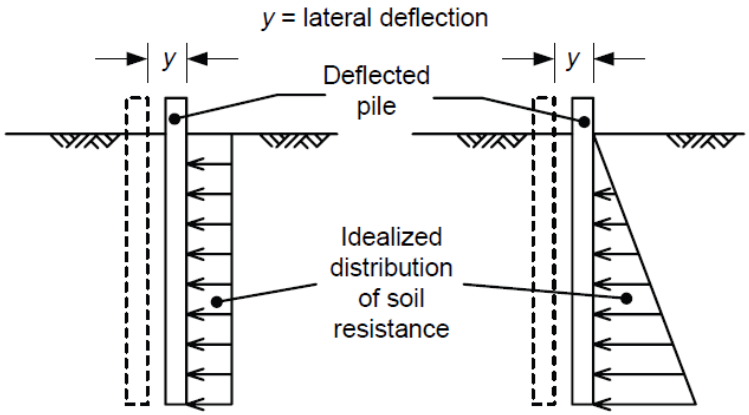

Stiff (Overconsolidated)Clay Sand

b. Size effect

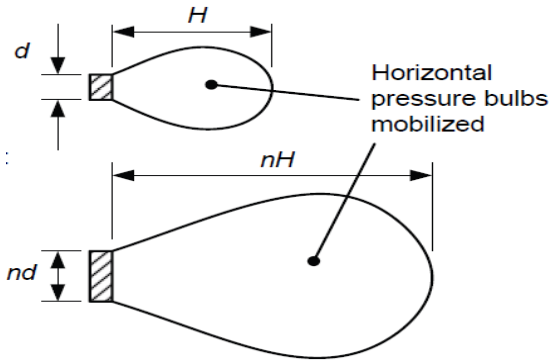

Figure 2.3 Idealized soil type and size effects (after Terzaghi, 1955)

2.3 Brom's Design Method

Restricting his work to driven piles, Broms (1964a, 1964b) presented methods for the design of laterally loaded piles in uniform soil profiles consisting of cohesive (clay) and cohesionless (sand) material, and for unrestrained (free-head) and restrained (fixed-head) pile-head conditions. In doing so, failure modes involving either the pile (formation of plastic hinges) or the soil (mobilization of ultimate lateral resistance) were proposed for short and long piles as shown in Figure 2.4. These failure modes recognized the relative importance of either pile or soil strength in governing the ultimate capacity of long or short piles, respectively.

In considering the ultimate lateral soil pressures acting against a laterally loaded pile, Broms (1964a, 1964b) considered the general behavior at ultimate conditions to be as shown in Figure 2.5. This depicts different deformation patterns of the soil in front of the laterally loaded pile depending on depth: Soil towards the surface exhibits upwards movement, while soil at depth only moves horizontally around the pile. Also, separation of the soil from the back of the deflected pile is shown for the cohesive soil case, while downwards movement of soil to fill the gap created at the back of the deflected pile is depicted for the cohesionless case. Such kinematic behavior indicates the need to distinguish between surficial and at depth soil resistance because of the relative freedom of soil near the surface to move upwards when loaded horizontally. Consequently, the surficial soil offers lesser resistance compared with the resistance at-depth which is derived from only horizontal movement as a result of overburden weight suppressing any upward movement. Both resistances are three-dimensional in nature, as is the soil behavior at the back of

the pile, reminding one that lateral pile behavior is a consequence of soil resistance mechanisms that vary around, as well as along, the pile.

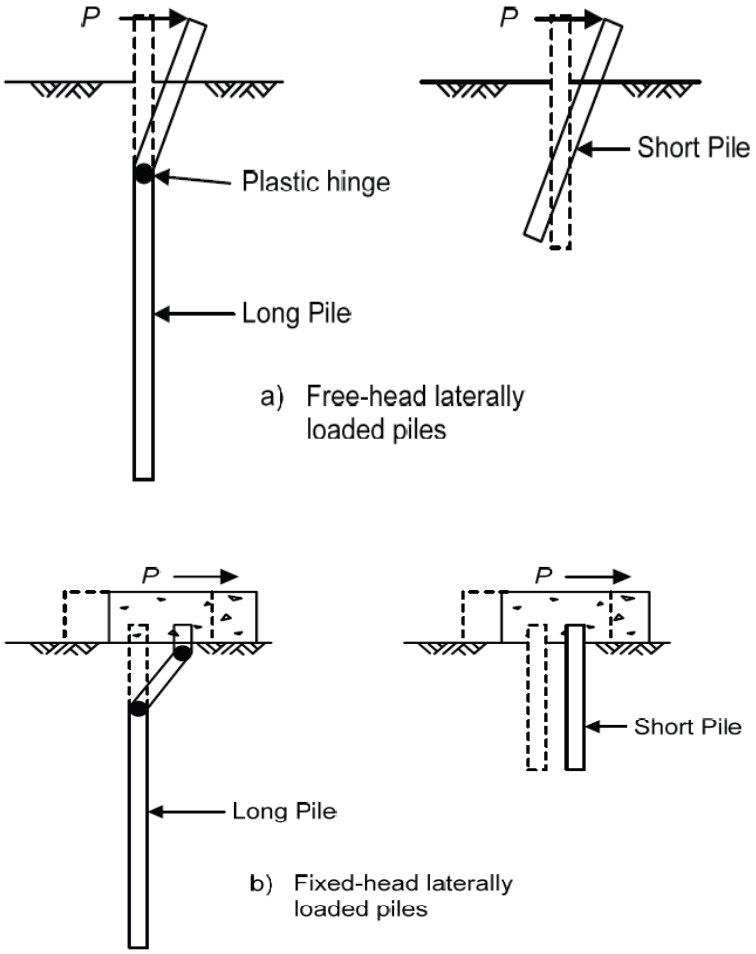

Figure 2.4 Failure modes proposed for short and long piles (after Broms, 1964a, 1964b)

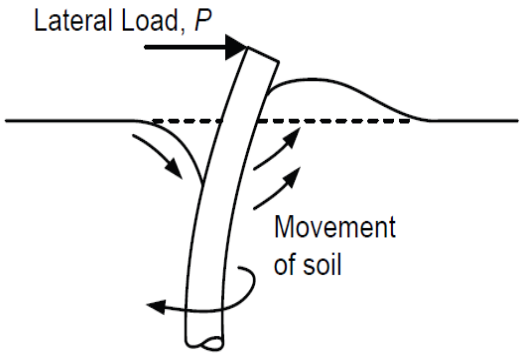

a) Ultimate behavior for cohesionless (sand) conditions

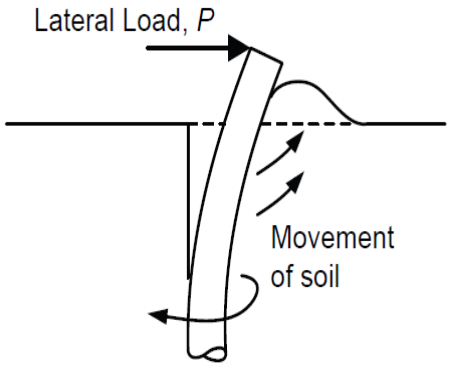

b) Ultimate behavior for cohesive (clay) conditions

Figure 2.5 General behaviors for ultimate conditions (after Broms, 1964a, 1964b)

In addition to ultimate behavior, Broms (1964a, 1964b) considered design at working loads and made some other noteworthy observations. As deflection was considered to govern working load design, linear subgrade reaction theory was utilized to produce dimensionless ground line lateral deflection versus dimensionless length plots for restrained and unrestrained pile-head conditions. These are shown in Figure 2.6 for a lateral load *P* applied at the ground line only, for both "cohesive" (constant subgrade modulus $= k_h$) and "cohesionless" (linearly increasing subgrade modulus $= n_h z$) soil conditions. Immediately apparent is the significant reduction in lateral deflection as a result of restraining the pile head.

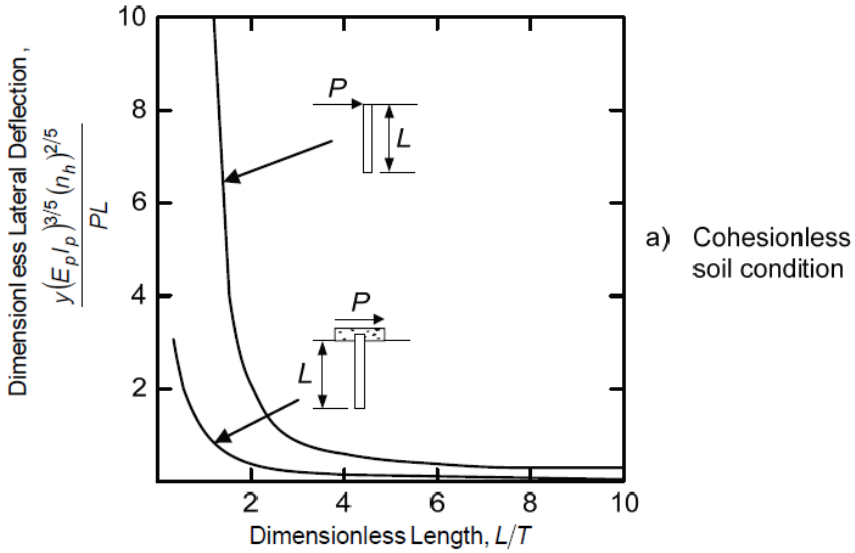

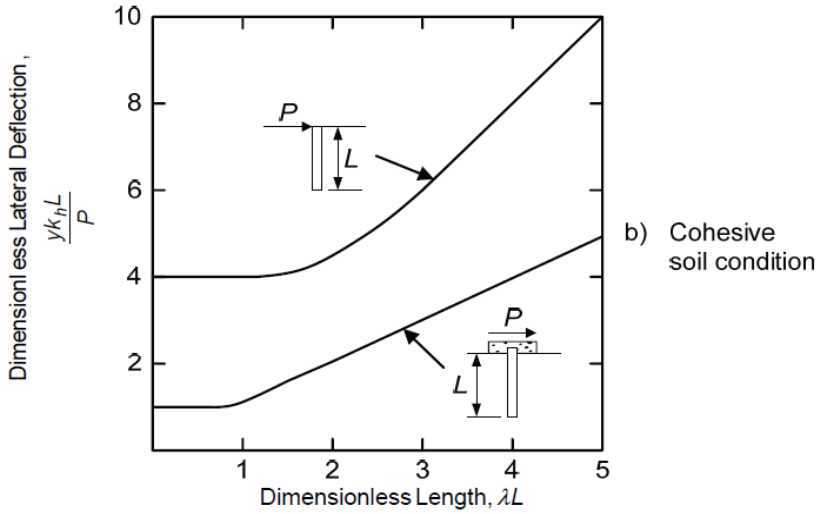

Figure 2.6 Broms (1964a, 1964b) lateral deflection design charts

Based on deflection behavior, rigid and flexible piles were as defined in Table 2.1.

Table 2.1 Rigid and flexible pile criteria from Broms (1964a, 1964b)

Soil Condition	Rigid Pile Criteria		Flexible Pile Criteria	
	Free-Headed	Fixed Headed	Free-Headed	Fixed Headed
Cohesive	$\lambda L < 1.5$	$\lambda L < 0.5$	$\lambda L > 2.5$	$\lambda L > 1.5$
Cohesionless	$\frac{L}{T} < 2.0$		$\frac{L}{T} < 2.0$	

In connection with this deflection behavior, reference was made to a "critical depth" for the cohesive soil condition case, in that the subgrade reaction within this depth was considered to control the ground line deflection of the pile. Such critical depths equal to dimensionless depths (λL) of 2.0 and 1.0 were given for fixed-head and free-head piles respectively, based on the observation from Table 2.1 that ground line deflections at these lengths are approximately the same as those assuming the pile is long (within 10%). This indicates that the way lateral soil resistance is mobilized is a function of the deflected shape of a pile, and the reduced deflection of a fixed-head pile compared with a similarly loaded free-head pile is due in part to the greater depth of soil mobilized by the deflected shape.

The work of Broms (1964a, 1964b) and subsequent design summary (Broms, 1965) provided greater insight into lateral pile-soil interaction with the use of suitable models and reasonable assumptions. Practicably, its use in the design of rigid piles was widespread (Allen, 1985) and

capable application to the design of drilled shafts demonstrated (Kulhawy and Chen, 1995). Nevertheless, the approach required the assignment of problems into particular categories that necessarily approximate behavior, and with the advent of computer technology analytical improvements were possible (Matlock and Grubbs, 1965). One such improvement was to model the soil using elasticity and plasticity theory in order to depict the continuous nature of soil in a more realistic way.

2.4 Continuum Approaches

A weakness of the subgrade reaction approach is the independence of each soil spring, whereby the response of any one spring is assumed to have no influence on the response of others. Real soil is inherently a particulate material and thus derives its resistance through innumerable load paths that can generally be considered in a continuous, interactive sense. As a result, mathematical elastic and plastic continuums have been applied extensively in modelling soil behavior with much success. Applied to laterally-loaded piles, the replacement of soil with a continuous elastic or elastic-plastic model therefore stands to reason, providing a more fundamental approach to modelling the actual interaction between the pile and soil entities. While of value from a fundamental point of view, the success of such an approach relies on the ability to model the soil, pile and the pile-soil interface behavior appropriately. This aspect is still a subject in need of further research, but the work undertaken to date has served to strengthen the general understanding of lateral pile-soil interaction, and more importantly provide an appropriate basis for consideration of pile-soil-pile interaction effects that characterize lateral pile-group behavior.

Continuum approaches, as defined here, comprise an assortment of solution techniques utilizing either the theory of elasticity alone or both the theory of elasticity and plasticity. These include fully three-dimensional analyses and simplifications using two-dimensional analyses (plane strain or plane stress). Three-dimensional analyses offer the most realistic approach to assessing pile-soil interaction and are divided into integral equation (or boundary element) method and differential method analysis categories. Boundary element analysis work will be discussed first given that this approach is considered to have been most useful in providing a framework in which to synthesize single pile lateral behavior from a general standpoint.

2.4.1 Boundary Element Single Pile Models

An advantage of the boundary element method over other methods is its use of surface discretization that provides for the greatest numerical efficiency when dealing with three-dimensional problems possessing low surface area to volume ratios, as is the case with pile foundation problems (Banerjee, 1976; Banerjee and Driscoll, 1976). This enables a three-dimensional solution with the least computational effort and is certainly a redeeming feature of the method. Boundary element methods use the Mindlin (1936) solution for lateral displacement induced by a horizontal point load (Figure 2.7) as the mechanism responsible for interdependency. Through numerical integration of this solution over a discretized pile surface, equating lateral displacements from the elastic soil (Mindlin's solution) and elastic pile (Bernoulli-Euler beam theory), and imposing equilibrium conditions, a simultaneous equation solution ensues to solve for unknown forces that then allows determination of pile actions.

Introducing this type of approach to assess lateral response of piles, Spillers and Stoll (1964) noted that the purely elastic solution generated very high lateral pressures against the pile near the surface that would result in yielding of real soil. Nonlinear behavior of the soil model was therefore introduced by specifying maximum permissible pressures mobilized against the pile based on plastic yield criteria, considered a "first modifying effect" towards reconciling results with observed behavior. This reiterated the need for attention to surficial soils when assessing lateral load behavior, and the need of non-linearity in the pile- soil system. Subsequent work developed the boundary element principle put forward by Spillers and Stoll to produce useful design information for various pile-soil configurations, albeit from a mostly linear-elastic perspective. Notable was the work of Poulos (1971a), Banerjee and Davies (1978), Davies and Budhu (1986), and Budhu and Davies (1987, 1988).

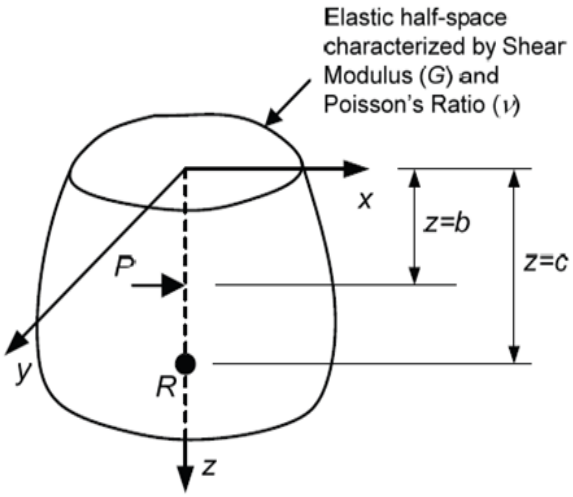

Figure 2.7 Mindlin (1936) solution

U_R = Lateral displacement at point R due to point load P

$$U_R = \frac{P}{16\pi G(1-v)}\left[\frac{3-4v}{|b-c|} + \frac{1+(1-v)(1-2v)}{b+c} + \frac{2bc}{(b+c)^3}\right] \qquad (2.11)$$

Poulos (1971a) choose a somewhat crude approach, starting with the depiction of a pile as a thin rectangular strip of width equal to the pile diameter (d), and possessing a length (L) and flexibility (E_pI_p) corresponding to that of the pile. A linear-elastic continuum with Young's modulus (E_s) constant with depth was used to represent the surrounding soil, and no separation between the pile and soil allowed. Any shear stresses at the pile edges were neglected, pile-soil interaction derived solely from uniform distribution of normal stress assumed across each pile-segment width, where pile lengths were discretized into standard 21 equal-length segments. Although a very crude approximation of actual behavior, the approach provided a consistent framework in which to assess the behavior of both rigid and flexible piles.

Such behavior was presented using the concept of pile head influence factors of the form given by the following equation below, where rotational influence factors were similarly defined to obtain rotation at the pile head.

$$\delta_h = I_{\delta p}\frac{P}{E_s L} + I_{\delta M}\frac{M}{E_s L^2} \qquad (2.12)$$

Where: δ_h = lateral deflection at pile head,

$I_{\delta p}$ =displacement influence factor for horizontal load only,

P =horizontal load (applied at pile head),

$I_{\delta M}$ =displacement influence factor for moment only, and

M =moment (applied at pile head).

Typical trends observed are shown in Figure 2.8 (a and b) where the parameter K_R represents a relative pile-soil stiffness measure, and the length-to-diameter (or slenderness) ratio, L/d, an appropriate parameter for distinguishing between rigid and flexible piles. In effect, K_R accounts for non-rigidity of the pile foundation and L/d accounts for embedment (Kuhlemeyer, 1979). Poulos (1972) noted that displacement and rotation at the pile head are virtually unaffected by the boundary condition at the pile tip when K_R values are less than about 0.01. Kuhlemeyer (1979) noted that this translates to an effective slenderness ratio at which flexible pile behavior can be assumed to apply, and such effective slenderness ratio values are plotted in Figure 2.9 against the ratio of the pile to soil modulus, E_pE_s. Shown are slenderness ratios corresponding to K_R values of 0.01 and 0.05. Kuhlemeyer considered that K_R = 0.01 was appropriate for displacement behavior at the pile head, but K_R =0.05 more appropriate for rotation behavior.

The work of Banerjee and Davies (1978) mainly served to provide a more rigorous boundary element technique whereby both normal and shear stresses around a cylindrical pile-soil interface were incorporated into the solution scheme using an a priori numerical procedure. Results for the soil modulus linearly increasing at the ground surface from both zero and half the pile tip modulus (i.e., triangular and trapezoidal distributions respectively) were also obtained, although these required an approximate solution scheme given that the Mindlin (1936) solution is strictly only valid for a constant modulus distribution with depth. These non-homogenous modulus cases exhibited a relative increase in the values of influence factors and transfer of pile actions to greater depths compared with the homogeneous modulus case. Relatively higher bending moments in the pile were also noted in the non-homogeneous cases.

Davies and Budhu (1986) and Budhu and Davies (1987, 1988) advanced on Banerjee and Davies (1978) by acknowledging different soil resistance patterns around a pile.

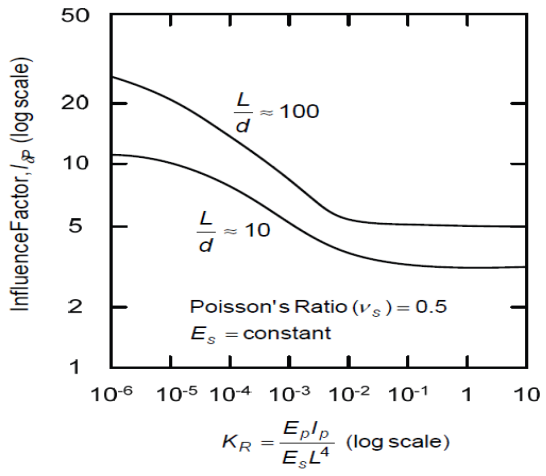

a. Influence factor for free headed pile

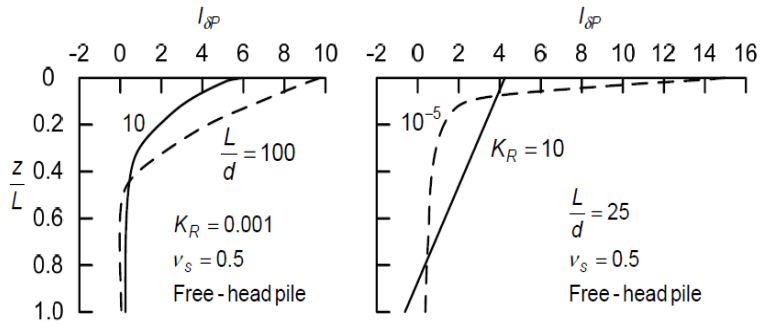

b. Typical displacement profiles showing effect of L/d and K_R

Figure 2.8 Typical trends for rigid and flexible piles (after Poulos and Davis, 1980)

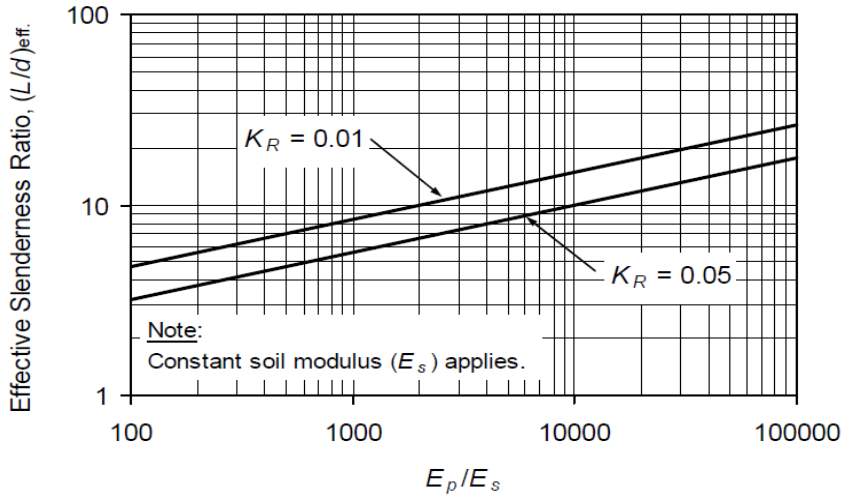

Figure 2.9 Apparent effective slenderness ratios for flexible pile behavior

Besides emphasizing the importance of nonlinear soil effects, the work of Davies and Budhu (1986) and Budhu and Davies (1987, 1988) also improved on prior elastic boundary element solutions by providing algebraic expressions to directly calculate pile head behavior for flexible piles. This approach was initiated by Kuhlemeyer (1979), who showed that, given flexible pile and elastic conditions, the independence of pile head displacement and rotation to pile length leads to behavior that is only a function of the pile-soil stiffness ratio. Also given are expressions for a parabolic distribution of Young's modulus with depth, as determined by Pender (1993) using the work reported by Gazetas (1991). Such information can be used as a means of back-calculating equivalent elastic soil moduli at small deflections using real load-deflection behavior. This is an important consideration when modelling pile load tests because the initial stiffness assigned to a soil model, particularly an elastic-plastic soil model, is one of the key parameters that control the nonlinear response of a modeled pile.

Idealization of the pile as a line element, necessary to avoid otherwise prohibitively expensive numerical computations, is also restrictive. This is because the governing integral equations can be satisfied only at the centerline of the pile, which in turn enforces limitations on the nature of surface tractions (i.e., normal and shear stresses) acting around the mathematical pile circumference (Banerjee and Driscoll, 1976).

2.4.2 Finite Element Method

Kuhlemeyer (1979a) has indicated that the critical length of a pile can be estimated as the length that results in a relative pile-soil stiffness factor, $K_R = E_p I_p \big/ E_s L^4$ of between 0.05 and 0.01 where the symbols are and E is the soil Young's modulus of the pile. Kuhlemeyer's basis for these values is the results of Poulos (1972); choosing the K_R value where the tip fixity condition has no effect upon the head response to head loads. He proposes that for a given pile and soil combination, there is a critical length to diameter ratio, beyond which the head response to head loads is unchanged by increasing the pile length. This suggests that if a pile has an effective length of less than three diameters, it may be necessary to use a more complex beam bending model than the simple beam theory which involves plane sections remaining plane. Even if the actual pile length is much greater than three diameters, then simple bending theory may still no longer be appropriate if the critical length is less than three diameters.

Kuhlemeyer (1979b) has used the solution for a cantilever response given by Timoshenko and Gere (1972), as an analytic check on his finite element model. That solution provides a more accurate response than the predictions of simple bending theory by taking account of shear deformations. Using the predicted tip deflection for the tip loaded stocky cantilever, it is possible to show that the answer is at least five percent in error when using simple bending theory for beams with a length to diameter ratio of less than three.

This suggests that piles with an effective length in the soil of less than three diameters are likely to require consideration of deviations from the behavior given by simple bending theory. This conclusion is based upon loading of the tip of a cantilever but should provide an indication of the more complex behavior arising from the distributed loading produced during interaction between the pile and soil. Thus, a lower limit to the length of piles, of three diameters, can be suggested for any lateral pile analysis that uses simple bending theory for the pile response.

An expression that Kuhlemeyer fitted to the results of Poulos (1972), appears to be in error since Poulos' original results cannot be reproduced by its use. Instead of the influence coefficient for head deflection due to head shear increasing with increasing length to diameter ratio, it decreases. This is also contrary to the finite element-based equations of Kuhlemeyer, which can be shown to include a term for the length to diameter ratio, when re-expressed in the form necessary for direct comparison with Poulos' results.

Randolph (1977) and (1981), also uses a semi-analytic finite element model to analyses the response of laterally loaded piles in an elastic soil mass. His resulting equations for the response of flexible piles can be expressed in a similar form to Kuhlemeyer's and are in broad agreement. Randolph (1977), has shown that the response of flexible piles in an elastic soil mass is a function of the relative stiffness of the soil and pile and the degree of inhomogeneity of the soil profile.

From dimensional analysis, Randolph has found the form of the expressions for head load deformation characteristics and used the two extremes of a uniform Young's modulus and one that is proportional to depth, to ascertain the correct power relationships. Again, expressions similar to Kuhlemeyer's are found for the uniform soil, but the expressions for the non-uniform profile are necessarily different. Randolph has then proposed expressions that include a non-homogeneity-related term and has checked their accuracy against the finite element results.

Randolph (1981) has presented the results of his finite element study in the form of simple equations that are convenient for design calculations using a small programmable calculator. His design charts allow bending moment, and deflected shape profiles to be calculated for any flexible pile in a wide range of soil Young's modulus profiles. The cornerstone of his presentation method is the pile "critical" length. By non-dimensionalizing, using the critical length, the expressions obtained for head response to head loading of flexible piles are greatly simplified.

Randolph (1977), and Kuhlemeyer (1979a), both use the same concept of results of symmetric, curve-fitted equations of response, based upon finite element studies using the economical semi-analytic model. This illustrates its power versatility in solving problems in geotechnical engineering that can be adequately approximated as being axially symmetric. The benefit of using the finite element method is the lack of difficult-to-verify simplifying assumptions, inherent in the modified Boundary Element method, leading to a confidence in the results that is governed only by the degree of discretization in the finite element mesh used.

While the fully three-dimensional finite element method has been used in a few instances (e.g. Desai and Appel, 1976) it remains an unpopular choice of approach, because of the small size of problem that it can economically solve. A parametric study using three-dimensional finite elements is not feasible, and most applications have been for a particular pile and soil.

From the expectation judgment can be made irrespective of the data and availability of construction material in recent decade before many researches are concerned on the behavior of laterally loaded pile in foundation construction and design principle especially in offshore construction. Even though from beam on elastic foundation design and analysis principle in 19^{th} century especially Winkler (1970) that is replacing soil medium by identical and same elastic spring, this principle ignores the non-linearity of soil behavior.

A study was conducted by Bransby and Springman (1995) in order to evaluate the short-term behavior of piles when subjected to lateral loading occurred by deformation of a clay layer under an adjacent surcharge load, using three-dimensional finite element analysis. The objective of the analysis was to search on the pile-clay interaction behavior.

The geometry modeled in this study was the same geometry modeled in centrifuge tests performed by Bransby (1995) in order to provide a comparison. Piles having 1.27m diameter and 19m length

were embedded in a 6m layer of clay overlying dense sand. There was a 5m distance between the rows and the piles were at a center-center spacing of 6.67m along the row.

Bransby and Springman (1995) concluded that, finite element analysis results were in close agreement with the results obtained from the centrifuge tests. Bending moment profiles were of the same shape with the test data and the magnitudes were close enough. Thus, Bransby and Springman (1995) suggested that, modelling the laterally loaded piles and pile groups using 3D finite element method is very useful both in design and to understand the soil and system behavior.

Another study was performed by Kahyaoglu et al. (2009) using 3D finite element analysis to investigate the behavior of single piles and a group of free-head piles subjected lateral soil movement. A number of numerical analysis was performed in order to figure out the force acting on passive piles with different pile spacing. Effect of pile spacing and the internal friction angle of the moving soil were determined by this parametric study.

Kahyaoglu *et al.* (2009) concluded that results of the analysis performed using Plaxis 3D Foundation and the experiments were in close agreement. As, the pile spacing getting larger, the loads acting on the piles increased. However, for the pile spacing larger than 8D, each pile behaved like an isolated single pile without arching effect. The computer analysis results also showed that as the pile spacing increased the residual load acting on the soil mass between piles increased.

As reported by Poulos and Davis (1980), the first attempts to study the lateral behavior of piles included two-dimensional finite element models in the horizontal plane. Several investigations have attempted to study the behavior of pile under lateral load (Muqtadir *et al*. 1986; Yang *et al*. 2005; and Karthigeyan *et al*., 2006, 2007) using 3D finite element analysis. Since the three-dimensional finite element analyses are widely used now, the analyses of laterally loaded piles are investigated by this approach in this study. The effects of pile shape for both circle and square cross-section on pile response are investigated in addition to the effect of slenderness ratio to explore the response of laterally loaded piles.

Poulos and Davis (1980) informed that the first tries included two-dimensional finite element models in the horizontal plane Baguelin and Frank (1979); general 3D finite element analysis recommended by Desai and Appel (1976), and axis-symmetric geometries by Banerjee and Davis (1978).Some recent work such as Yang and Jeremic (2002) used 3D Finite Element Methods of a laterally loaded pile

driven in layered and uniform soil profiles so that numerically achieve p-y curves and compare them to experimental ones.

Mostafa and EI Naggar (2002), Wang et al. (1998), EI Naggar and Novak (1996), Kagawa (1992), and Poulos and Davis (1980) agreed that using FEM analysis is feasible for the design of large structures only. This is due to the cost of the specialized software, the time needed for non-linear analysis, the time required for model creation, the difficulty in explanation of the result in terms of usual pile (beam) variables, and the un-certainties related with soil non-linear modelling in 3D.

Poulos *et al.* (1996) presented a two-stage analysis involving finite element method and boundary element method. The finite element method was used to evaluate the free-field movements generated by an unsupported excavation without presence of piles, and then these soil movements were used as input into a boundary element program to analyze the pile behavior. The FE program (AVPULL) simulated the plane-strain unsupported excavation, with the soil modeled by eight node iso-parametric finite elements, following Tresca failure criterion. In the boundary element program (PALLAS), the pile was idealized as an elastic beam and the soil as an elastic continuum, but with limiting pressures (P_u) applied to the pile. P_u was assumed to be $9C_u$ (undrained shear strength of the soil). Based on the results of the "standard" problem and parametric studies, a series of design charts were presented for the maximum bending moment and deflection in a single pile. The key factors influencing the pile response of a single pile were found to be excavation depth, soil properties, pile properties and the pile head condition. The limitation of this method is that it cannot apply to pile group with cap.

Given the complexity of nonlinear pile-soil interaction, it would appear that modelling lateral behavior in any way other than with three-dimensional models using nonlinear soil models and interface elements must constitute a compromise. However, consideration of the ratio of pile to soil stiffness, commonly in the region of several orders of magnitude, suggests benefit in viewing pile-soil interaction more from the standpoint of pile behavior. Trochanis *et al.* (1988, 1991a, 1991b), for example, noted that inclusion of their inelastic soil model increased pile deflections but did not change the deflected shape of the pile when plotted relative to the pile length and maximum displacement. The so called normalized deflected shape was considered to depend only on the elastic properties of the pile and soil, and for the case of equal soil properties was controlled

solely by the slenderness ratio of the pile. Well-behaved pile behavior was thus exhibited regardless of the soil behavior crude rudimentary.

Yang and Jeremić (2002), using a three-dimensional finite element model with separation and slippage capabilities, noted similar behavior when modelling lateral response in layered elastic-plastic soils. Two layered-soil cases were considered: One depicting a medium dense sand layer within a soft clay deposit, the other depicting a soft clay layer within a medium dense sand deposit. In both cases the top of the distinct layer was located at a depth of four pile diameters and was four pile diameters in thickness. The top of the pile was unrestrained and loaded horizontally but located above the ground surface so that both moment and horizontal loading applied at the ground line. Under lateral loading the two cases developed significantly different distributions of soil pressures along the pile length, but the pile displacement profiles and pile-head displacements were almost the same.

The influence on the initial stiffness from diameter was investigated by Sorensen et al. (2010), Lesny and Wiemann (2006) by use of numerical modelling. Sorensen et al. (2010) model piles with diameters of 1 to 7 m with an embedment length of 20 m. The shear force was applied to the pile at some height above the soil surface and the relative density (I_d) of the soil was varied between 0.13 and 0.8. The initial stiffness of the *p-y* curves was described by a function of depth, diameter and internal friction angle of the sand, where the combined expression shows a power dependency of each factor.

The modified initial stiffness of the *p-y* curves described by Sorensen *et al.* (2010) was for a location in the North Sea west of Denmark compared to both standard *p-y* curve formulations (API 2007) and a numerical model, Augustesen *et al.* (2010). The analyzed pile was in dense sand and had a diameter of 4 m and an embedment length of 22 m. The conclusion was that the standard *p-y* curves underestimates the stiffness at shallow depth and overestimates the stiffness at large depth, resulting in too stiff pile response. In addition, the *p-y* curves based on the modified initial stiffness was in reasonable concordance with the numerical model.

Lesny and Wiemann (2006) analyzed piles with a diameter of 1 to 6 m and embedment lengths of 10.6 m to 38.9 m. The pile length had been chosen to fulfill a critical embedment length criterion to ensure a rigid fixation in the soil. The objective was to adjust the modulus of subgrade reaction

to ensure a consistent stiffness with the critical embedment length criteria and the numerical model for large diameter piles. The analyses showed that a parabolic function fits the numerical model, and that the function is inversely proportional to the diameter.

Fan and Long (2005) applied a 3D finite element program to investigate the soil response of laterally loaded pile in sand. The influence from pile properties, stiffness and diameter, initial horizontal stress on pile (coefficient of horizontal earth pressure) and soil dilatancy was investigated and the results were compared to existing methods for predicting ultimate capacity. The numerical analyses presented by Fan and Long (2005) showed that the influence from the pile stiffness on the soil response was insignificant whereas the ultimate capacity had a non-linear dependency with pile diameter. In addition, an increased initial horizontal stress gave increased initial stiffness and an apparent increase of ultimate capacity. The soil dilatancy had a significant influence on the soil capacity, with increasing capacity with increasing dilatancy.

Achmus *et al.* (2007) describe the findings of a numerical study of static and cyclic loaded piles with diameters of 7.5 m and an embedment length of 30 m in dense or medium dense sand. The numerical model showed that the stiffness of a large diameter pile subjected to static loading was overestimated by use of the standard *p-y* curves. In addition, the analyses showed that the relative difference to the standard *p-y* curves was independent of the height of the load above the ground line. Based on soil parameters obtained from cyclic triaxial tests an expression for the dependency of the oedo-metric stiffness modulus with number of cycles has been setup and applied to the numerical model. The results of the cyclic numerical models showed an increased displacement with increasing number of cycles, and a tendency that the rate of deformation decreases with increasing density of the sand and with decreasing load height above surface.

Zania and Hededal (2011) presented results of numerical investigations of a 2.0 m pile, in which the focus has been to quantify the effect of pile stiffness and pile-soil friction on the behavior of the pile. The effect of the pile stiffness on ultimate capacity as well as the *p-y* curves was found negligible, as long as the flexibility criteria for a rigid pile were met (criteria defined by e.g. Poulos and Davis (1980)). As expected, increasing interface shear strength increases the distance from the pile toe to the point of zero deflection. Furthermore, the stiffness of the *p-y* curves increased. The finite element analyses described by Zania and Hededal (2011) showed in addition that the ultimate

capacity increased with increasing pile-soil interface strength. The numerical analyses consistently showed higher capacities than predicted by the standard p-y curves. This may be attributed to the negligence of the contribution of side shear resistance to the ultimate capacity when applying the standard curves, and to the inappropriate variation of the normalized ultimate soil resistance with depth.

Consideration of pile curvature is also instructive. Disregarding pile failure and the associated excessive local rotations, the radius of curvature of a pile is large with respect to its diameter. Even in the extreme case of a magnitude 8 earthquake, Margason and Holloway (1977) estimated the radius of curvature to be of the order of 60 m. Given that pile diameters are in the order of one meter, the large ratio of radius of curvature to diameter demands highly continuous horizontal displacements along the length of a pile. Therefore, in terms of behavior along the pile at and in the vicinity of a given depth, practically constant behavior is implied and suggests the possibility of assessing pile-soil interaction in a more local form.

The finite element method (FEM) is a powerful tool in handling soil-pile interaction in a rigorous manner. Various formulations are presently available to model the actual behavior of the soil-pile system, ranging from true non-linear 3D analysis (Faruque and Desai, 1982) to elastic, quasi-3D analysis (Desai, 1977; Kuhlemeyer, 1979; Baguelin et al, 1979; Randolph, 1981). The quasi-3D finite element formulations take advantage of the symmetry of the problem and expand the displacement field in terms of a Fourier series. The latter solution procedure is therefore more economical. During the solution process, the soil-pile system is broken up into elements of finite size. Each element can be assigned unique properties so that non-homogeneous and non-linear soil behavior can be included. Sophisticated stress-strain and strength models can be used to model the soil-pile interface. Structural elements are used to model the pile.

Randolph (1981) presented results of his parametric studies using elastic, quasi-3D finite element modelling in the form of algebraic equations fitted to the solutions. Comparison with solutions from the elastic continuum approach showed good agreements. This is not surprising as both methods model the soil as an elastic material (Poulos and Randolph, 1982; Poulos, 1982). The advantage of the elastic finite element method is that soil non-homogeneity and variation of soil parameters with depth can be considered.

For piles in layered soils under small working loads, although the solutions proposed by Davisson and Gill (1963) and Pise (1982) can be used, they require the soil stiffness to be constant with depth for each layer. This may not sufficiently represent the actual soil profiles, especially when soil stiffness varies with depth. In this paper, a variational approach, which has been successfully used by Shen and Teh (2004) for a laterally loaded single pile in one-layer soil, is employed to numerically solve the problem of a laterally loaded pile in a two-layer soil system using the theory of subgrade reaction. The soil stiffness, which is represented by modulus of subgrade reaction of soils, can be either constant with depth or vary linearly with depth in each layer. The proposed solution can be particularly useful for layered soil conditions, such as for drilled shafts socketed in rock with overburden sand or clay layer. Soil stiffness variation with depth can be more accurately modeled in the proposed solution compared with existing solutions for a layered soil system.

Fan & Long (2005) applied a 3D finite element program to investigate the soil response of laterally loaded pile in sand. The influence from pile properties, stiffness and diameter, initial horizontal stress on pile (coefficient of horizontal earth pressure) and soil dilatancy was investigated and the results were compared to existing methods for predicting ultimate capacity. The numerical analyses presented by Fan & Long (2005) showed that the influence from the pile stiffness on the soil response was insignificant whereas the ultimate capacity had a non-linear dependency with pile diameter. In addition, an increased initial horizontal stress gave increased initial stiffness and an apparent increase of ultimate capacity. The soil dilatancy had a significant influence on the soil capacity, with increasing capacity with increasing dilatancy.

Yang and Jeremi´c (2002) conducted numerical analyses using finite element method on single laterally loaded pile in elastic-plastic soil model. Pile behavior was tested in uniform sand, clay and layered soil deposits. Based on the results obtained from numerical analysis authors developed *p-y* curves and compared them with *p-y* curves obtained by McVay *et al.* (1995) and Reese *et al.* (1974). Pile was modeled to be made of aluminum, squared shape with 0.429 m in width and about 12 m long with 11.3 m embedded in the soil. The authors concluded that the use of three-dimensional finite element model, with the use of very simple constitutive soil model can give good approximation of laterally loaded pile behavior.

2.5 Ultimate Lateral Resistance

Structures on pile foundations may be subjected to lateral forces and movements as a result of ship impact and wave action in harbor and offshore structures, retaining walls, high wind forces in transmission-tower foundations, and lateral accelerations acting on structures in earthquake zones. Therefore, one key issue for pile design may be estimation of the ultimate lateral resistance. Various methods have been proposed to estimate the ultimate lateral load capacity H_u (Hansen, 1961; Broms,1964; Petrasovits and Award, 1972; Prasad and Chari, 1999 and Zhang et a1., 2005).

One of the most popular methods for estimating H_u is Broms' method (Lee et al., 2010). For unrestrained or free-headed piles, Broms (1964) assumed that the ultimate soil resistance is equal to three times the passive Rankine earth pressure (Poulos and Davis, 1980).

There are many different definitions regarding the ultimate pile capacity either from deflection or from load point view. It can be determined based on the excessive lateral displacement of the pile head or the rotation of the pile (Hu, et al. 2006). According to Sawwaf (2006), the ultimate lateral capacities can be defined as the loads corresponding to the lateral displacements at the pile head equal to around 10% of the diameter of the pile. As stated by Dickin and Nazir (1999), it can also be obtained from the p-y curve as the point where the curve turns into linear or considerably linear. It can also be defined as the maximum load from the p-y curve when the load cannot be increased with deflection. In the Helmer's field test in Virginia, in order to avoid additional deflection, loading has been terminated once the tests reached desired deflections.

A horizontal load test was carried out on a pile consists of placing two piles at some distance from each other and either pulling them toward each other or pushing them apart. The resulting load displacement curve for one pile gives the horizontal load H_o versus the horizontal displacement y_o (Figure 2.10). From this curve, an ultimate load H_{ou} can be defined as the horizontal load H_o corresponding to a displacement equal to one-tenth of the pile diameter (B/10) (Briaud, 1997).

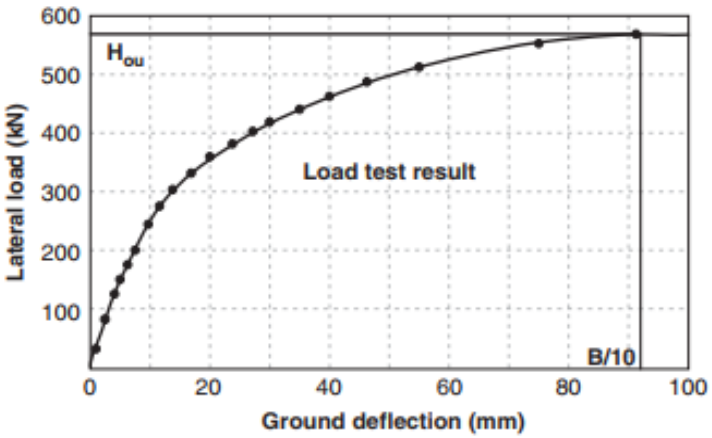

Figure 2.10 Load test result (Briaud 1997)

Also, in finite element method the control factor in evaluating the ultimate lateral load capacity of the piles is the yield of the maximum allowed lateral displacement at the pile head which is taken to be *10%* of the pile diameter as it is more compliant with the design criterion (ASTM STP-835, 1983 and USACE, 1998).

According to British Standard as recommended in BS EN 1997-1:2004+A1:2013, 7.6.1.1(3), the ultimate horizontal load measured at deflection equal to *10%* of the pile's diameter when it is difficult to define the ultimate limit state from the loading deflection curve.

2.6 Constitutive Models

Soil is a complicated material that behaves non-linearly and often shows anisotropic and time dependent behavior when subjected to stresses. Generally, soil behaves differently in primary loading, unloading and reloading. It exhibits non-linear behavior well below the failure condition with stress dependent stiffness. Soil undergoes plastic deformation and is inconsistent in dilatancy and also experiences small strain stiffness at very low strains and upon stress reversal. In addition to soil behavior, its failure in three-dimensional state of stress is extremely complicated. Numerous criteria have been devised to explain the condition for failure of a material under such loading state.

Currently, various constitutive models for the soil have been developed. These models cover a wide range of soil features such as anisotropy, cyclic loading, creep etc. The selection of a constitutive model for a geotechnical application depends on the mechanical properties of the soil.

(i.e. permeability, stiffness and strength), previous history on the mechanical properties of the soil and the stress changes that will occur in feature (Wood, D., Muir., 1990).

In the finite element analysis, reliable predictions can be achieved by using an appropriate constitutive model for a particular geotechnical problem. In general, the criterion for the soil model evaluation should always be a balance between the requirements from the continuum mechanics aspect, the requirements of realistic representation of soil behavior from the laboratory testing aspect, convenience of parameter derivation and simplicity in computational application. The application of some constitutive models in Plaxis finite element model are briefly discussed below used for this study.

2.6.1 Linear Elastic Model

The use of the linear elastic model is quite common to model massive structures in the soil or bedrock layers that include piles and so on (Brinkgreve, R.B.J. & Broere, W., 2006). This model represents Hooke's law of isotropic linear elasticity used for modelling the stress–strain relationship of the pile material. Linear elastic constitutive model is probably the most common model used to approximate the stress-strain relationship of materials. Linear elastic models involve two elastic stiffness parameters namely Young's modulus (E) and Poisson's ratio (ν). The linear elastic model is not suitable to model soil because soil behaviour is highly nonlinear and irreversible, but it is appropriate to model stiff volumes in soil like concrete structures.

2.6.2 Mohr Coulomb Model

The Mohr Coulomb Model is a linear elastic and perfectly plastic model. It involves five parameters, both elastic and plastic behavior parameters i.e. Young's modulus (E) and Poisson's ratio (ν) for soil elasticity, friction angle (ϕ) and cohesion (c), for soil plasticity and the dilatancy angle (ψ).

The stiffness behavior below the failure line is assumed to be linear elastic according to Hook's law. Hence, the model does not accurately predict deformation behavior before failure, especially in situation where the stress levels are changing or multiple different stresses paths are allowed. However, the model does not show softening behavior after peak strength. Soft soils like normally consolidated clays, generally show a decreasing mean effective stress during undrained shearing,

whereas the Mohr-Coulomb's model would predict a constant mean effective stress in this case, which results in an over prediction of the shear strength (Plaxis 3D Foundation Manual, 2004).

The soil in the problems of this paper is modeled as elasto-plastic material. The basic principle of elasto-plasticity is that strains and strain rates are decomposed into an elastic part and plastic part as shown in Figure 2.11.

Hooke's law is used to relate the stress rates to the elastic strain rates. According to the classical theory of plasticity, plastic strain rates are proportional to the derivative of the yield function with respect to the stresses. This means that the plastic strain rates can be represented as vectors perpendicular to the yield surface. This classical form of the theory is referred to as associated plasticity. However, for Mohr-Coulomb type yield functions, the theory of associated plasticity overestimates dilatancy (Plaxis 3D Foundation Manual, 2004).

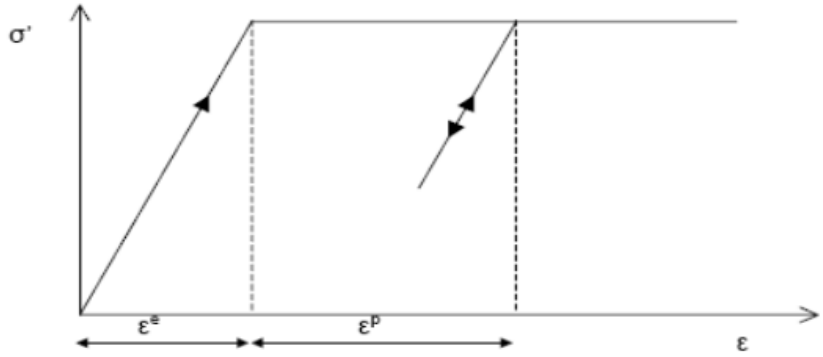

Figure 2.11 Basic idea of an elastic perfectly plastic model

The Mohr-Coulomb yield condition is an extension of Coulomb's friction law to general states of stress. In fact, this condition ensures that Coulomb's friction law is obeyed in any plane within a material element. The full Mohr-Coulomb yield condition consists of six yield functions when formulated in terms of principal stresses and six plastic potential functions (Plaxis 3D Foundation Manual, 2004).

The two plastic model parameters appearing in the yield functions are the well-known friction angle ϕ and the cohesion c. The condition f_i=0 for all yield functions together (where f_i is used to

denote each individual yield function) represent a hexagonal cone principal stress space as shown in the Figure 2.12.

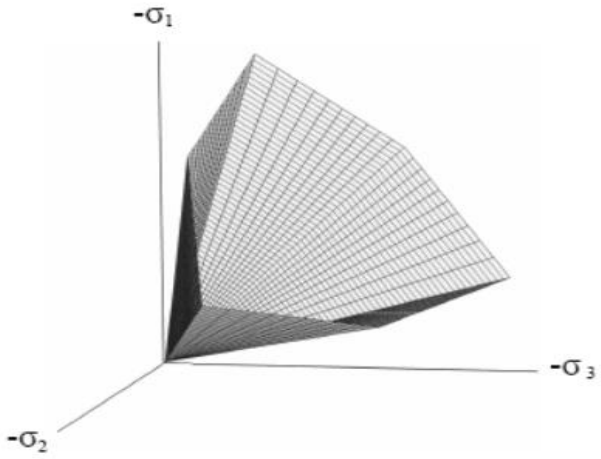

Figure 2.12 The Mohr-Coulomb yield surface in principal stress space (c = 0)

The plastic potential functions contain a third plasticity parameter, the dilatancy angle ψ. This parameter is required to model positive plastic volumetric strain increments (dilatancy) as actually observed for dense soils. For stress states within the yield surface, the behavior is elastic and obeys Hooke's law isotropic linear elasticity, as discussed above (Plaxis 3D Foundation Manual, 2004).

CHAPTER 3 : NUMERICAL MODELLING

3.1 Introduction

In this study, numerical modelling was used to investigate behaviour of laterally loaded piles embedded in layered soils of Addis Ababa. Verification of the study with full-scale lateral load tests result from the literature was used to control the accuracy of the numerical model results. After verification of finite element analysis solution, a parametric study has been conducted (chapter-4). Variations in the factors such as the embedment depth of the pile, pile diameter, and site condition were studied. Three-dimensional geotechnical finite element package Plaxis 3D Foundation was used in all analyses for this purpose. In this chapter properties and main functions of the 3D finite element methodology were presented briefly for better understanding of the model designs.

3.2 Introduction to Plaxis 3D Foundation

Plaxis 3D Foundation is a three-dimensional finite element program used to perform deformation and stability analysis for various types of geotechnical structures such as foundations, anchors and sheet piles. The program uses a convenient graphical user interface that enables users to generate a geometry model and a finite element mesh quickly and easily. Plaxis 3D Foundation is an implicit element solver relating forces and displacements by demanding equilibrium in every point in the model.

The generation of a three-dimensional finite element model is based on the model geometry such as volumes, surfaces, lines and points. To create the soil stratigraphy different boreholes can be defined. Boreholes are locations in the drawn area at which the information on the position of soil layers and the water table is given. The program will interpolate the soil layer position between each borehole.

The sign convention used by Plaxis 3D Foundation was based on the Cartesian coordinate system as shown in Figure 3.1.

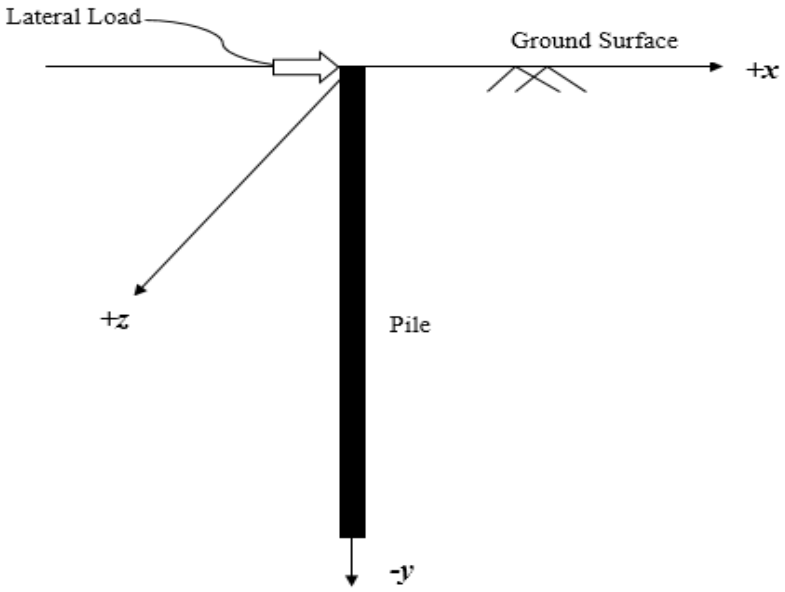

Figure 3.1 General three-dimensional coordinate system and sign convention for the model

The creation of the model basically consists of two parts, generation of the model and calculation phase. The model geometry is a composition of boreholes and work planes. Only one borehole is created in the numerical modelling, as no information on the soil stratigraphy at the site is available, i.e. the soil layers are assumed to be horizontal and homogenous. The work planes are used in order to define loads and structures at different vertical levels. Soil and material properties can be added using material library in Plaxis 3D Foundation, where standards values of the material properties of construction materials can be found. For these numerical approaches, the soil material is assignment depending on the soil properties obtained from correlation of different parameters using SPT-N values, UCS and triaxial tests obtained from the geotechnical laboratory and field tests.

Plaxis 3D Foundation consists of two parts which are input and output program. Input program is used for the definition of the model and assignment of analysis properties. At the beginning of the input program, project properties are asked from the user. Model boundaries in two horizontal directions (x and z) and unit system used in analyses are defined in this part. Input program includes five main components that are soil, structures, mesh, water levels and staged construction. In soil mode, soil stratigraphy is assigned to the model by creating boreholes. In addition, ground water level of a specific point is defined also with boreholes. Multiple boreholes can be defined in any

number at any point. Work planes are horizontal planes with different y-coordinates that show the top view of the model geometry. They were used to draw, activate and deactivate the structural elements and loads. Each work-plane holds the same geometry lines but vertical distance between them may vary. Within work-planes, points, line sand clusters were used to describe a 2D geometry model.

Plaxis 3D Foundation interpolates layer thicknesses and ground water levels that were assigned in every borehole. Desired non-uniform three-dimensional soil profiles and water level can be obtained with this way. In structures mode, all kinds of geometric entities, structural elements and their configurations were assigned. In addition, boundary conditions; predefined displacement or loading of a point, line or a surface can be defined in this part. Both soil and structure modes include material sets option which was used for the definition of material properties of soil and structural elements. In mesh mode, geometry was divided into mesh elements with desired amount of fineness.

Plaxis 3D Foundation has five default mesh element distributions. These are very coarse, coarse, medium, fine and very fine mesh generations. In addition, desired amount of local fineness of a specific volume or geometric entity can be achieved with fineness factor option. In water levels mode, water levels outside of the model can be defined for the simulation of external water pressures. Additionally, it can be used as phreatic level for partially saturated soils. After finalization of all geometric entries, calculation stages were arranged in staged construction mode according to the purpose of the analysis. All geometric elements can be activated or deactivated for every stage. Besides, analysis properties of each stage such as calculation type, maximum number of iteration and error tolerance can be defined separately. After setup of all stages, analysis can be conducted.

Plaxis 3D Foundation provides extensive ways for the documentation of the analysis results. Output program was presented all numerical analysis results in variety of forms including curves, diagrams and tables. It mainly consists of the results of deformations and stresses. In addition, force results are presented for structural elements. This chapter is devoted to introduce the details of constitutive models, material properties, and finite element modelling used in the performed parametric study.

3.3 Generation of the Model

3.3.1 Model Geometry

In this part of the research, numerical modelling was conducted on a single pile in layered soil by using Plaxis 3D Foundation FEM package. The pile was modeled using an embedded pile model available in Plaxis 3D Foundation. The model geometry depends on both the diameter of pile and its length. The soil is layered in each site, and the cross section of the soil block was pre-defined in the model tab on the project properties window. Based on the pile geometry, the limits of the soil contour were defined as the x_{min}, x_{max} and z_{min}, z_{max}. The depth (y-axis) was applied using the "create borehole" button, in this function groundwater table level can also be selected. The top boundary of the soil layer is at y = 0, and the bottom boundary of the soil layer is a function of pile diameter and its length. Once the soil block was drawn, the soil properties can be assigned to it.

According to Karthigeyan *et al.* (2006 and 2007) for static lateral load condition, the soil mass dimension depends on the pile diameter and length. The width of soil mass was taken as 40D, in which, D is the pile diameter or pile width. The soil mass effect on the pile response is diminishing for the width more than 40D. The height of soil mass was taken as L+20D, in which, L is the length of pile as shown in Figure 3.2.

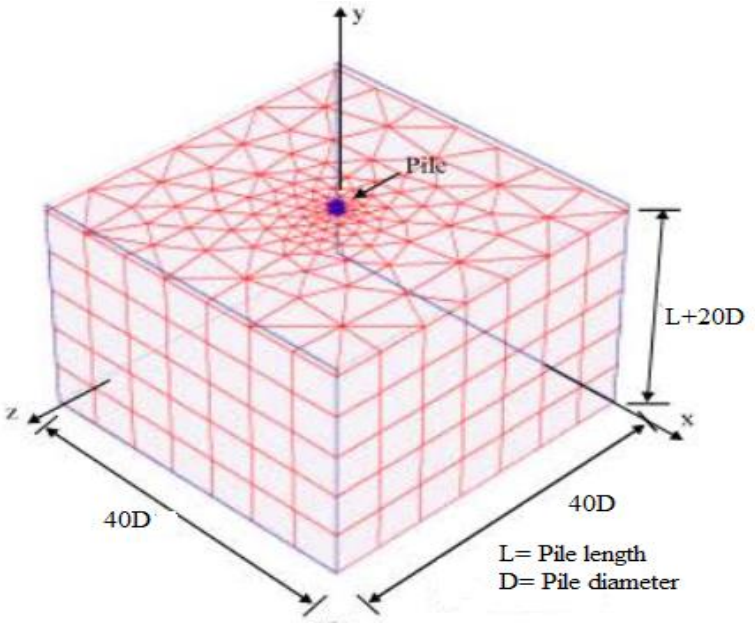

Figure 3.2 Model geometry, Karthigeyan *et al.* (2006 and 2007)

Table 3.1 3D FEM model dimensions (design of experiments)

Embedded pile length L(m)	Pile diameter D (m)	Width of soil mass along X (m)	Length of soil mass along Z (m)	Height of soil mass along Y (m)
24	0.65	26	26	37
	0.9	36	36	42
	1.15	46	46	47
	1.4	56	56	52
27	0.65	26	26	40
	0.9	36	36	45
	1.15	46	46	50
	1.4	56	56	55
30	0.65	26	26	43
	0.9	36	36	48
	1.15	46	46	53
	1.4	56	56	58
33	0.65	26	26	46
	0.9	36	36	51
	1.15	46	46	56
	1.4	56	56	61

3.3.2 Model Properties

Finite element analysis software Plaxis 3D Foundation was used for the investigation of the behavior of laterally loaded pile. In order to carry out a parametric study, other properties should be kept constant while the effect of the change in a certain property was being investigated. Therefore, the interpretation of parametric study results can be more complex, since the effect of several factors will interfere with each other. In addition, real laterally loaded pile model with all external boundaries will require much more 3D mesh elements which cause longer calculation times.

Embedded pile option in Plaxis 3D Foundation was used to model the vertical pile and its properties in all analyses. This option was given the opportunity of modelling piles as structural members with a definite rigidity and mechanical properties.

Before systematically investigating the factors affecting the pile-soil interaction behavior, the boundary size, surface fixity conditions and mesh generation effects were studied as it is necessary in order to establish correct geometry and model of the problem.

3.3.3 Model Boundary Fixities

The boundaries of the soil in the model must be constrained in the vertical and lateral directions where the displacement of the soil due to the lateral load is negligible. In order to minimize the boundary effects in the model many authors suggested different locations of these boundaries. The horizontal length extent of 40D (40 times of the pile diameter) and vertical depth extent of L+20D (length of a pile plus 20 times diameter of a pile) is sufficient after which no appreciable stress and strain variation effect was observed by Karthigeyan *et al.* (2006 and 2007).

Therefore, boundaries of the model were placed at sufficient distances from the pile so that the influence of the boundaries on the deformations of the pile is minimized. Three separate boundary conditions were imposed onto the model. Nodes on both lateral boundaries of the model were fixed against horizontal movement ($u_x = u_z = 0$), yet free to move in the horizontal direction. Meanwhile, nodes on the bottom boundary of the model were fixed against all directions ($u_x = u_y = u_z = 0$), whereas the top boundary was free to move in all directions.

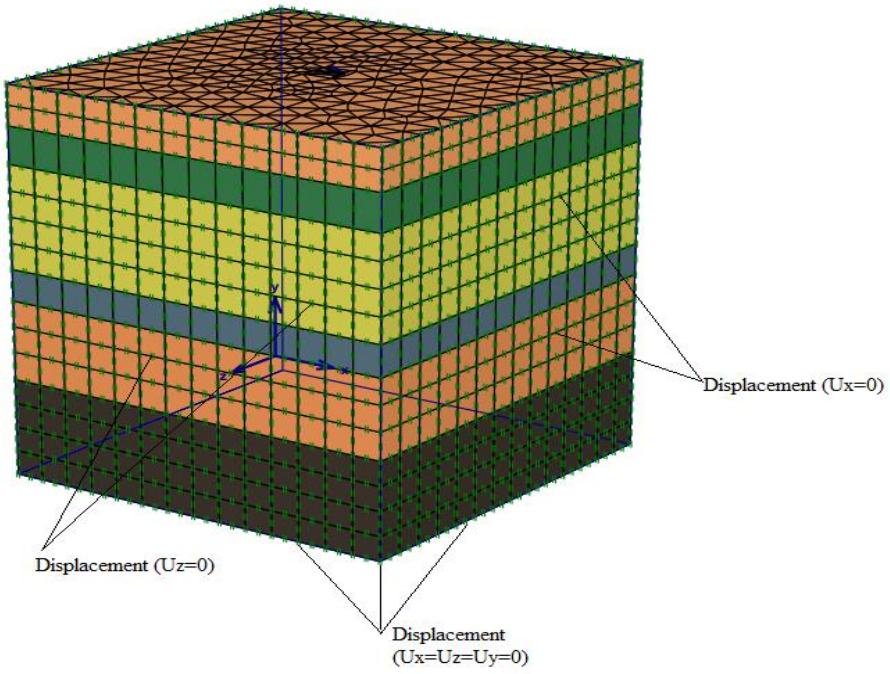

Figure 3.3 Boundary conditions

It is desirable to select the size/geometry of the model large enough so that boundaries are far away from the area where we are making calculations, and that stress-strain distributions in the soil are not affected from the geometrical constraints near the boundaries. However, long calculation times in three dimensional analyses make this procedure inefficient.

Therefore, the size/geometry of the model and distance to the boundaries were studied to determine the optimum dimensions sufficient for an accurate model. The deflections in the soil were investigated as a result of pile resistance are not affected or interrupted because of the model boundaries.

3.3.4 Mesh Generation

In order to perform the finite element calculations, the geometry has to be divided into elements. A composition of finite elements is called a finite element mesh. The basic soil elements of a 3D finite element mesh were represented by the 15-node wedge elements. These elements were generated from the 6-node triangular elements. The 15-node wedge element was composed of 6-node triangles in horizontal direction and 8-node quadrilaterals in vertical direction.

The model was meshed using the automatic mesh generation tool in Plaxis 3D Foundation. The element was provided a second-order interpolation of displacements as shown in Figure 3.4. Plaxis 3D Foundation uses three local coordinates (ξ, η, ζ), the shape functions have the property that the function value is equal to unity at node *i*, and zero at the other nodes. This type of element has three translational degrees of freedom in each node and is generated from 6 nodes triangular wedge elements, suitable for a two-dimensional mesh.

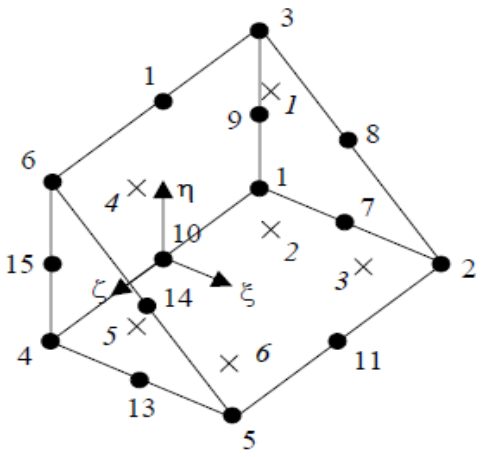

Figure 3.4 Local numbering and positioning of nodes (•) and integration points (x) of a 10-node wedge element in Plaxis 3D Foundation (Plaxis 3D Foundation Manual, 2006)

Typical 2D and 3D meshes used in this study were presented in Figure 3.5 and Figure 3.6, respectively. The mesh element size can be adjusted by using a general mesh size varying from very coarse to very fine and also by using line, cluster and point refinements. Very fines mesh should be avoided in order to reduce the number of elements, thus to reduce the memory consumption and calculation time. The program does not allow entering a new structural element or a new soil cluster after the mesh was generated. If a new element or cluster was added to the geometry model, the mesh generation should be repeated with the new input.

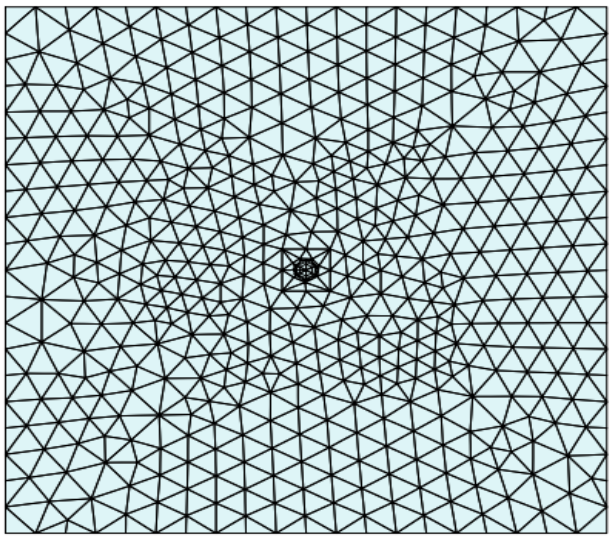

Figure 3.5 Mesh generation of the cross section of a typical 2D FE model

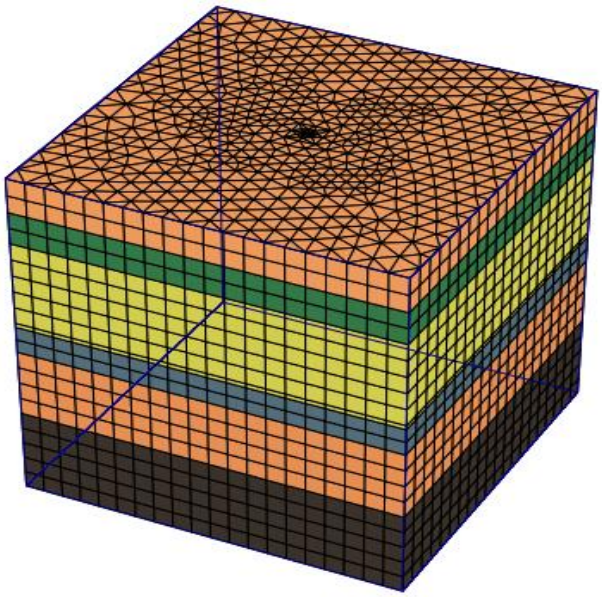

Figure 3.6 Mesh generation of a typical 3D FE model

3D finite element mesh was composed of elements, nodes and stress points. While generating the mesh, the geometry was divided into 15-node wedge elements. As mentioned before, these elements were composed of the 6-node triangles in x-z direction, as generated by 2D mesh generation. Moreover, 8-node quadrilateral faces were generated in y-direction.

3.3.5 Sensitivity Analysis

As mentioned above, in the finite element calculations, the model has to be divided into elements which compose the "finite element mesh". The finite element mesh size will possibly influence the results. To investigate the influence of number of elements or mesh coarseness on the behaviour of laterally loaded pile foundation, five different finite element meshes were performed. These were done by varying their number and sizes keeping material properties and all other parameters constant. For this purpose, a horizontal load of 250kN was applied at the pile head. The generated number of elements and the head deflection of a pile is given in Table 3.2.

Table 3.2 Influence of mesh size on head deflection

Model	Mesh Coarseness	Number of elements	Head deflection (mm)
1	Very Coarse	1062	5.70
2	Coarse	1740	5.96
3	Medium	3484	6.01
4	Fine	7686	6.13
5	Very Fine	27552	6.16

Figure 3.8 shows the influence of mesh density on the head deflection of the pile. As shown from this figure head deflection is increases with increases number of elements till the number of elements reach 7686, after that an increasing in number of elements has no significant effect on the head deflection of pile. It can be said that mesh is converged with 7686 elements because there is no significant change in deflection when the number of elements increased to 27552. Therefore model 4 (fine mesh) was used to investigate the general behaviour of the laterally loaded pile foundation.

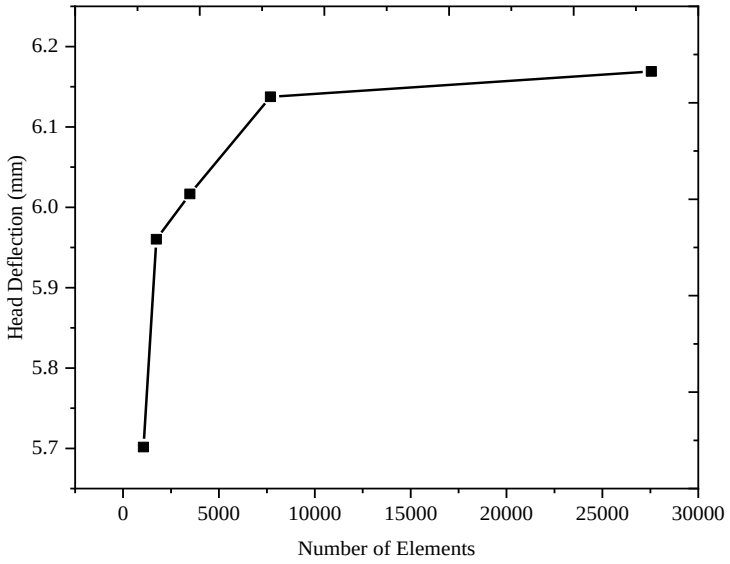

Figure 3.7 Influence of mesh density on head deflection of the laterally loaded pile

3.3.6 Calculation Process

At this phase the construction of the model and loads applied were staged. The first phase is the initial phase, where the initial stresses in the soil are computed using the K_o- procedure. In this procedure the initial vertical stresses were computed using submerged soil unit weight. Then, related horizontal stresses were computed using the coefficient of lateral earth pressure at rest $K_o \cong 1-\sin\phi$, assuming normally consolidated soil.

Following the initial phase, a second phase called the installation phase was initiated. In the installation phase the pile foundation was constructed, the pile and interface surfaces were activated. Afterwards, the lateral load was applied at the ground surface of the top head of the pile. The load was applied using same intervals of load, and each interval corresponds to a different phase. The calculation phase was staged in this order, because the displacements were reset to zero after the initial stresses have been calculated and the foundation has been installed. This was done to calculate the lateral deflections, bending moments and shear forces created by the applied loads.

The staging is summarized below:

1. Calculation of initial stresses using the K_0 - procedure.
2. The interface is activated and the pile was installed.
3. The horizontal load was applied in different phases corresponding to increments of load.

A calculation process in Plaxis 3D Foundation was divided into calculation phases. In each calculation phase, a number of calculation steps are needed since the non-linear behaviour of the soil requires loadings in small proportions (load steps) as shown in Figure 3.8.

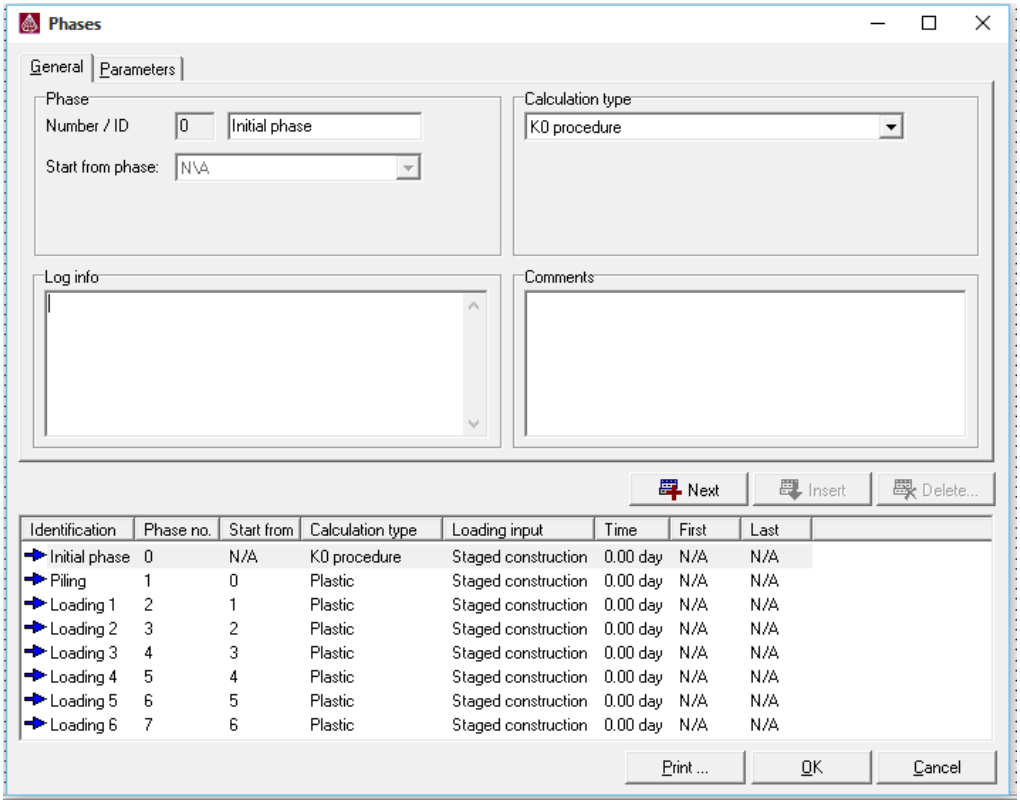

Figure 3.8 Calculation phases in Plaxis 3D Foundation

3.3.7 Interface Element

In order to achieve a good relationship between the pile structure and the soil volume, an interface was created. Interfaces were joint elements to be added to the surfaces to allow for a proper modelling of soil-structure interaction. Interfaces were used to simulate the contact between a plate (from the pile structure surfaces) and the surrounding soil. An interface can be created next to the plate or geogrid elements or between two soil volumes. In the model the interface was created next to the pile plates. The thickness of the interface was zero, which means that the pair of nodes were located with the same coordinates. The interface consists of 16 nodes quadrilateral shaped elements. Interface elements are numerically integrated using 3 Gauss integration points. Figure 3.9 shows the position of the nodes and integration points.

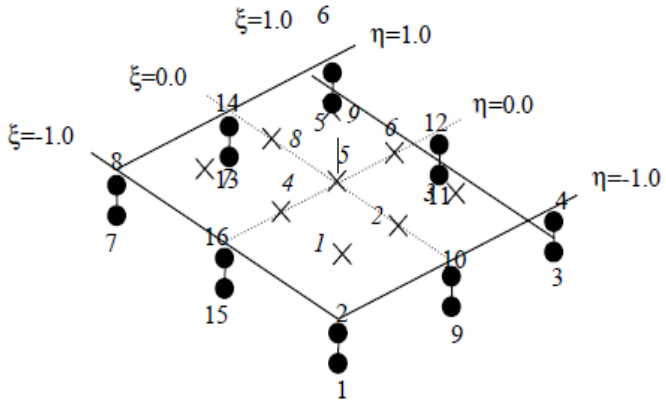

Figure 3.9 Local numbering and positioning of nodes (Σ) and integration points (x) of a 16-node interface element (Plaxis 3D Foundation Manual, 2006)

The interface elements have pairs of nodes instead of single nodes. The distance between the two nodes of a node pair is zero. The aim of these interface nodes is to allow for differential displacements between the node pairs slipping and gapping.

The interface stiffness and strength can be defined depending on the kind of analysis, and it is controlled by the parameter R_{inter}. A rigid interface, perfectly rough soil-structure, is used when the interface should not have a reduced strength with respect to the strength of the surrounding soil. The strength of these interfaces was assigned as rigid (which corresponds to $R_{inter} = 1.0$). It behaves as an element with the same material properties as the adjacent soil element. In thin layer element method, the contact between structure and soil was described as perfectly rough. The material behaviour in the contact area (the thin element) was simulated by the material behaviour of the soil (Table 3.3, Table 3.4 and Table 3.5).

The following rules are applied to calculate the interface properties from the soil properties in the related data set and value of R_{inter}.

$$c_{inter} = c_{soil} \qquad (3.1)$$

$$\tan\phi_{inter} = \tan\phi_{soil} \qquad (3.2)$$

Where: c_{inter} - Cohesion of the interface

c_{soil} - Cohesion of the soil

ϕ_{inter} - Interface friction angle

ϕ_{soil} - Soil friction angle

3.4 Selection of an Appropriate Constitutive Model and Input Parameters

3.4.1 Constitutive Model

Based on the data collected from AAICEC (site-I), CBE Head Quarter (site-II) and Mixed Used Building (site-III) in Addis Ababa, the parameters are not elastic in behavior. Their inelastic behavior under static loading can be described by elasto-plastic constitutive model. According to the constitutive model options available in Plaxis 3D Foundation, Mohr-Coloumb's soil model was used for static analysis. Although it is well known that, the more advanced soil constitutive models can capture the nonlinear stress-strain behavior of soils more accurately, they also require significant number of material model parameters to be input. Therefore Mohr-Coulomb model was considered to be adequate for the content of this study. And the reinforced concrete pile was modeled as linear elastic material in this study.

3.4.2 Soil and Material Parameters

For this study, three sites were considered as study areas located in Addis Ababa, Ethiopia. This are:

I. Addis Africa International Convention and Exhibition Centre (AAICEC) - *Site-I*

The project site is located in Addis Ababa, Bole Sub-City, around CMC. The project site is characterized by flat topography with an average elevation of 2402 m a.s.l.

II. New Headquarter Building Commercial Bank of Ethiopia (CBE) - *Site-II*

The New Headquarter Building Commercial Bank of Ethiopia (CBE) project is located in central Addis Ababa, Kirkos sub city, around the national theatre.

III. Mixed Use Building project- *Site - III*

The project site is located in Addis Ababa, Kirkos sub city around Bulgaria roundabout.

3.4.2.1 Determination of basic soil parameter for the numerical model

Some of the soil parameters used for the analysis of the foundation were obtained from geotechnical reports; however, some necessary data were not included in the investigation report. Therefore, the parameters which could not be obtained directly from the laboratory tests, have been indirectly derived by using empirical correlations based on the recommendations of different literature, international geotechnical codes and standards. The data used for this study can be categorized in the following group;

1) Stiffness parameters; modulus of elasticity (Es) and Poisson's ratio (ν)
2) Shear strength parameters; angle of internal friction(ϕ) and soil cohesion(c)
3) Unit weight or density of the soil (γ): saturated unit weight (γ_{sat}) and unsaturated unit weight (γ_{unsat})

1) Stiffness parameters

a) Young's Modulus of Elasticity, E_s

The stiffness modulus E_s is a basic parameter that describes the load-deformation behaviour of soils and governs the results of deformation related problems. Several methods are available for estimating the stiffness modulus of a soil as described by (Bowles, 1996). Unconfined compression tests, tri-axial compression tests and in situ tests are among the test methods. The geotechnical investigation reports have included stiffness modulus of values for the different layers but some of them were not conducted. Elastic modulus of the completely weathered rock was taken from literature recommendations given by (Gu, 2008). After the modulus elasticity (Es) is determined from correlation, which is used as input value in Plaxis 3D Foundation software. The SPT based soil and rock classification systems are given Appendix A, Table A.1. Typical values of Young's modulus for granular and cohesive materials according to USCS are given in Table A.2 and Table A.3, respectively in the Appendix-A.

b) **Poisson's Ratio,** ν

Poisson's ratio is property of materials that describes volume change of the material in a direction perpendicular to application of a load. It is defined as the ratio of the lateral expansion to the axial compression of soils. (Bowles 1996) recommend a range of values of Poison's ratio between 0.4 and 0.5 for most clay and 0.2 to 0.4 for medium to dense cohesion less soil. In this research, the value of poison's ratio for each layer of ground condition was obtained from typical values from different literatures. And the typical values of Poisson's ratio for soils and other materials according to Bowls are given in Table A.4, in the Appendix-A.

2) Shear Strength Parameter

Shear strength parameters, namely, angle of internal friction (ϕ) and cohesion (c) are taken from literature recommendation given by (Braiud 2013). According to Bowls (1977), PI and SPT-N can be used to estimate the angle of internal friction (ϕ) and unconfined compressive strength of cohesive soils (q_u) respectively.

3) Unit weight or density of the soil

The Soil density is another soil property that the software takes as in put data. Therefore, the saturated unit weight and unsaturated unit weight of all layers was taken from the investigation report and taking typical values from the literature.

Geotechnical properties of both soil and rock materials used for input parameters of FEM software are presented in Table 3.3, Table 3.4 and Table 3.5 for site-I, site-II and site-III respectively. Further, the material properties from the empirical correlation and typical parameter values of soils and rocks were used to determine the composite properties of materials by combining the Young's modulus and Poisson's ratio. Tables 3.6 summarize the engineering properties of the piles.

Table 3.3 Geotechnical properties of Addis Africa International Convention and Exhibition Share Company Building Site (Site-I)

Strata Description	Elevation (m)	E (MPa)	ν	γ_{unsat} (kN/m^3)	γ_{sat} (kN/m^3)	c (MPa)	ϕ (°)
Medium stiff to stiff, highly plastic clay soil	5.5	20	0.3	18	20	0.04	6
Slightly to moderately weathered ignimbrite rock	10.6	300	0.27	20	22	0.03	41
Medium stiff to very stiff clayey silt soil	24.7	15	0.3	17	19.5	0.03	5
Moderately weathered vesicular basalt rock	29	1000	0.26	22.5	24	5	42
Very stiff clayey silt soil	39.8	25	0.3	17	19.5	0.03	5
Slightly to moderately weathered basalt rock	53	1200	0.26	23	26	5	45

Table 3.4 Geotechnical properties of CBE Head Quarter Building Site (Site-II)

Strata Description	Elevation (m)	E (MPa)	ν	γ_{unsat} (kN/m^3)	γ_{sat} (kN/m^3)	c (MPa)	ϕ (°)
Soft organic silty clay soil	4	12	0.3	16.5	18	0.028	5
Silty clay soil	6.6	13	0.3	17	19.5	0.03	6
Highly weathered basalt rock	8.8	400	0.27	20	22.5	0.03	42
Medium strong, slightly to moderately weathered basalt rock	15	1000	0.26	22	24	5	42
Silty clay soil	18.2	13	0.3	17	19.5	0.03	6
Stiff, sandy clayey silt soil	21	12	0.3	15	18.5	0	28
Highly weathered s*coriaceous* (Scoria) rock	25.5	300	0.27	20	22.5	0.03	42
Moderately weathered basalt rock	39	1000	0.27	22	24	5	42
Stiff, swelling clayey silt soil	45	14	0.3	17	19.5	0.03	5
Moderately weathered basalt rock	52	1000	0.27	22	24	5	42
Strong slightly fractured, fresh to faintly weathered basalt rock	61	1500	0.19	26	28	5	45
Moderately weathered basalt rock	75	1000	0.26	22	24	5	42
Strong slightly fractured, fresh to faintly weathered basalt rock	83	1500	0.19	26	28	5	45

Table 3.5 Geotechnical properties of Mixed-Used Building Project Site (Site-III)

Strata Description	Elevation (m)	E (MPa)	ν	γ_{unsat} (kN/m^3)	γ_{sat} (kN/m^3)	c (MPa)	ϕ (°)
Backfill	0.45	12	0.3	16	18.5	0.015	28
Medium stiff clayey silt soil;	4.4	13	0.3	17	19.5	0.03	5
Moderately weathered, moderately jointed ignimbrite rock;	7.4	300	0.27	20	22	0.03	42
Loose to dense silty sand	14.5	25	0.3	18	20	0.005	32
Silty gravel soil;	16	100	0.28	19	21	0	33
Moderately to highly weathered basalt rock;	22.5	1000	0.24	22.5	24	5	42
Slightly to moderately weathered basalt rock;	40.3	1200	0.26	23	26	5	45
Very stiff to hard sandy SILT soil.	50	15	0.3	16	19.5	0.012	28

The average location of ground water table for site-I, Site-II and Site-III was 6 m, 5.5 m and 5 m respectively.

3.4.2.2 Parameters of reinforced concrete circular pile used for the model

The actual length and diameter of the piles used for parametric study were obtained from foundation recommendation report of site-I and the engineering properties of the reinforced concrete is taken from Ethiopian Building Code of Standard (EBCS).

Table 3.6 Pile Parameters

Parameter	Symbol	Pile-1	Pile-2	Pile-3	Pile-4	Unit
Material	-	Concrete	Concrete	Concrete	Concrete	-
Modulus of elasticity	E	30	30	30	30	GPa
Poisson's ratio	ν	0.15	0.15	0.15	0.15	-
Unit weight	γ	25	25	25	25	kN/m^3
Length	L	24	27	30	33	m

Table 3.7 Variation of pile diameter

Pile length L(m)	Pile diameter D(m)
24	0.65 0.9 1.15 1.4
27	0.65 0.9 1.15 1.4
30	0.65 0.9 1.15 1.4
33	0.65 0.9 1.15 1.4

3.5 Validation of Numerical Model

The finite element approach was used in this study to investigate the behaviour of pile when subjected to lateral loads. This section assesses the accuracy of the finite element approach in analyzing laterally loaded piles and to verify certain details of the finite element such as pile displacement. According to literature, there are number of published cases of full-scale lateral pile response subjected to lateral loads. Thus, it deals with a full-scale laterally loaded pile (Ismael, 1998) to make a comparison with present study of laterally loaded piles. For the case of laterally loaded piles embedded in layered medium some assumptions are made due to the inaccuracy of soil data obtained from the site and laboratory.

This section used to assess the accuracy of the finite element approach in analyzing laterally loaded piles and to verify certain details of the finite element such as pile displacement. Verification example was worked out to compare the result obtained by finite element analysis to those obtained from experimental study. The comparative case includes full-scale lateral load tests reported by (Ismael, 1998). The results of laboratory and field tests are used to identify the soil profiles and soil properties that are well instrumented.

Table 3.8 Geotechnical properties of the soil layer

Parameters	Name	Medium dense cemented silty sand layer	Medium dense to very dense silty sand	Pile	Unit
Unsaturated Soil Weight	γ_{unsat}	18	19	25	kNm^{-3}
Saturated soil weight	γ_{sat}	18	19	-	kNm^{-3}
Young's Modulus	E	13000	13000	2.00E+09	kPa
Poisson's Ratio	ν	0.3	0.3	0.15	-
Cohesion	c	20	1	-	kPa
Friction Angle	ϕ	35	45	-	°

The case study deals with lateral load in which the deflection response of bored piles in cemented sand was examined by field test on a single pile under lateral load (Ismael, 1998). All piles were

0.3 m in diameter and had a length of 3 or 5 m. The site of this load test was in Kuwait. The surface soil to a depth of 3.5 m was characterized by having both component of shear strength, both effective parameters. The soil profile consists of a medium dense cemented silty sand layer to a depth of 3 m. This is underlain by a medium dense to very dense silty sand with cemented lumps to the bottom of the borehole. The same load sequence as pile tests was applied to the pile after completing the whole geotechnical model for lateral pile tests. The properties of soil in the both cases are listed in Table 3.8.

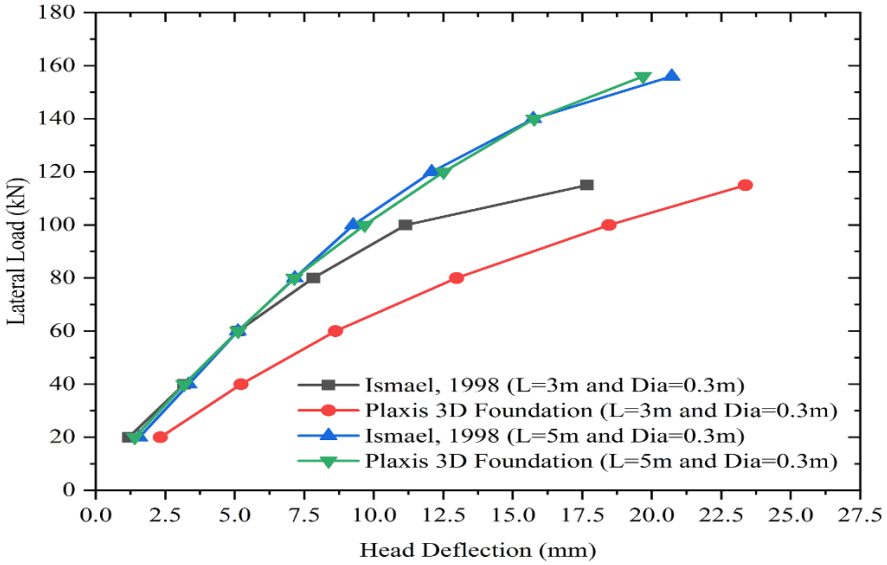

Figure 3.10 Comparison of finite element result with field test data from Ismael (1998)

The comparison between the finite element result and layered sand field test data is shown in Figure 3.10. The pile with a length of 5 m is highly resistance to the lateral load from the second pile length value. Comparable data were obtained between the experimental results of the three piles and the present simulation model. The results obtained from the numerical simulation for a pile of 5 m is relatively closed with the result obtained from the field test. Whilst the result from the numerical simulation is not too closed in case of 3 m long pile, it may be due to nonhomogeneous soil around the pile in field.

CHAPTER 4 : PARAMETRIC STUDIES AND ANALYSIS

4.1 Introduction

In this chapter, a parametric study was conducted on a laterally loaded pile embedded in layered soil conditions using Plaxis 3D Foundation. One of the purposes for this study was to investigate the laterally loaded pile by varying; length of the piles, pile diameter and site condition under static lateral loading. The analysis was performed on the model with the same characteristics except pile length, pile diameter and site condition.

The main objective of this study is to investigate the behaviour of laterally loaded pile embedded in layered in soils of Addis Ababa. As shown in chapter-3, a Plaxis 3D Foundation model has been developed to study the behaviour of laterally loaded pile. In addition, to ensure the reliability of the results obtained by the developed model, was compared with a full-scale laterally loaded pile (Ismael, 1998) to make a comparison with current study of laterally loaded piles. In this chapter, the 3D finite element method results were compiled and presented.

4.2 Parameter Analysis

In order to evaluate the effect of some parameters due to laterally loaded pile on the deformation analysis, a parameter analysis was performed. In this analysis some important parameters; pile length, pile diameter and site condition were analyzed by changing the values of each of them according to the procedure and methodology.

4.3 Results and Discussion

The parametric study is carried out in three stages:

1. Overall variation and analysis of results of deflection, shear force and bending moment with respect to the three types of soil profiles of Addis Ababa.
2. Analysis of head deflection results with respect to length and diameter of pile.
3. Analyzing the result of ultimate lateral load carrying capacity of pile with respect to length and diameter of pile.

4.3.1 Effect of Pile Diameter on Head Deflection of Pile

The variation of the piles head deflection due to the loads applied at the piles head are drawn in Figure 4.1, Figure 4.2 and Figure 4.3 for site-I, site-II and site-III, respectively for different embedded length and diameter of pile. These graphs show the change of lateral load and corresponding lateral deflection at the pile head in *x* direction. It can be seen from the figures that the variation of the pile head displacement with the applied loads are nonlinear. In Plaxis 3D Foundation the pile was modeled with diameter of pile 0.65m, 0.9 m, 1.15 m and 1.4 m.

In this section the effect of pile diameter and length on the head deflection of laterally loaded pile is discussed as follows. And the effect of site condition on the head deflection of the pile is discussed.

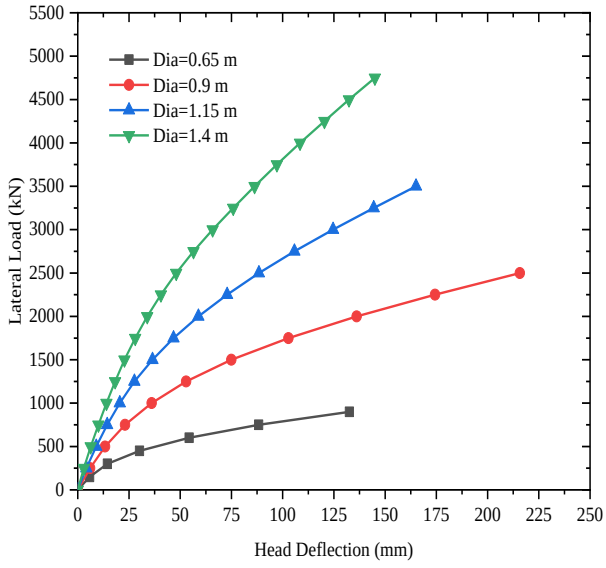

a. Length of pile=24m

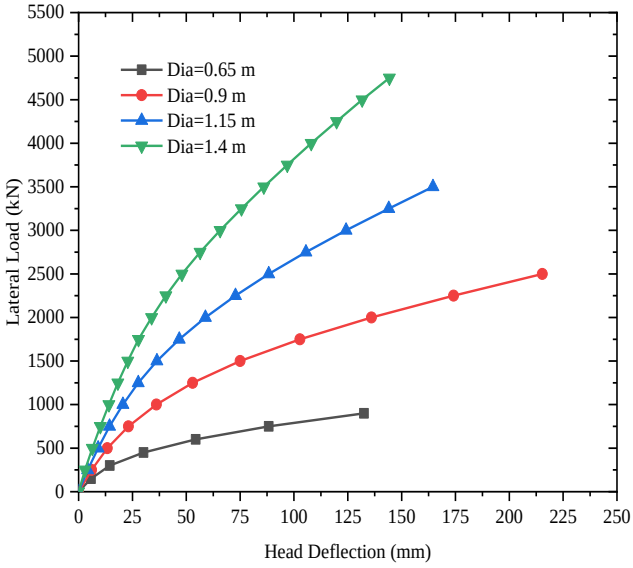

b. Length of pile=27m

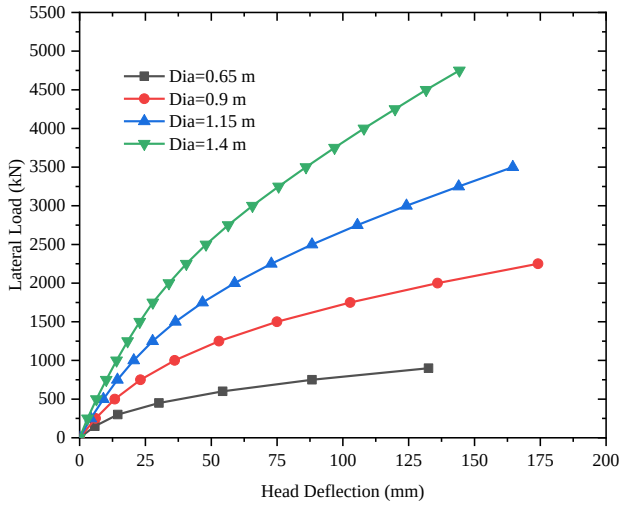

c. Length of pile=30m

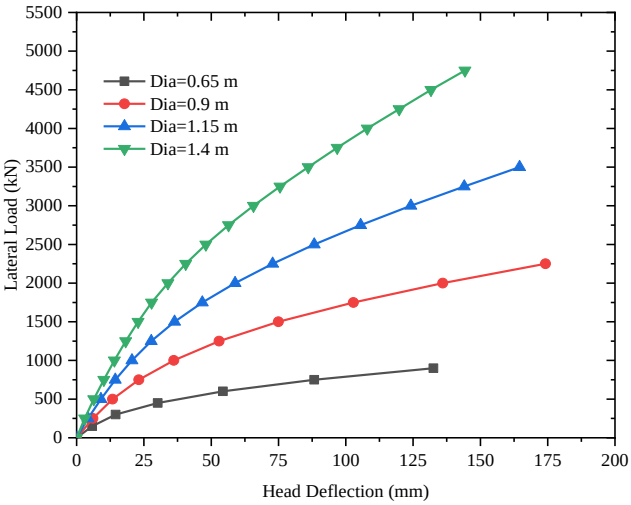

d. Length of pile=33m

Figure 4.1 Lateral load versus head deflection for *site-I*

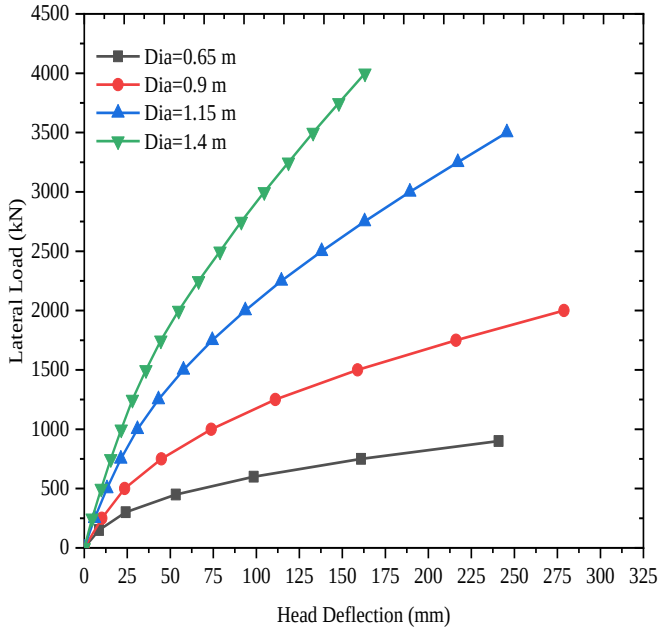

a. Length of pile=24m

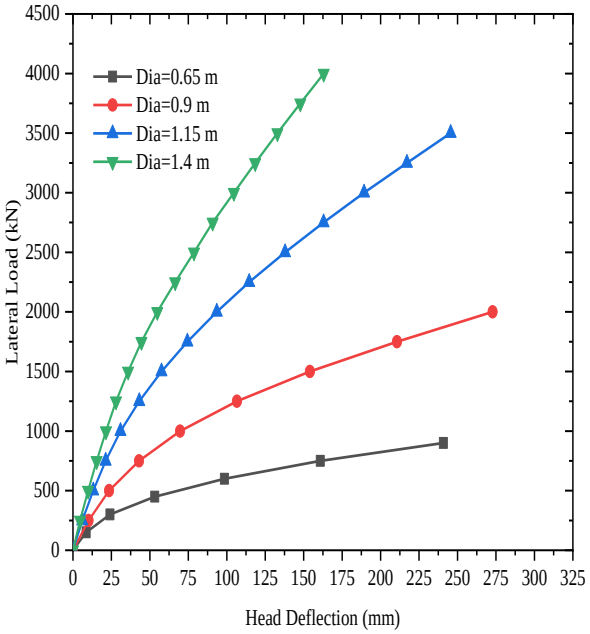

b. Length of pile=27m

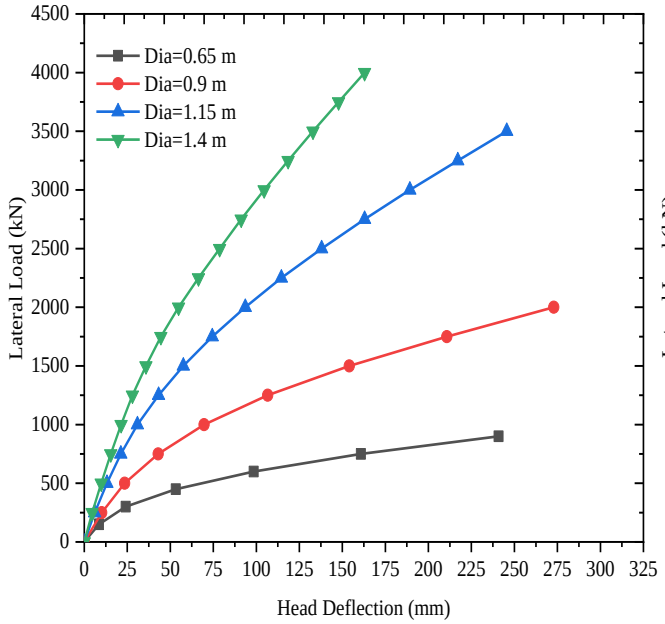

c. Length of pile=30m

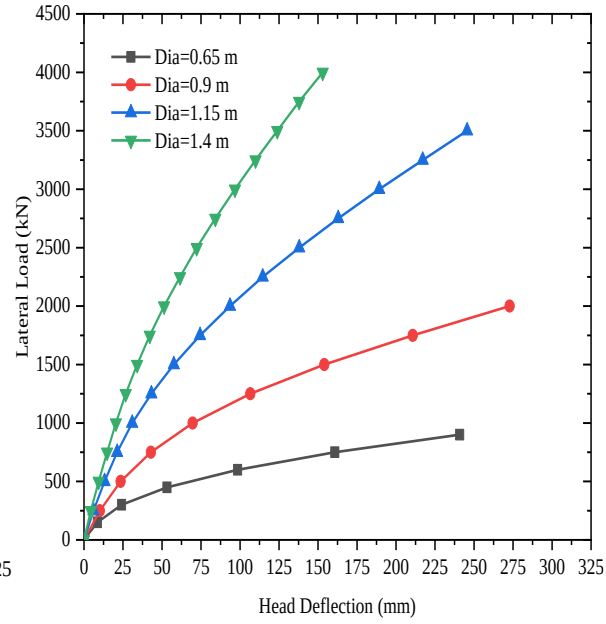

d. Length of pile=33m

Figure 4.2 Lateral load versus head deflection for *site-II*

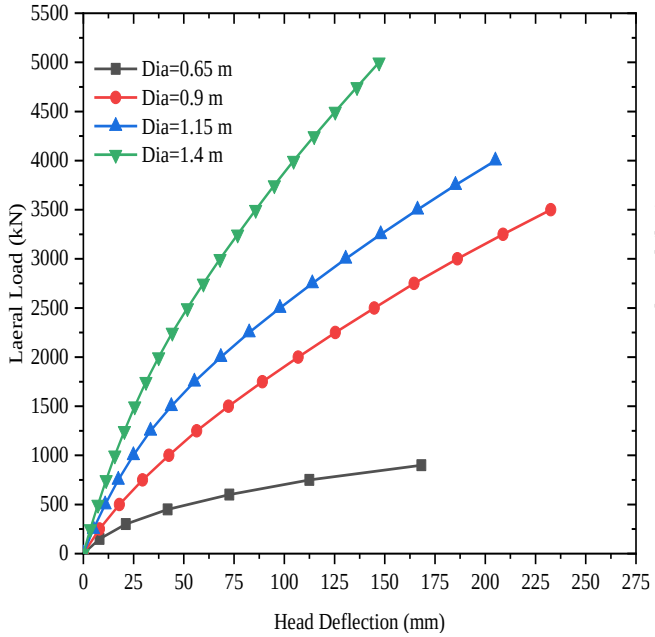

a. Length of pile=24m

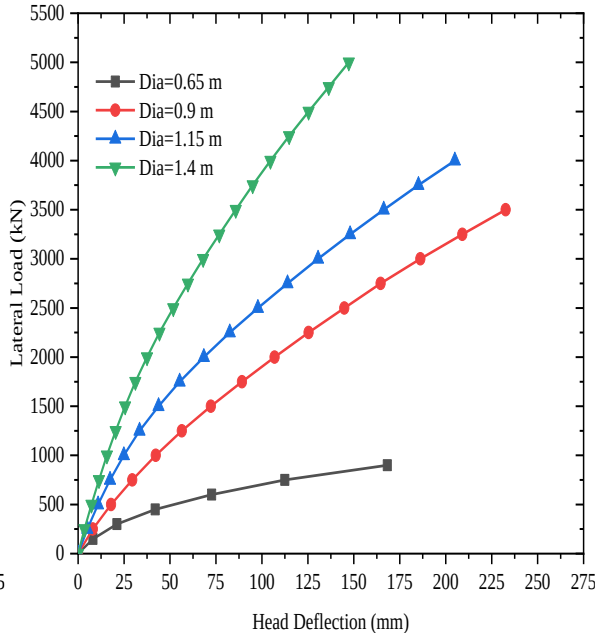

b. Length of pile=27m

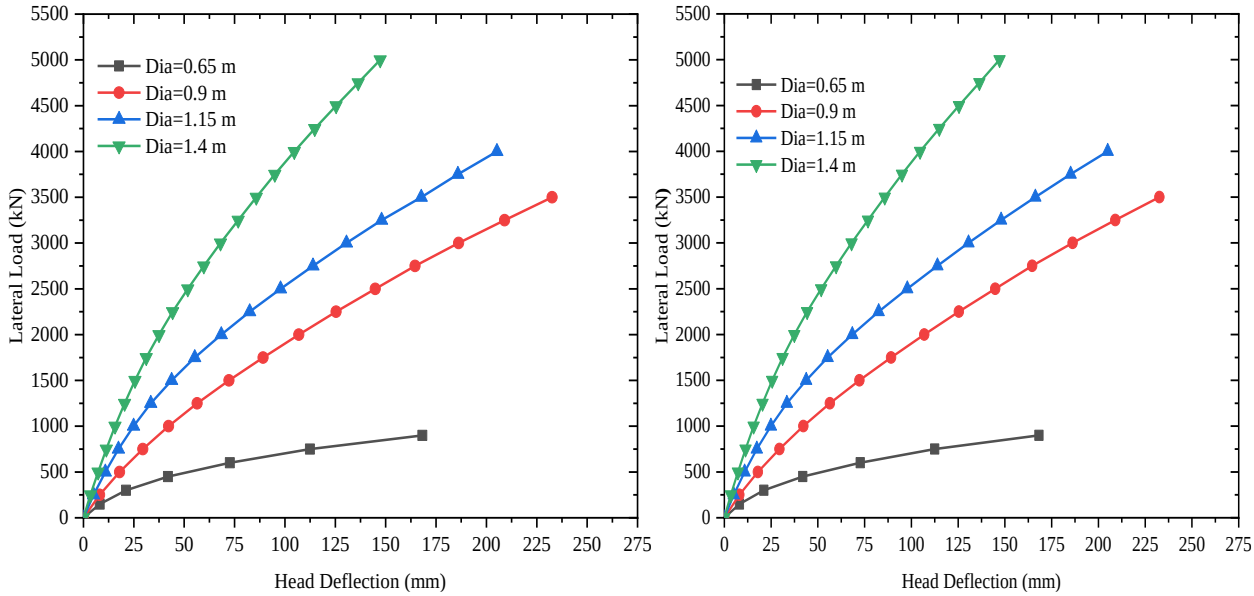

c. Length of pile=30m

d. Length of pile=33m

Figure 4.3 Lateral load versus head deflection for *site-III*

Figure 4.1, Figure 4.2 and Figure 4.3 shows change of lateral load and corresponding lateral head deflection at the pile head in *x* direction (*p-y* curves) at the end of FEM analysis in the site-I, site-II and site-III. It is also observed in the *p-y* graph as the diameter of the pile increase with decrease in head deflection and vis versa. This was due to the pile stiffness, EI, increase with increase in moment of inertia I which depends on the diameter of the pile.

As stated before, most of the time the head deflection of laterally loaded pile is depends on the strength and the stiffness behaviour of the soil layer exist near to the ground surface. Thus, when comparison is made between the geotechnical properties of first layers of three sites (Table 3.6, Table 3.7 and Table 3.8), site-II has soft organic silty clay with relatively small value of strength parameters. When the comparison was made between Figure 4.1, Figure 4.2 and Figure 4.3, as expected the head deflection of the pile embedded in site-II has greatest values than the other two sites.

From the geotechnical properties of the layers, Table 3.6, Table 3.7 and Table 3.8 shows that for site-II a hard strata was found at a depth of 6.6 m from the ground surface with thickness 2.2 m but for site-I a hard strata was found at a depth of 5.5 m from the ground surface with thickness of

5.1 m and for site-III a hard strata was found at a depth of 4.4 m from the ground surface with thickness of 3 m. Thus, the thickness of the hard strata of site-II is small and its location from the ground surface is deep relative to the other two sites. As a result, piles embedded in site-II has greatest values of head deflection relative to site-I and site-III (Figure 4.1, Figure 4.2 and Figure 4.3) with different pile diameter with the application of static lateral load. Therefore, the thickness and the location of the layers were determined the head deflection of the pile.

Table 4.1 shows that the effect of site condition on the head deflection of laterally loaded pile. The result was obtained from FEM analysis with the application of lateral load of 750 kN at the pile head for different diameter and length of the pile. As discussed in the above head deflection is increase with increase in diameter of a pile and the deflection value of the pile embedded in Site-II was greatest from the other two sites.

Table 4.1 The effect of site condition on the result of pile head deflection

Pile length (m)	Site	Head deflection (mm)			
		D=0.65m	D=0.9m	D=1.15m	D=1.4 m
L=24	I	88.31	23.08	14.35	10.07
	II	160.83	44.82	21.29	15.41
	III	112.46	29.47	17.37	11.36
L=27	I	88.29	23.13	14.38	10.11
	II	160.83	42.97	21.30	15.41
	III	112.46	29.47	17.36	11.35
L=30	I	88.29	23.13	14.38	10.11
	II	160.83	42.98	21.29	15.41
	III	112.44	29.47	17.36	11.35
L=33	I	88.29	23.13	14.38	10.11
	II	160.83	42.94	21.29	15.41
	III	112.50	29.47	17.36	11.35

4.3.2 Effect of Length of the Pile on Head Deflection

The parametric study was carried out by varying the length of the pile and the deformation is obtained from Plaxis output. This parameter was varied for different pile length of 24 m, 27 m, 30 m and 33 m in the study. Figure 4.1, Figure 4.2 and Figure 4.3 shows that the results obtained from Plaxis 3D Foundation analysis. The pile head deflection and lateral load are obtained. It was

observed that the length of the pile increased without increase in head deflection because the embedded length of the pile is greater than its critical length. All piles in this study were considered as flexible piles because they have length greater than its critical length L_c (Table C.l, Appendix C).

4.3.3 Ultimate Lateral Resistance

The ultimate lateral resistance and working load deflections of single piles depends on the dimensions, strength, and flexibility of the individual pile, and on the deformation characteristics of the soil surrounding the loaded pile. The ultimate lateral resistance of a laterally loaded pile will be governed by either the ultimate lateral resistance of the surrounding soil or by the yield or ultimate moment resistance of the pile section.

The failure criterion considered in this analysis is the yield of the maximum ultimate lateral displacement at pile head, where the lateral load capacity of pile is reached when the ultimate lateral displacement yields at head of pile. The ultimate lateral displacement at pile head depends on some factors such as pile type, soil type, and type of structure carried by the pile, but it mainly depends on pile diameter.

The ultimate lateral load capacity of a pile referred in this thesis is taken as the loads corresponding to the lateral deflection at the pile head equal to around 10% of the diameter of the pile. In real design, the pile capacity may be even limited to deflection requirements, in another word, service limit conditions.

4.3.4 Ultimate Lateral Load Capacity from Numerical Results

In all the cases studied, the load required to displace the pile head a horizontal distance equal to 10% of the pile diameter is assumed as the ultimate lateral load capacity of the pile. These ultimate loads are given in Table B-1, Table B-2 and Table B-3, Appendix B.

The effects of diameter and length with different L/D ratio of a pile on its ultimate lateral load capacity is shown in Figure 4.4 and Figure 4.5 which are obtained from 3D finite element method analyses at all three sites.

4.3.4.1 Effect of Diameter of the Pile on Lateral Load Capacity

To study the effect of diameter on lateral load capacity of a pile having length 24 m, 27 m, 30 m and 33 m length with different diameters, 0.65 m, 0.90 m, 1.15 m and 1.4m were considered. The results are given in Figure 4.4 (a, b and c) for *Site-I, Site-II and Site-III* respectively, which indicates that lateral load capacity increases with increasing diameter of the pile. This was due to the increase in surface area. Also, the pile stiffness, EI, increases with increase in moment of inertia I which depends on the diameter of pile.

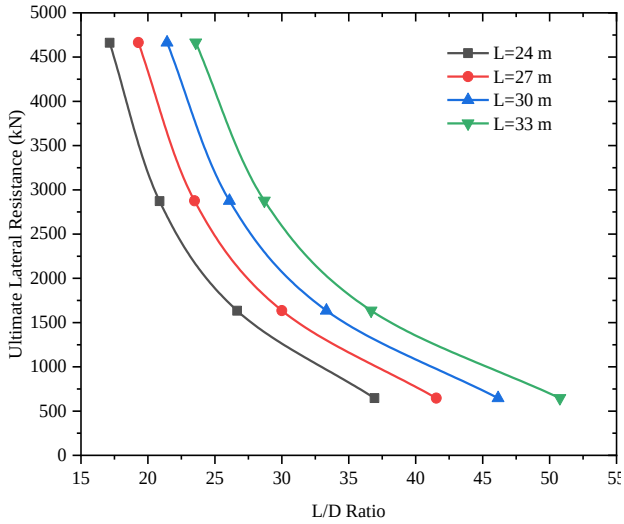

a. Site-I

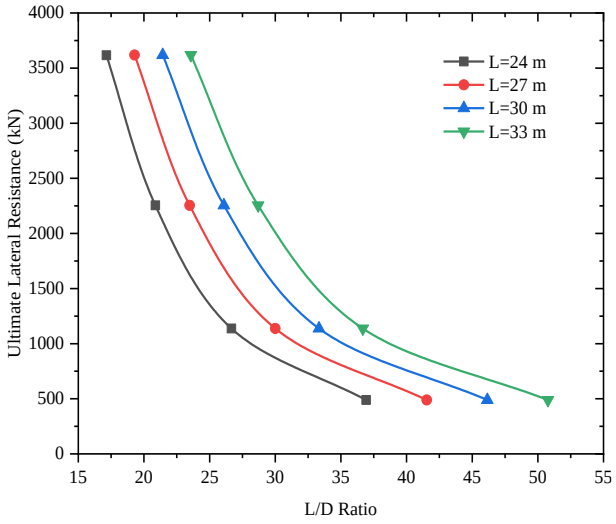

b. Site-II

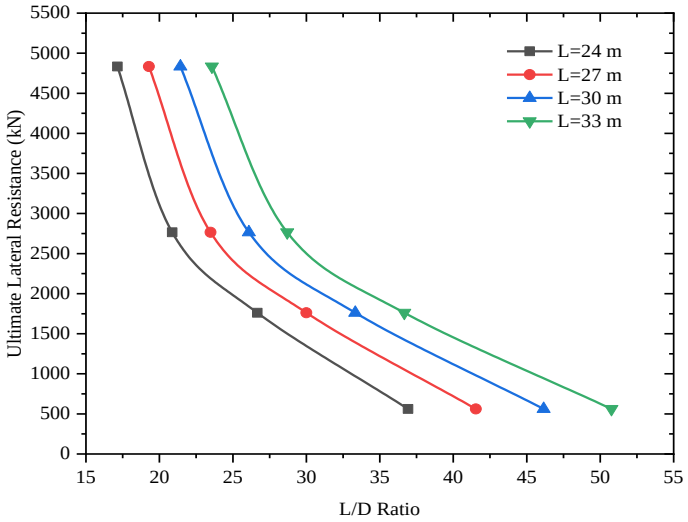

c. Site-III

Figure 4.4 Ultimate lateral resistance (decrease in diameter)

Figure 4.4 (a, b and c) shows that ultimate lateral resistance is increase with decrease in L/D ratio. This implies that L/D with constant pile length and decreasing pile diameter, the ultimate lateral resistance of the pile decreased and he reverse is true.

Figure 4.4 (b) shows that the ultimate lateral resistance was small relative to Figure 4.4 (a) and Figure 4.4 (c) for similar loading condition. This is because of the stiffness and strength properties of upper layer of the soil and, the location and thickness of hard strata near to the ground surface as it was discussed in section 4.2.1. Generally, laterally loaded piles embedded in site-II have a smaller ultimate lateral resistance than the other two sites.

4.3.4.2 Effect of Length of the Pile on Lateral Load Capacity

To study the effect of length of the pile on lateral load capacity, 0.65 m, 0.9 m and 1.15 m and 1.4 m diameter piles of different lengths i.e. 24 m, 27 m, 30 m and 33 m were considered. The results are given in Table B.1, Table B.2 and Table B.3 in the Appendix for *Site-I, Site-II and Site-III* respectively, which indicates there is no any considerable change in lateral load capacity with increase in length as shown in the Figure 4.5 (a, b and c).

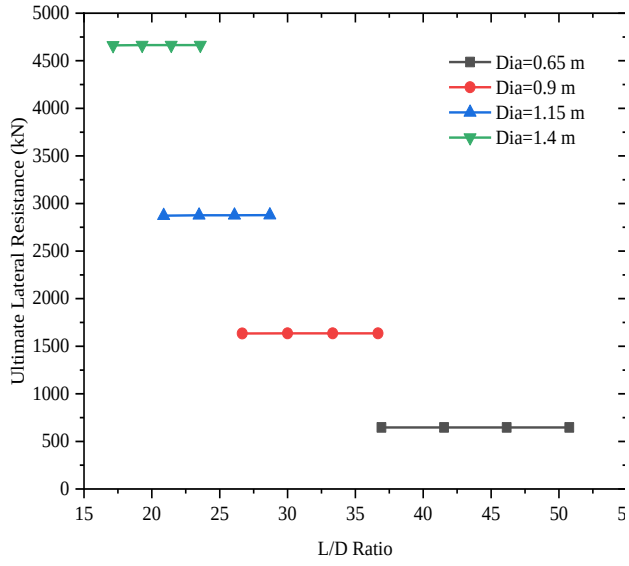

a. Site-I

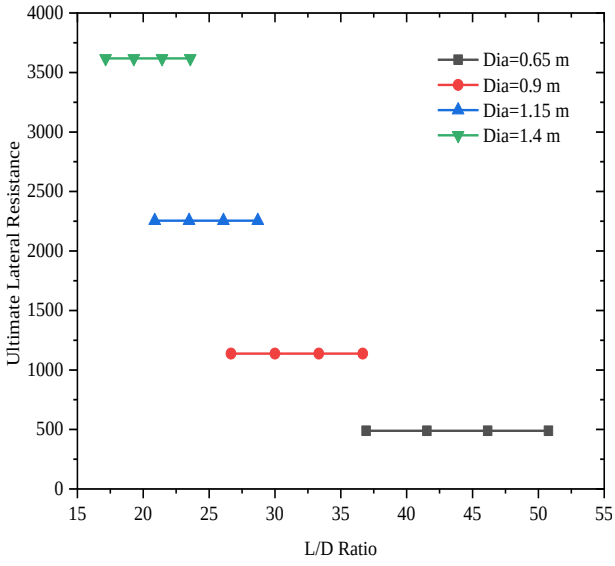

b. Site-II

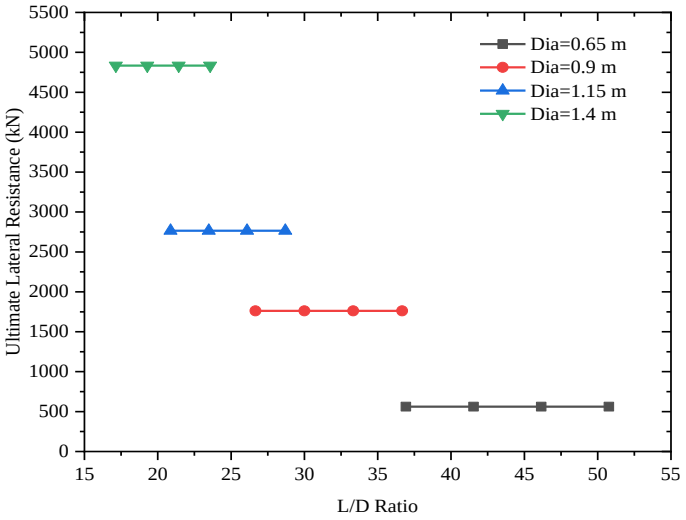

c. site-III

Figure 4.5 Ultimate lateral resistance (increase in length)

Figure 4.5 (a, b and c) shows that ultimate lateral resistance is constant with increase in L/D ratio. This implies that L/D ratio with constant pile diameter and decreasing pile length, the ultimate lateral resistance of the pile remains unchanged. This is because the embedded length of the pile is greater than the critical length (L_c) of the pile (Table C.1, Appendix C).

4.3.5 Effect of Diameter on the Deflection of the Pile

Figure 4.6, Figure 4.7 and Figure 4.8 shows the pile deflection along the pile axis with different length and diameter, obtained from Plaxis 3D Foundation results. The figures were plotted using dimensionless parameters as normalized deflection versus normalized length of a pile (δ/D vs y/L). The result is obtained by applying lateral load of H= 750 kN, pile having diameter 0.65 m, 0.9 m, 1.15 m and 1.4m at its head with different length.

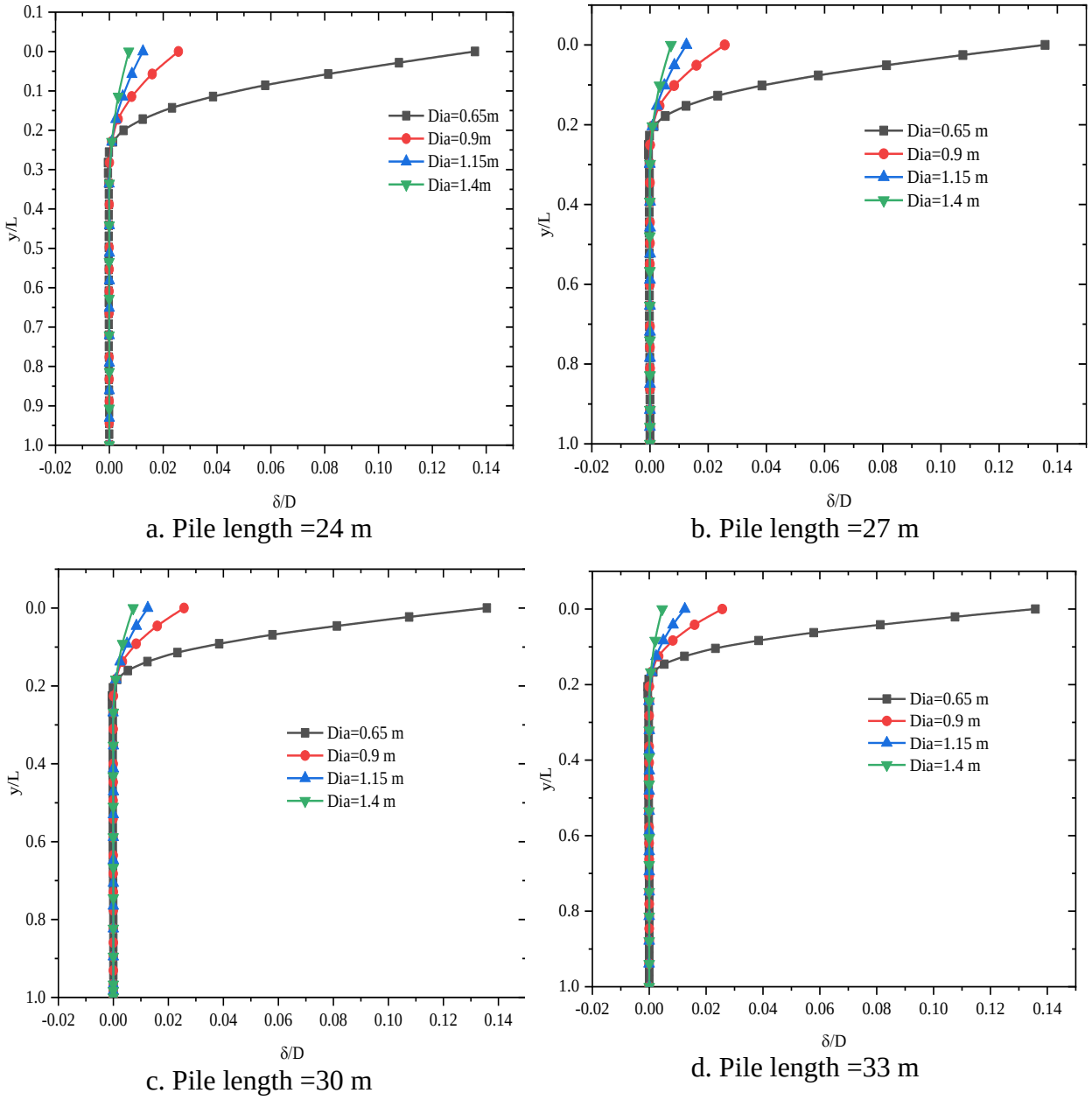

a. Pile length =24 m

b. Pile length =27 m

c. Pile length =30 m

d. Pile length =33 m

Figure 4.6 Lateral Deflection versus pile length for Site-I

Figure 4.6 shows the normalized lateral displacement in *x* direction along the normalized pile depth at the end of FEM analysis in the site-I. The maximum lateral displacement at the shaft head in the x direction is occurred at the ground surface corresponding to each diameter of the pile. As it can be seen in the graph that at some length of a pile the deflection was diminished to zero. Figure 4.6 (a), Figure 4.6 (b), Figure 4.6 (c) and Figure 4.6 (d) shows that the deflection of pile was diminished at y/L= 0.21, 0.20, 0.19 and 0.19 respectively. This indicates that when the pile length

increases the depth of a pile at which deflection getting zero is insignificant. Increase in diameter of the pile with decrease deflection of pile head in x direction for all diameter as shown in Figure 4.6. This was due to the increased in stiffness of a pile.

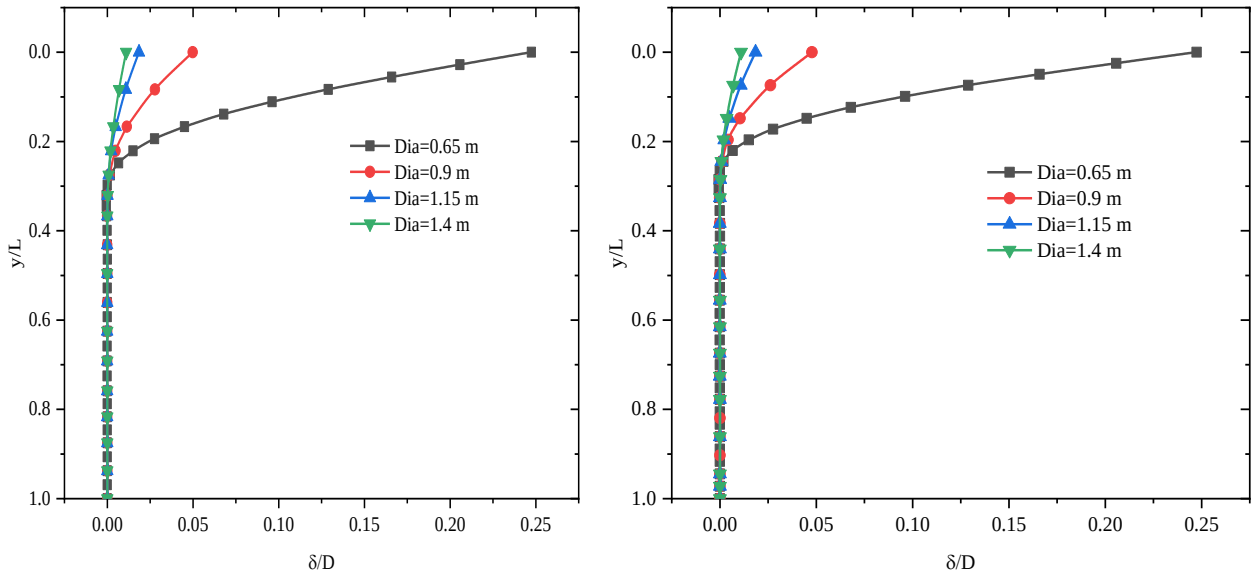

a. Pile length =24m

b. Pile length =27m

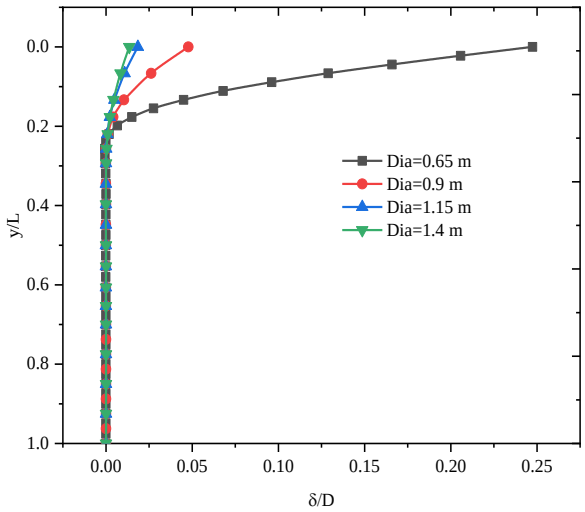

c. Pile length =30m

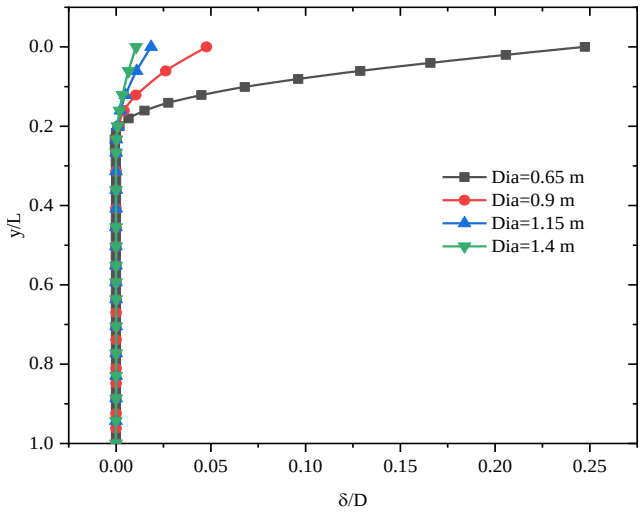

d. Pile length =33m

Figure 4.7 Lateral Deflection versus pile length for Site-II

Figure 4.7 shows the normalized lateral displacement in *x* direction along the normalized pile depth at the end of FEM analysis in the site-II. The maximum lateral displacement at the shaft head in the x direction is occurred at the ground surface corresponding to each diameter of the pile. As it

can be seen in the graph that at some length of a pile the deflection getting to zero. Figure 4.7 (a), Figure 4.7 (b), Figure 4.7 (c) and Figure 4.7 (d) shows that the deflection of pile is diminished at y/L= 0.22, 0.21, 0.2 and 0.19 respectively. This indicated that increase in pile length there was insignificant change in depth of a pile at which deflection is diminished to zero. Increase in diameter of the pile with decrease deflection of pile in x direction for all diameter as shown in Figure 4.7. This was due to the increase in surface area of a pile.

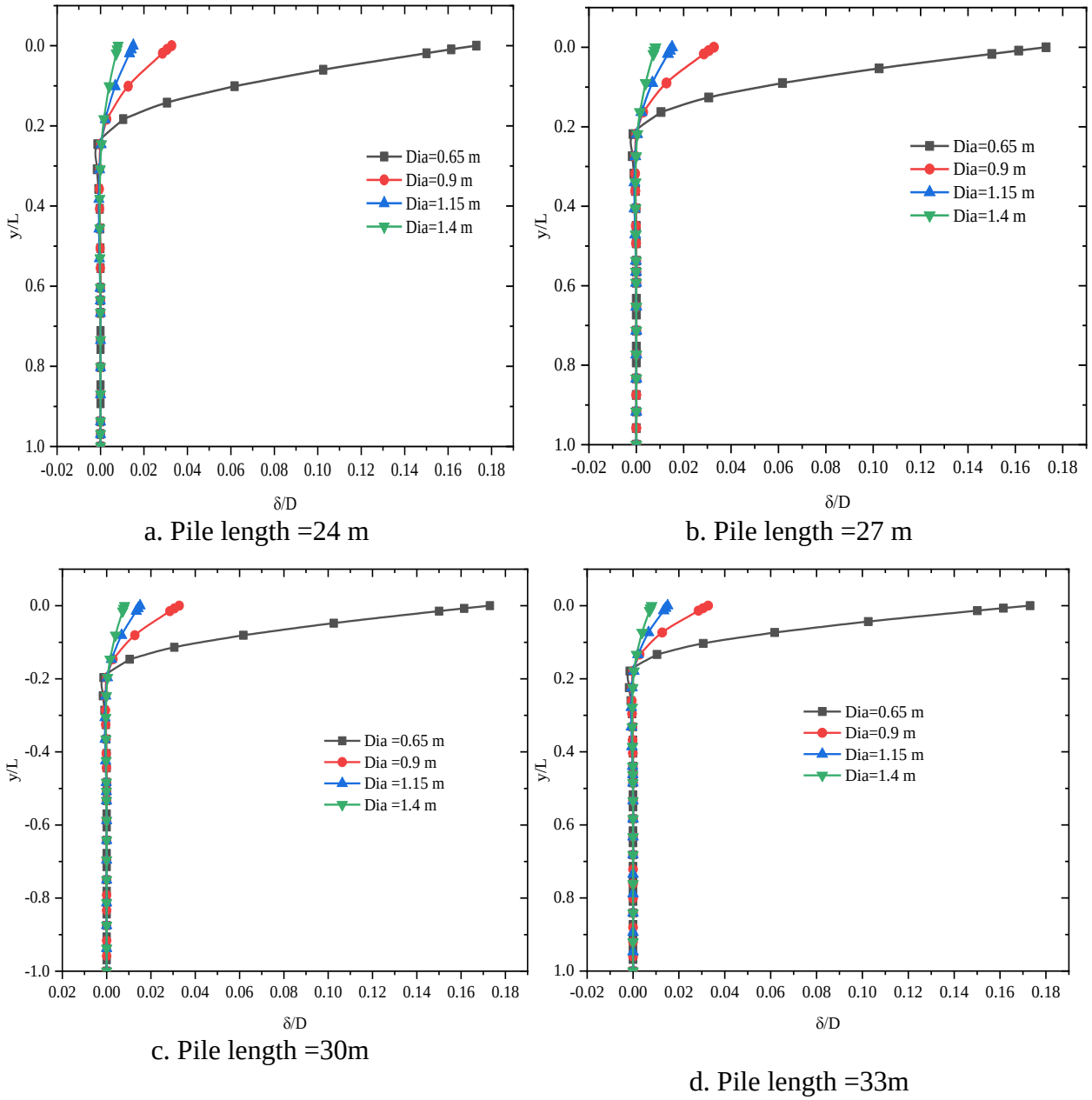

a. Pile length =24 m

b. Pile length =27 m

c. Pile length =30m

d. Pile length =33m

Figure 4.8 Lateral Deflection versus pile length Site-III

Figure 4.8 shows the normalized lateral displacement in *x* direction along the normalized pile depth at the end of FEM analysis in the site-III. The maximum lateral displacement at the shaft head in the x direction is occurred at the ground surface corresponding to each diameter of the pile. As it can be seen in the graph that at some length of a pile the deflection getting to zero. Figure 4.8 (a), Figure 4.8 (b), Figure 4.8 (c) and Figure 4.8 (d) shows that the deflection of pile is diminished at y/L= 0.21, 0.20, 0.19 and 0.19 respectively. And in the four figures there is a negative deflection occurred when diameter of a pile D=0.65 m. Increase in diameter of the pile with decrease deflection of pile in x direction for all diameter as shown in Figure 4.8. This was due to the increase in stiffness of a pile. Although, it was observed that the length of the pile increased without increase in the depth of zero deflection.

From Figure 4.6, Figure 4.7 and Figure 4.8 it can be observed that the magnitudes of δ/D are large for site-II relative to the other two sites. This was indicated that when the pile is embedded in site-II its deflection more significant than the other two sites with same loading conditions.

4.3.6 Effect of Diameter on the Bending Moment Distribution Along the Pile

Figure 4.9, Figure 4.10 and Figure 4.11 shows normalized bending moment distribution along the pile with different length and diameter obtained from Plaxis 3D Foundation results. The figures are plotted using dimensionless parameters as normalized bending moment versus normalized length of a pile (M/(H*L) vs y/L). The result is obtained by applying lateral load of H=750 kN pile having diameter 0.65 m, 0.9 m, 1.15 m and 1.4 m at its head.

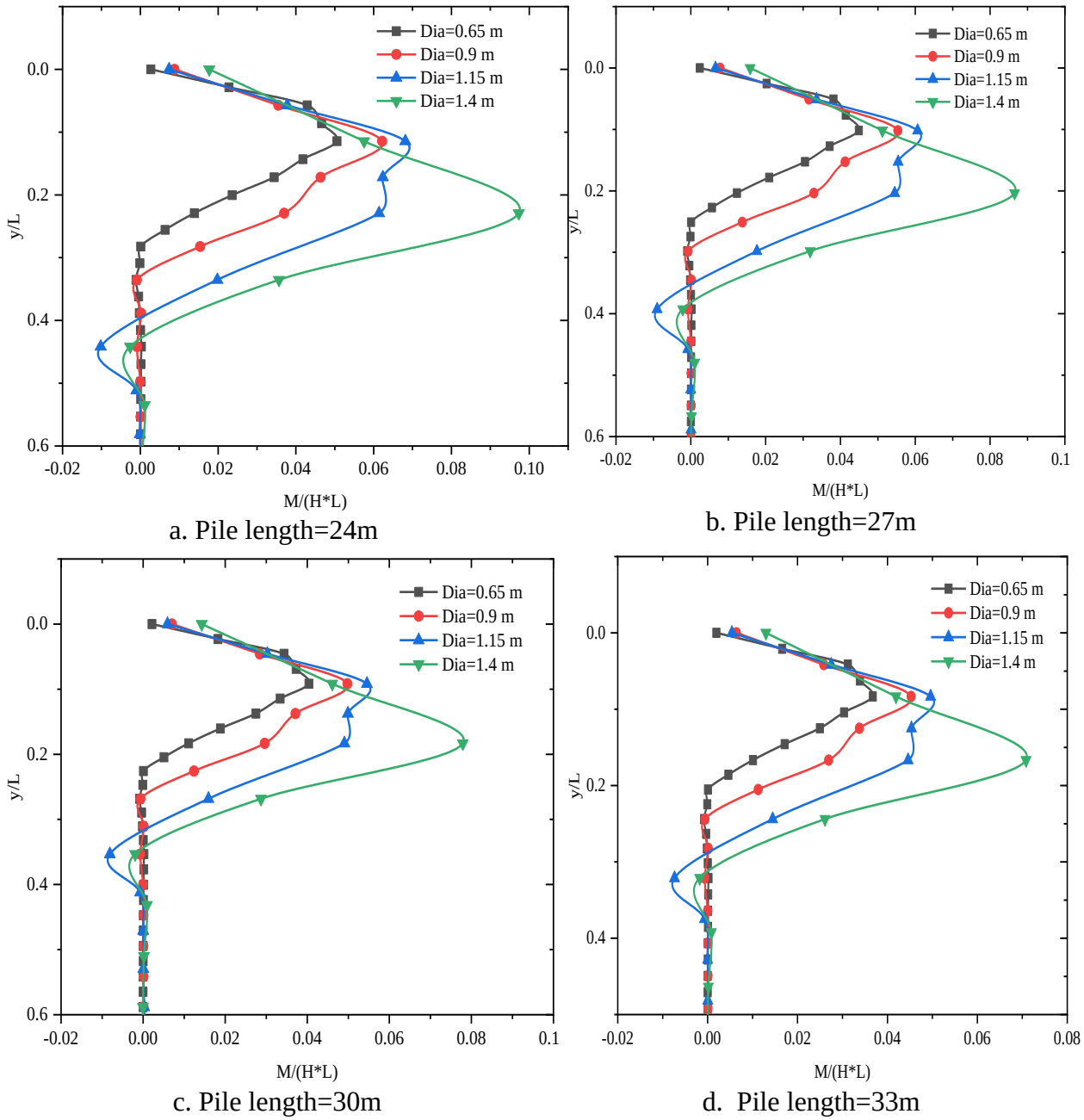

a. Pile length=24m

b. Pile length=27m

c. Pile length=30m

d. Pile length=33m

Figure 4.9 Bending moment versus pile length for Site-I

Figure 4.9 shows the distribution of normalized bending moment (M_3) along the normalized pile depth at the end of FEM analysis in the site-I. If the structure has a local system of axes (1, 2, 3), the first direction is always the axial direction. The other directions (second and third) will always be perpendicular to the structure axis. The bending moment M_3 is the bending moment formed because of the bending around the third axis.

As it can be seen in the curve that the maximum bending moment varies with increase in pile diameter. As shown in the figures negative moment was produced when pile having diameter of 1.15 m and 1.4 m.

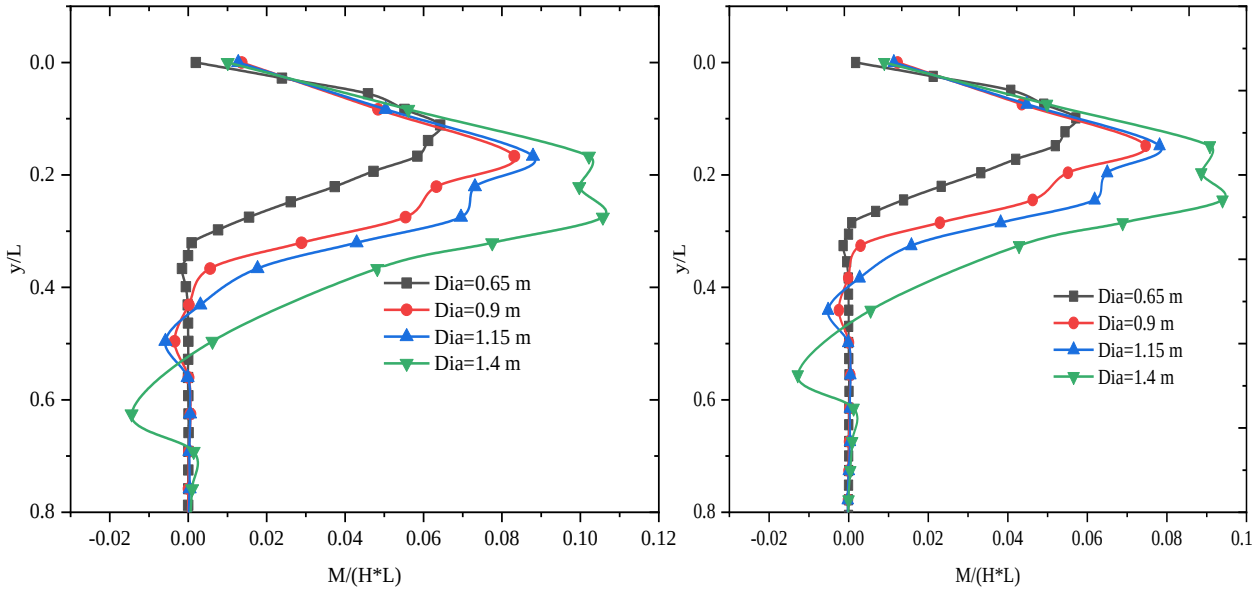

a. Pile length=24m

b. Pile length=27m

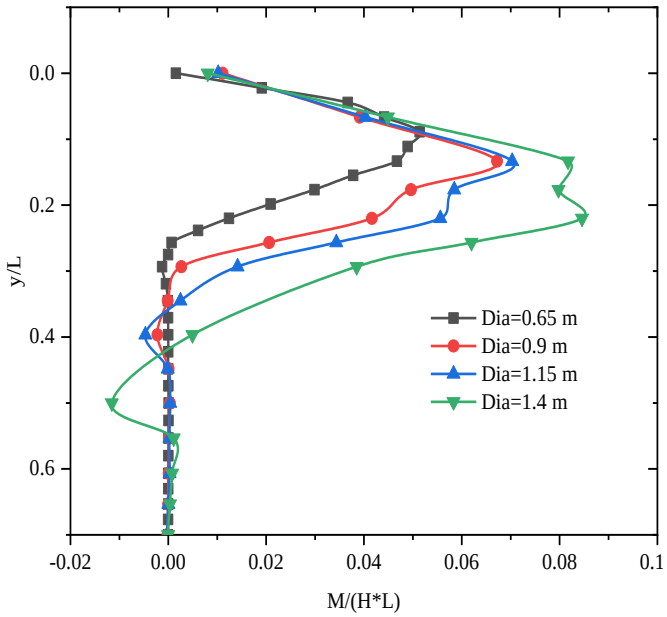

c. Pile length=30m

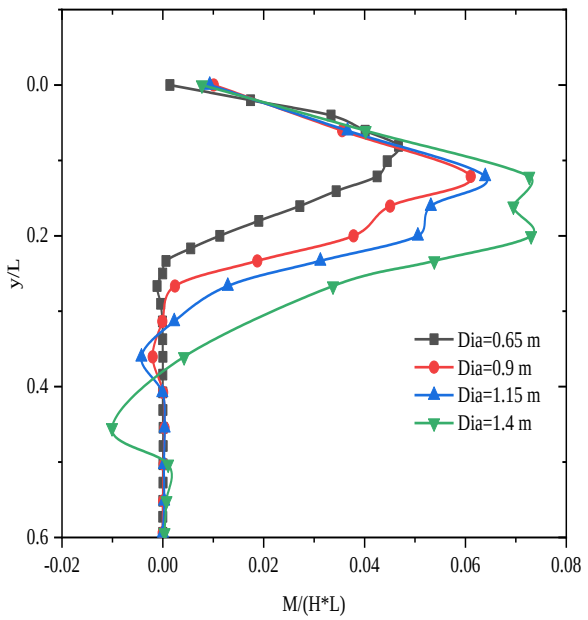

d. Pile length=33m

Figure 4.10 Bending moment versus pile length for Site-II

Figure 4.10 shows the distribution of normalized bending moment (M_3) along the normalized pile depth at the end of FEM analysis for site-II. As it can be seen in the curve that the maximum bending moment varies with increase in pile diameter. Figure 4.10(a) to Figure 4.10(d) shows that when the diameter of a pile increases the bending moment increases.

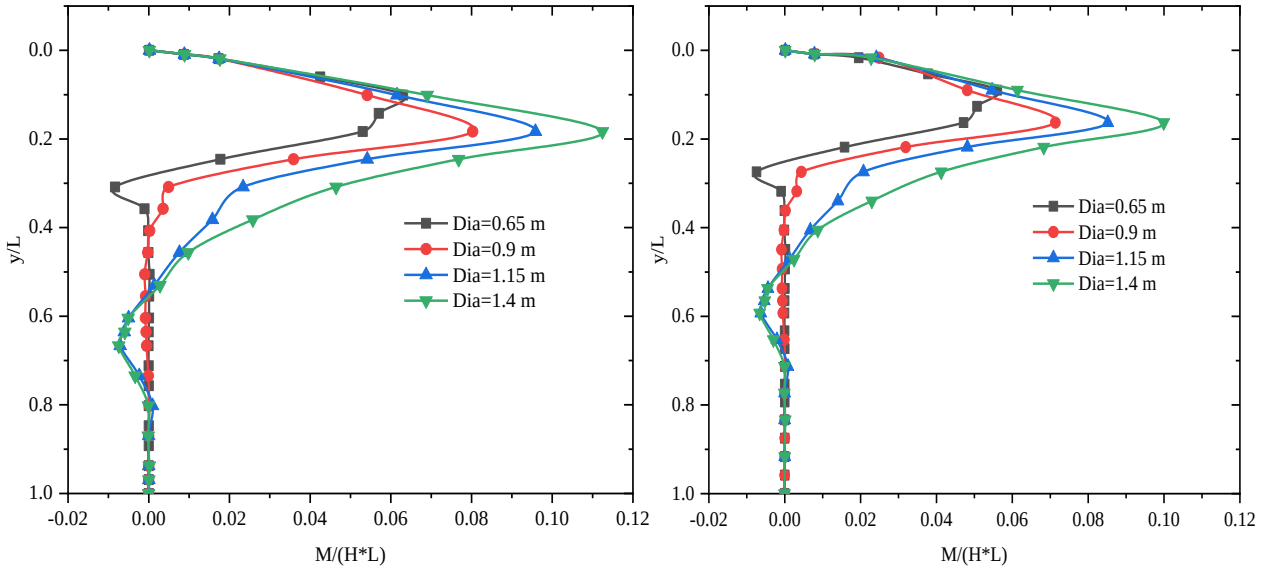

a. Pile length=24m

b. Pile length=27m

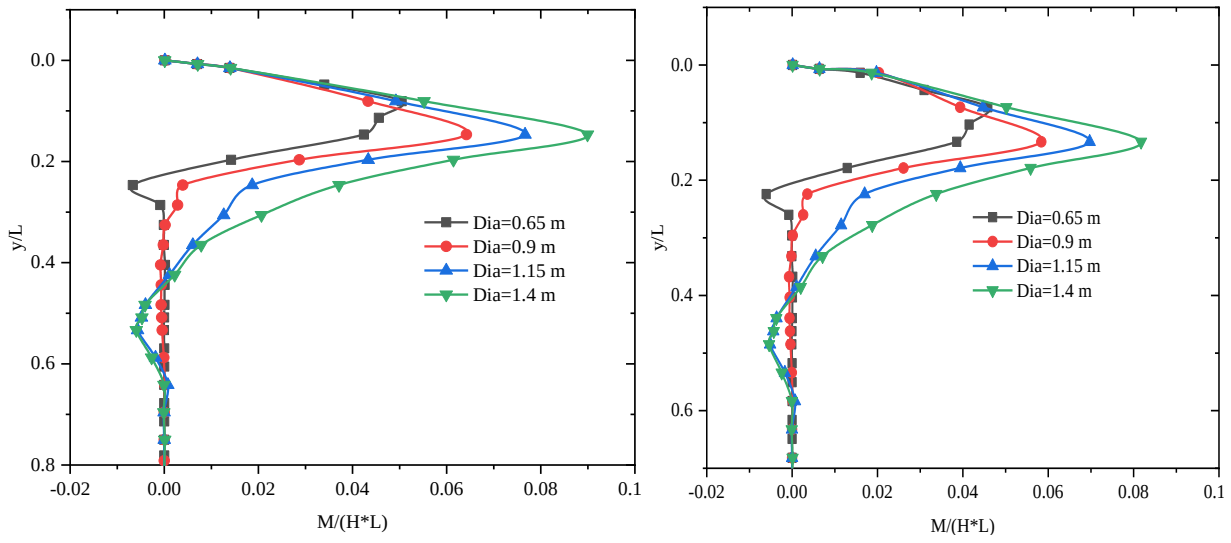

c. Length of pile=30m

d. Length of pile=33m

Figure 4.11 Bending moment versus pile length for Site-III

Figure 4.11 shows the distribution of normalized bending moment (M_3) along the normalized pile depth at the end of FEM analysis in the site-III. Figure 4.11 (a) to Figure 4.11 (d) shows that as the diameter of the pile increases with increase in bending moment.

As it can be seen in the curve that the maximum bending moment varies with increase in pile diameter. It can be observed that the negative moment is occurred when the pile diameter 1.15 m and 1.4 m.

Figure 4.9, Figure 4.10 and Figure 4.11 shows that the bending moment is constant with increase in pile length before normalization of bending moment. After normalizing of bending moment, the increase in pile length leads to decrease in bending moment.

4.3.7 Effect of Diameter on Shear Force Distribution Along the Pile

Figure 4.12, Figure 4.13 and Figure 4.14 shows that shear distribution along the pile with different length and diameter obtained from Plaxis 3D Foundation results. The figures are plotted using dimensionless parameters as normalized shear versus normalized length of pile (S/H vs y/L). The result is obtained by applying a typical lateral load of H=750 kN pile having diameter 0.65 m, 0.9 m, 1.15 m and 1.4m at its head.

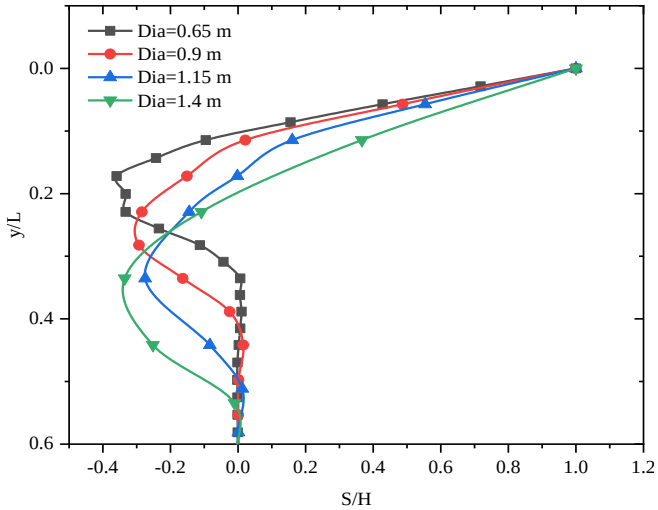

a. Pile length =24 m

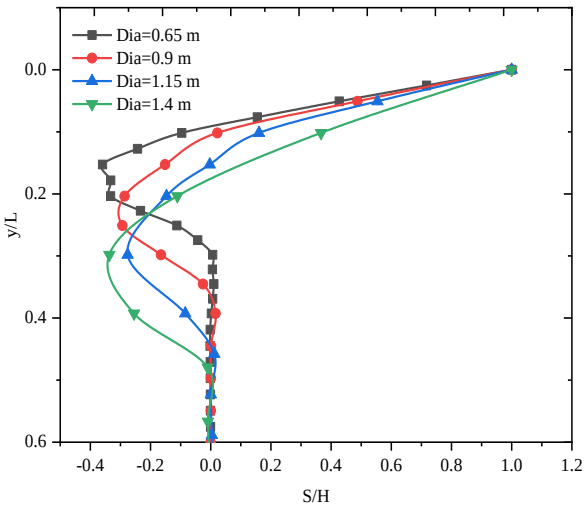

b. Pile length =27 m

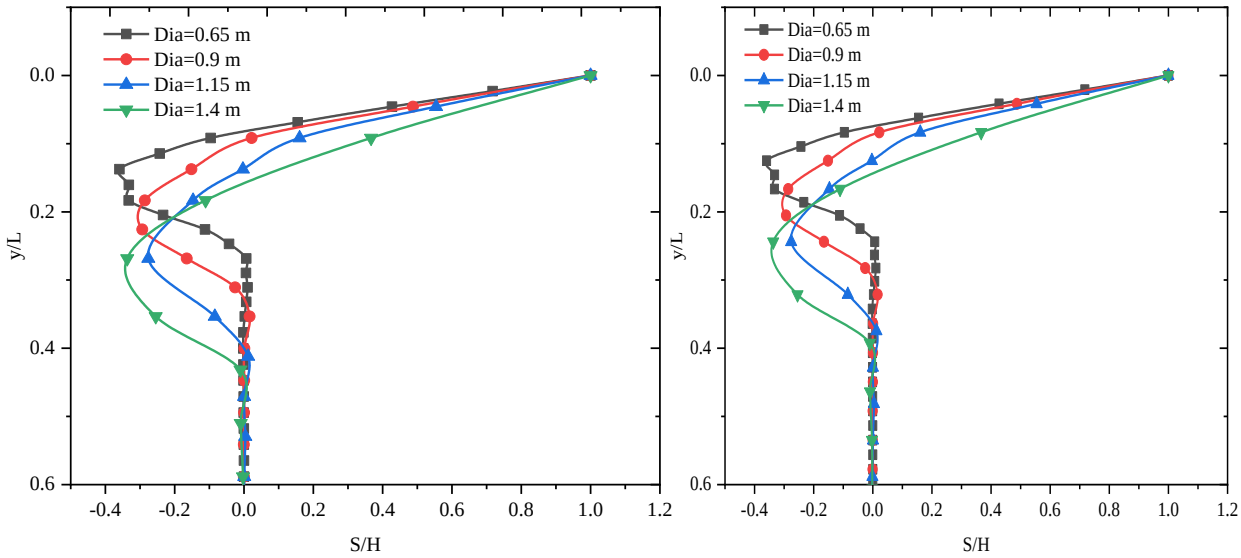

c. Pile length=30 m d. Pile length=33 m

Figure 4.12 Shear force versus pile length for Site-I

Figure 4.12 shows the distribution of normalized shear force along the normalized pile depth at the end of FEM analysis in the site-I. The shear force over the 2nd beam axis is denoted as Q_{12}. As it can be observed in the graph that the maximum shear force is occurred at the ground surface and maximum negative shear force occurs below the ground surface for different diameter and length of a pile. As it can be seen in the curve that the maximum shear force varies with increase in pile diameter but constant with increase in pile length.

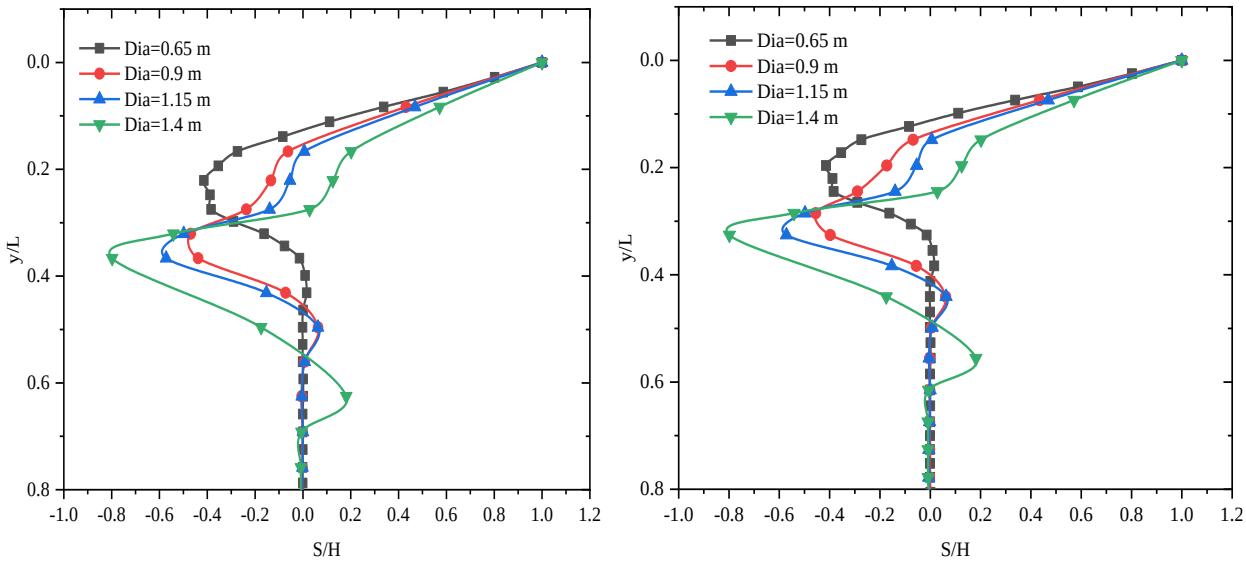

a. Pile length=24m b. Pile length=27m

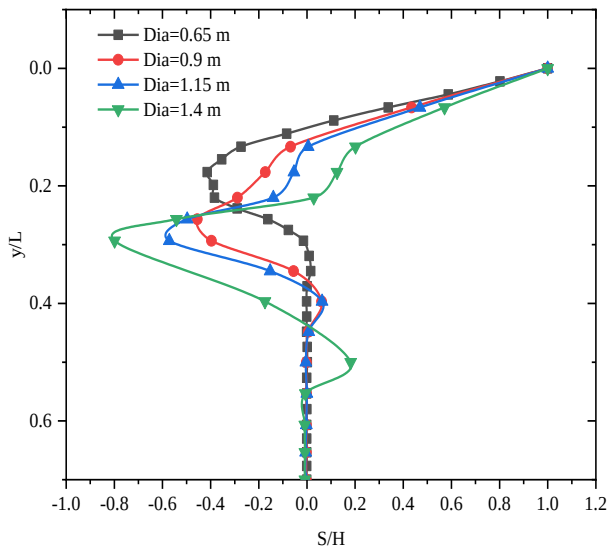

c. Pile length=30m

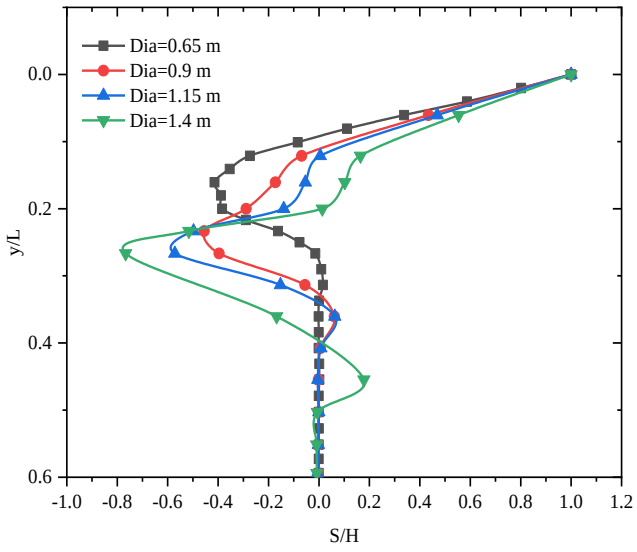

d. Pile length=33m

Figure 4.13 Shear force versus pile length for Site-II

Figure 4.13 shows the distribution of normalized shear force along the normalized pile depth at the end of FEM analysis in the site-II. As it can be observed in the graph that the maximum shear force is occurred at the ground surface for different diameter and length of a pile. As it can be seen in the curve that the maximum shear force varies with increase in pile diameter but constant with increase in pile length.

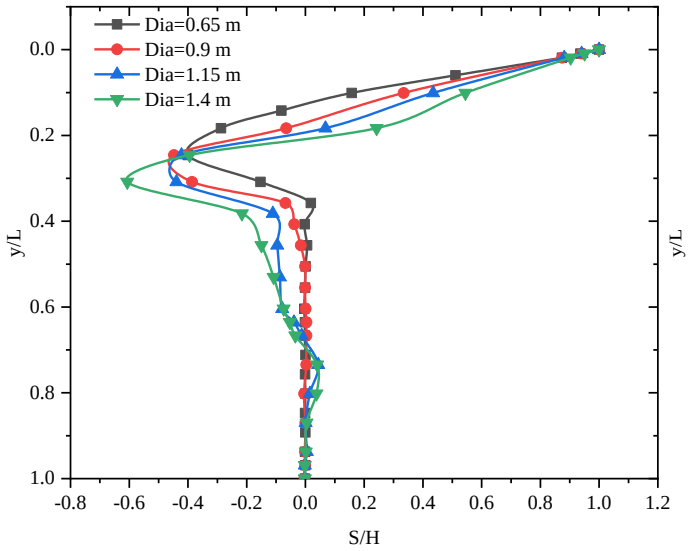

a. Pile length=24m

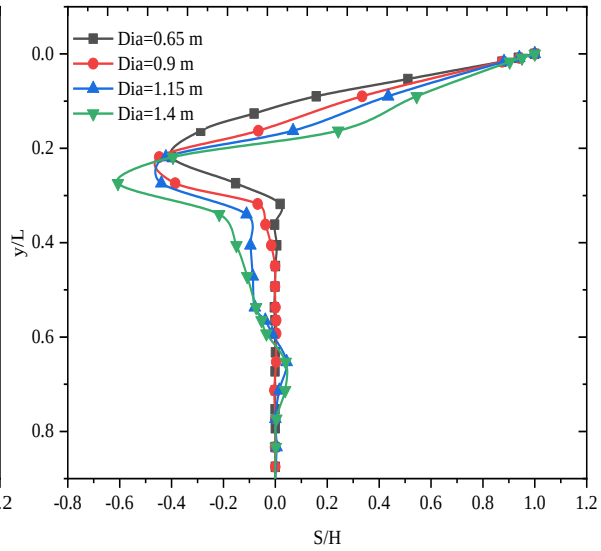

b. Pile length=27m

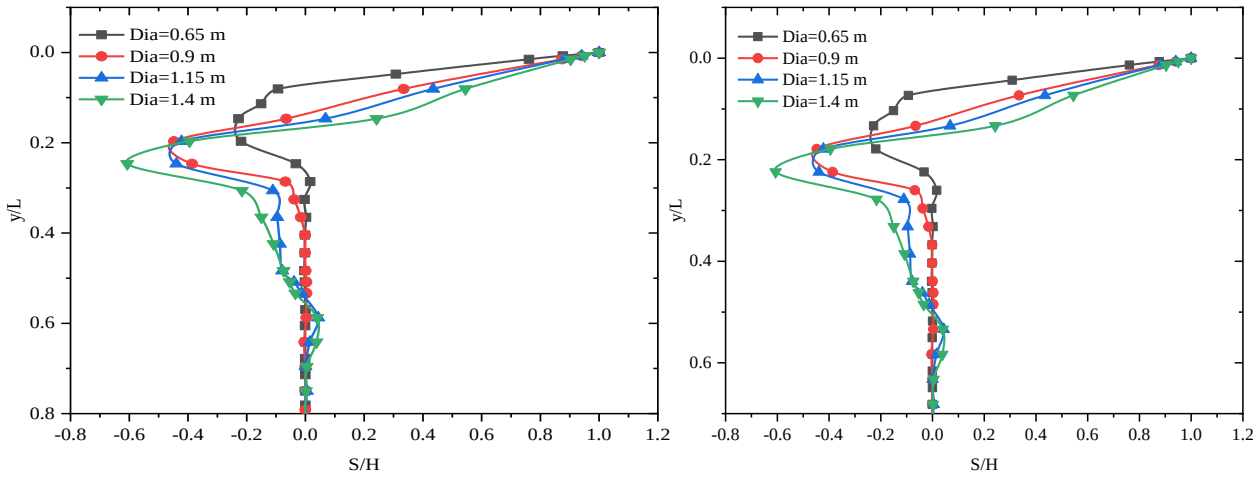

c. Pile length=30m d. Pile length=33m

Figure 4.14 Shear force versus pile length for Site-III

Figure 4.14 shows the distribution of normalized shear force along the normalized pile depth at the end of FEM analysis in the site-III. As it can be observed in the graph that the maximum shear force is occurred at the ground surface for different diameter and length of a pile. As it can be seen in the curve that the maximum shear force varies with increase in pile diameter but constant with increase in pile length.

CHAPTER 5 : CONCLUSIONS AND RECOMMENDATIONS

5.1 Conclusions

The main objective of this thesis was to study the behaviour of laterally loaded pile foundation embedded in layered soils considering the effect of pile diameter, pile length and site conditions using FEM. The main conclusions and recommendations drawn through the numerical modelling of laterally loaded pile developed in this study are summarized in this chapter.

In this study a numerical model was developed using Plaxis 3D Foundation software to analyses laterally loaded pile as three dimensional problems. The model, accounts for the effect of pile diameter, pile length and site condition on the behaviour of laterally loaded pile. The model was validated by comparing its results with the results of filed test available in the literature. The results of this numerical model were found in reasonable agreement with the results of field test available in the literature.

The results of the analyses show that pile diameter and site condition affect the behaviour of laterally loaded piles. But when the pile length is beyond the critical length, the finite element method results show that the behaviour of laterally loaded pile is unchanged, the increase in pile length is insignificant. And the diameter of the pile greatly affects the response of the laterally loaded piles. The most important observations regarding the result obtained from the numerical analysis of behaviour of laterally loaded pile foundation can be summarized as follows:

- Diameter of the pile was increased from 650 mm to 1400 mm. As expected, head deflection of the pile decreased by 73.8%, 40.8% and 27.6% when the pile diameter increases from 650 mm to 900 mm, 900 mm to 1150 mm and 1150 mm to 1400 mm respectively with different pile length. Increase in diameter of pile reduces head deflection of the pile due to increase in structural stiffness.
- As expected, the lateral load capacity of pile increases by 50.6%, 43.1% and 36.4% when the pile diameter increases from 650 mm to 900 mm, 900 mm to 1150 mm and 1150 mm to 1400 mm respectively for different pile length since pile stiffness, EI, increases with increase in moment of inertia I which depends on the diameter of pile.

- The head deflection, ultimate lateral capacity of laterally loaded pile remains constant with increase in length for constant pile diameter since the embedment length of pile is greater than its critical length.
- The bending moment attains a maximum positive value below the pile head due to free headed and gradually decreases in a curvilinear manner with increasing depth.
- As expected, the larger diameter pile gives minimum deflection but greater bending moment value. Whereas smaller diameter pile gives maximum deflection but lesser bending moment value.
- The analysis shows that the location and the thickness of hard strata greatly affects the response of laterally loaded pile. The presence of soft organic silty clay and the location and the thickness of hard stratum in site-II reduces the ultimate lateral capacity of the pile by 24.3% and 19.2% relative to site-I and Site-II.
- In this study the effect of pile length on the head deflection and ultimate lateral resistance was negligible. For economical design of laterally loaded pile the selection of pile length is very important. For laterally loaded pile the length of the pile is more than its critical length the design will be uneconomical.

5.2 Recommendations

- Most of soil and rock parameters required for numerical analysis used in this study were obtained from correlation of some geotechnical properties of soils and rocks, and taking typical values from different literatures. Only very limited parameters are directly taken from test result. This is due to lack of adequate laboratory and field test results for different soil layers at different depth. This can be raised as one significant drawback in this study. A better simulation result of FEM could have been obtained, if most soil parameters have been directly determined from laboratory and field test results.
- In this thesis load was applied at the head of the pile on the ground surface. It is recommended to investigate, when the lateral load is applying eccentrically through extension of piles to some distance from the ground surface.
- In this research, the dynamic behavior of the laterally loaded pile is not taken into consideration. Therefore, future study is required to consider the dynamic load and its effect on the lateral capacity and the behaviour of laterally loaded pile.

- In this study, flexible and free headed pile was considered. It is recommended to investigate behaviour of laterally loaded pile with rigid conditions.

References

Anderson, J. B., Townsend, F. C., and Grajales, B. (2003). Case history evaluation of laterally loaded piles. ASCE, Journal of Geoechnical and Geo-enviromental Engineering, 129(3), 187-196.

Ashour, M. and Norris, G. (2000). Modelling Lateral Soil-Pile Response Based on Soil Pile Interaction. ASCE, Journal of Geotchnical and Geoenviromental Engineering, 126(5), 420-428.

B.S.Chawhan, S.S.Quadri, P.G.Rakaraddi,. (2012). Behavior of Lateral Resistance of Flexible Piles in Layered Soils. Journal of Mechanical and Civil Engineering, 02(05), 07-11.

Banerjee, P. K. and Davies, T. G. (1978). The Behaviour of Axially and Laterally Loaded Single Pile Embedded in Non-homogeneous Soils. Geotechnique, 28(3), 309-326.

Banerjee, P. K. and Driscoll, R. M. C. (1976). Three- dimensional analysis of raked pile groups. Proc. ICE, 2(61), 683-671.

Bathe, K.-J. (1996). Finite Element Procedures . Upper Saddle River, New Jersey : Prentice Hall.

Bransby, M. F. (1999). Selection of p-y Curves for the design of Single Laterally Loaded Pile. International Journal of Numerical and Analytical Methods in Geomechanics, 23(5), 1909-1926.

Briaud, Jean-Louis. (2013). Geotechnical Engineering: Unsaturated and Saturated Soils. Hoboken, New Jersey: John Wiley & Sons, Inc.

Broere, R.B.J. Brinkgreve and W. (2006). Plaxis 3D Foundation Version 1.5 User Manual. DELFT, Netherlands.

Broms, B. B. (1964a). Latreral Resistance of Pile in Cohesionless soils. Journal of Soil Mechanics and Foundation Division, ASCE , 90(3), 123-156.

Broms, B. B. (1964b). Lateral Resistance of Piles in Cohesive soils. Journal of Soil Mechanics and Foundation Division, ASCE, 91(3), 27-63.

Broms, B. B. (1965). Design of Laterally Loaded Piles. Journal of Soil Mechanics and Foundation Division, ASCE, 91(3), 79-99.

Budhu, M. and Davies, T. G. (1987). Nonlinear Analysis of Laterally Loaded Piles in Cohesionless Soils. Canadian Geotchnical Journal, 114(1), 289-296.

Budhu, M. and Davies, T. G. (1988). Analysis of Laterally Loaded Piles in Soft Clay. Journal of Geotchnical Engineering, ASCE, 114(1), 21-39.

C.S., Muqtadir A. and Desai. (1986). Three-dimensional analysis of pile group foundation. International Journal for Numerical and Analytical Method in Geomechanics, 10(5), 41-58.

Davies, T. G. and Budhu, M. (1986). Non-linear Anaysis of Laterally Loaded Piles in heavily Over-Consolidated Clays. Geotechnique, 4, 527-538.

Douglas, D. J. & Davis, E. H. (1964). The movement of buried footings due to moment and horizontal load and the movement of anchor plate. Geotechnique, 14(3), 115-132.

Duncan, J. M., Evans, L. T. J., and Ooi, P. S. K. (1994). Lateral Load Analysis of single pile and and drilled shaft. Journal of Geotchnical Engineering, ASCE, 120(5), 1018-1033.

Gabr, M. A., Lunne, T., and Powell, J. J. (1994). p-y Analysis of Laterally Loaded Pile in Clay Using DMT. Journal of Geotechnical Engineering Division, ASCE, 120(5), 816-837.

Gazetas, G. (1991). Foundation Engineering Book. In G. Gazetas, Foundation Vibration (Second ed.). Van Nostrand, New York.

Gu, D.X. Effect of Weathering on Strength and Modulus of Basalt and Siltstone. American Rock Mechanics Association, 2008.

Hetenyi, M. (1946). Beam on Elastic Foundation. Ann Arbor, Michigan : The University of Michigan Press.

Hirai, and Hiroyoshi. (2012). A Winkler model approach for vertically and laterally loaded piles. International Journal for Numerical and Analytical Methods in Geomechanics, 36(29), 1869–1897.

Ilyas, T., Leung, C. F., Chow, Y. K., and Budi, S. S. (2004). Centrifuge Model Study of Laterally Loaded Pile Group. ASCE, Journal of Geotchnical and Geoenviromental Engineering, 130(3), 274-285.

Jamaludin, A., and Hussein, A. N. (1998). The Performance of Large Diameter Bored Piles Used for Road Project in Malaysia. Proceedings of the 3rd International Geotchnical Seminar on Deep Foundation on Bored and Auger Piles, (pp. 335-338). Ghent, Belgium.

Kézdi, Á., and Rétháti, L. (1974). Hand Book of Soil Mechanics. Elsevier.

Kuhlemeyer, R. L. (1979). Static and Dynamic Laterally Loaded Floadting Piles. Journal of Geotchnical Enginering Division, ASCE, 105(2), 289-304.

Matlock, H. (1958). Soil Modulus for Laterally Loaded piles. Trans., ASCE, 123, 1077-1081.

Matlock, H. (1970). Correlation for Design for Design of Laterally Loaded Piles in Soft Clays. Proceedings of the 2nd Annual OTC. Dallas, Texas.

Matlock, H. and Grubbs, B. R. (1965). Lateral Resistance of Piles in Cohesive Soils. Journal of Soil Mechanics and Foundation Division, ASCE, 91(1), 185-188.

Matlock, H., and Reese, L. C. (1960). Generalized Solution for Laterally Loaded Piles. Journal of Soil Mechanics and Foundation Division, ASCE, 86(5), 63-91.

McClelland, B. and Focht, J. A., Jr. (1958b). Soil Modulus for Laterally Loaded Piles. Trans., ASCE, 123, 1081-1086.

McClelland, B. and J. A. Focht Jr. (1958a). Soil Modulus for Laterally Loaded Piles. Journal of Geotchnical Engineering, ASCE, 123(3), 1049-1063.

McVay, M., Casper, R. and Shang, T.I. (1995). Lateral response of three-row group in loose to dense sands at 3D and 5D spacing. Journal of Geotechnical Engineering, ASCE, 121(5), 436-441.

Mindlin, R. D. (1936). Force at Point in the Interior of a Semi-Infinite Solid. Journal of Physics, 7, 195-202.

N.F.Ismael. (1998). Lateral loading tests on bored piles in cemented sands. Proceedings of the 3rd International Geotchnical Seminar on Deep Foundation on Bored and Auger piles, (pp. 137-144). Ghent, Belguim .

Ng, C. W. W., Zhang, L., and Nip, D. C. N. (2001). Response of Laterally Loaded Large Diameter Boared Pile Groups. Journal of Geotechnical and Enviromental Engineering, ASCE, 127(8), 658-669.

Poulos, H. G. (1971a). Behaviour of Laterally Loaded Piles: I-Single Piles. Journal of Soil Mechanics and Foundation Divisions, ASCE, 97(5), 711-731.

Poulos, H. G. (1971b). Behaviour of Laterally Loaded Piles: II-Pile Groups. Journal of Soil Mechanics and Foundation Division, ASCE, 97(5), 733-751.

Poulos, H. G. (1972). Behaviour of Laterally Loaded Piles: III-Socketed Piles. Journal of Soil Mechanics and Foundation Division, ASCE, 98(4), 341-360.

Poulos, H. G., and Davis, E. H. (1980). Pile Foundation Analysis and Design. New York: John Wiley and Sons.

Poulos, H.G., and Hull, T.S.,. (1989). The Role of Analytical Geomechanics in Foundation Engineering, Current Principle and Practice (GSP 22). Proceedings of the ASCE, 2, pp. 1578-1606. New York.

R. Salgado, F.S. Tehrani, M. Prezzi. (2014). Analysis of laterally loaded pile groups in multilayered elastic soil. Computers and Geotechnics, 62(18), 136–153.

Randolph, M. (1981). The Response of Flexible Piles to the Lateral Loading. Géotechnique, 31(2), 247-259.

Randolph, M. F. and Houlsby, G. T. (1984). The Limiting Pressure on a Circular Pile Loaded Laterally in Cohesive Soils. Géotechnique, 34(4), 613-623.

Reese, L. (1984). Hand Book on Design and Construction of Piles and Drilled Shafts Under Lateral Load. Federal HighWay Administration .

Reese, L. C., Cox, W. R., and Koop, F. D. (1975). Filed Testing and Analysis of Laterally Loaded Piles in Stiff Clay. In Proceedings, 7th Annual Offshore Technology Conference, (pp. 671-690). Houston, Texas.

Reese, L.C. and Van Impe W. F. (2001). Single Piles and Pile Groups Under Lateral Loading. New York: A.A Balkema Publishers.

Sahu, Amit Jain & A.K. (2016). Numerical Study on Response of Laterally Loaded Piles in Soils. Imperial Journal of Interdisciplinary Research (IJIR), 2(10), 2454-1362.

Scott, R. F. (1981). Foundation Anaysis . Engel Wood, NJ.: Prentice-Hall.

Skempton, A. W. (1986). Standard penetration test procedures and the effects in sands of overburden pressure, relative density, particle size, aging and over consolidation. Geotechnique, 36(3), 425-447.

Terzaghi, K. (1955). Evaluation of coefficient of subgrade reaction. Geotechniques, 5(4), 297-326.

Trochanis, A. M., Bielak, J., and Christiano, P. (1991a). Three-Dimensional Nonlinear Study of Piles. Journal of Geotchnical Engineering, ASCE, 117(3), 429-447.

Vesić, A. (1961a). Beams on Elastic Subgrade and Winkler's Hypothesis. ISMFE, 1, 845-850.

Vesić, A. B. (1961b). Bending of Beams Resting on Isotropic Elastic soils. Journal of Engineering Mechanics Divisions, ASCE, 87(2), 35-53.

Wu, D., Broms, B. B., and Choa, V. (1998). Design of Laterally Loaded piles in Cohesive Soils Using p-y Curves. Journal of the Soil Mechanics and Foundations Division, ASCE, 38(2), 17-26.

Yang, Z. and Jeremić, B. (2002). Numerical Analysis of Pile Behaviour Under Lateral Loads in Layared Elastic-Plastic Soils. Journal of Numerical and Analytical Methods in Geomechanics, 26, 1385-1406.

Zania, V. and Hededal, O. (2011). The Effect of Soil Pile Interface Behaviour on Laterally Loaded Piles. Proceedings of the 13th International Conference on Civil, Structural and Environmental Engineering Computing.

Zienkiewicz, O. C. (1977). The Finte Element Method. London: McGraw-Hill.

Appendix A - Geotechnical properties of soil

Typical values of soil Young's modulus for different soils according to USCS.

In general, the soil stiffness and elastic modulus depends on the consistency and the parking (density) of the soil. Typical values of soil Young's modulus are given below as guideline.

Table A.1 Typical values SPT - Based soil and rock classification systems (Skempton, 1986)

Sand	N_{60}	
	0-3	Very Loose
	3-8	Loose
	8-25	Medium
	25-42	Dense
	42-58	Very Dense
Clays	N_{60}	
	0-4	Very Soft
	4-8	soft
	8-15	Firm
	15-30	Stiff
	30-60	Very Stiff
	>60	Hard
Week Rock	N_{60}	
	0-80	Very Weak
	80-200	Weak
	>200	Moderately Weak to Very Strong

Table A.2 Typical values of Young's modulus (MPa) for granular materials (Kézdi&Rétháti, 1974 and Prat et al., 1995)

USCS	Description	Loose	Medium	Dense
GW, SW	Gravels/Sand well-graded	30-80	80-160	160-320
SP	Sand, uniform	10-30	30-50	50-80
GM, SM	Sand/Gravel silty	7-12	12-20	20-30

Table A.3 Typical values of Young's modulus (MPa) for cohesive materials (Kézdi and Rétháti, 1974 and Prat et al., 1995)

USCS	Description	Very soft to soft	Medium	Stiff to very stiff	Hard
ML	Silts with slight plasticity	2.5 – 8	10 – 15	15 -40	40 – 80
ML, CL	Silts with low plasticity	1.5 – 6	6 -10	10 – 30	30 -60
CL	Clays with low-medium plasticity	0.5 – 5	5 -8	8 – 30	30 – 70
CH	Clays with high plasticity	0.35 – 4	4 -7	7 – 20	20 – 32
OL	Organic silts	-	0.5 -5	-	-
OH	Organic clays	-	0.5 -4	-	-

Table A.4 Typical values of Poisson's ratio for soils and other material, Bowels (1977)

Types of Soils	ν
Clay (Saturated)	0.4-0.5
Clay (Unsaturated)	0.1-0.3
Sandy Clay	0.2-0.3
Silt	0.3-0.35
Sand- Dense	0.2-0.4
Sand -Coarse (Void Ratio=0.4-0.7)	0.15
Sand-Fine (Void Ratio=0.4-0.7)	0.25
Rock	0.1-0.4 (Depending on type of Rock)
Loess	0.1-0.3
Ice	0.36
Concrete	0.15

Appendix B - Ultimate Capacity from Numerical Results

Table B.1 Lateral load capacity and lateral deflection for the case of *site-I*

Length of pile(m)	Diameter of pile (m)	L/D ratio	Lateral load capacity (kN)	Head deflection (mm)
24	0.65	36.92	646.98	65
	0.9	26.67	1634.74	90
	1.15	20.87	2872.65	115
	1.4	17.14	4661.38	140
27	0.65	41.54	647.03	65
	0.9	30	1635.03	90
	1.15	23.48	2876.86	115
	1.4	19.29	4664.88	140
30	0.65	46.15	647.04	65
	0.9	33.33	1635.74	90
	1.15	26.08	2876.95	115
	1.4	21.43	4665.37	140
33	0.65	50.77	647.06	65
	0.9	36.67	1635.78	90
	1.15	28.69	2877.24	115
	1.4	23.57	4665.33	140

Table B.2 Lateral load capacity and lateral deflection for the case of *site-II*

Length of pile(m)	Diameter of pile (m)	L/D ratio	Lateral load capacity (kN)	Head deflection (mm)
24	0.65	36.92	489.01	65
	0.9	26.67	1137.40	90
	1.15	20.87	2254.50	115
	1.4	17.14	3616.67	140
27	0.65	41.54	489.02	65
	0.9	30	1137.46	90
	1.15	23.48	2254.52	115
	1.4	19.28	3618.34	140
30	0.65	46.15	489.02	65
	0.9	33.33	1137.46	90
	1.15	26.087	2254.46	115
	1.4	21.4286	3618.83	140
33	0.65	50.7692	489.022	65
	0.9	36.6667	1137.55	90
	1.15	28.6957	2254.47	115
	1.4	23.5714	3618.93	140

Table B.3 Lateral load capacity and lateral deflection for the case of *site-III*

Length of pile(m)	Diameter of pile (m)	L/D ratio	Lateral load capacity (kN)	Head deflection (mm)
24	0.65	36.92	562.08	65
	0.9	26.67	1761.56	90
	1.15	20.88	2766.16	115
	1.4	17.14	4833.59	140
27	0.65	41.54	562.51	65
	0.9	30	1761.71	90
	1.15	23.48	2766.20	115
	1.4	19.28	4833.61	140
30	0.65	46.15	562.45	65
	0.9	33.33	1761.72	90
	1.15	26.08	2766.28	115
	1.4	21.43	4833.69	140
33	0.65	50.77	562.45	65
	0.9	36.67	1761.72	90
	1.15	28.69	2766.29	115
	1.4	23.57	4834.30	140

Appendix C - Approximation the actual soil profile in to single homogenous layer

Due to the layered nature of soil deposits, the magnitude of E_s may vary with depth. For layered profile, Bowles (1987) recommended using a weighted average value of E_{av} as shown in Equation:

$$E_{av} = \frac{\sum_{i=1}^{n} E_{s(i)} H_i}{\sum_{i=1}^{n} H_i} \qquad \text{(C.1)}$$

Where: $Es(i)$= soil modulus of elasticity within a depth H_i

H_i = ith soil layer thickness

Based on the above equation the weighted average values of Young's modulus of elasticity (E_{av}) are 420MPa, 560MPa and 585MPa for site-I, site-II and site-III respectively.

Table C.1 Calculated values of critical length of the pile

Pile diameter (m)	Critical length of pile L_c (m)		
	Site-I	Site-II	Site-III
0.65	8.4	7.8	7.74
0.9	11.6	10.8	10.72
1.15	14.8	13.8	13.69
1.4	18.0	16.8	16.67